

Summer 2009

# Membrane properties of intact rock cores of Burlington Limestone, Jefferson Dolomite, Darrington Phyllite, and low permeability concrete

Megan Hart



Department: Geosciences and Geological and Petroleum Engineering

# MEMBRANE PROPERTIES OF INTACT ROCK CORES OF BURLINGTON LIMESTONE, JEFFERSON DOLOMITE, DARRINGTON PHYLLITE, AND LOW PERMEABILITY CONCRETE

by

MEGAN LEANORE HART

A DISSERTATION

Presented to the Faculty of the Graduate School of the

MISSOURI UNIVERSITY OF SCIENCE & TECHNOLOGY

In Partial Fulfillment of the Requirements for the Degree

DOCTOR OF PHILOSOPHY

In

GEOLOGICAL ENGINEERING

2009

Approved by

Baojun Bai, Co-Advisor
Norbert Maerz, Co-Advisor
Jeffery Cawlfield
J. David Rogers
Paul E. Parris

PUBLICATION DISSERTATION OPTION

This dissertation has been prepared in publication format. Section 1, pages 1-17, has been added to supply background information and serve as a literature review for the remainder of the dissertation. Paper 1, pages 18 - 53, is prepared and accepted in the style used by Geochimica et Cosmochimica Acta submitted June, 2008. Paper 2, pages 54 -74, is prepared in the style used by Journal of Geotechnical and Geoenvironmental Engineering (as a note) and was submitted for publication in June, 2008. Paper 3, pages 75 - 99, is accepted and prepared in the style used by, Hydrogeology submitted June, 2008. Section 2, pages 100 - 101 is a final overall summary and conclusions chapter.

# ABSTRACT

A number of laboratory studies have shown that clays exhibit membrane properties. However, little research has been performed on lithologies outside of pure clays. Recently, research focusing on mixed sand and clay membrane properties for engineering applications was performed. Still, literature only suggests the possibilities of membrane properties, osmotic or reverse-osmotic, associated with other naturally occurring 'tight' rock types. Therefore, the objectives of this research was to perform a series of hyperfiltration experiments using actual rock discs of Quarry Ridge Jefferson Dolomite, Darrington Phyllite, Lower Burlington Limestone, and low permeability concrete to determine if tight lithologies can function as membranes.

# ACKNOWLEDGMENTS

I could never have succeeded in the manner that I have if it were not for the support and love furnished by my family. They always believed in me and stood behind me, even when I did not and probably when they shouldn't have done so (like when I was learning how to drive). So, here's to my family for believing in a stubborn and strong-minded person even though they have no clue what I have spent the last few years of my life doing!

My deepest gratitude goes to my committee for adding breadth to my doctorate and knowledge base. I also wish to recognize Dr. T. Michael Whitworth for his assistance and technical expertise during the time I performed my experiments.

To all the people and friends I have worked with, worked beside, and learned from; to the secretaries and administrative assistants (Beth, Joan, Katherine, Pam and Ellen) that have copied, collated, called about the (insert various problem here) problem, and made me coffee; and finally my cats and puppy who came home to me even when they couldn't stand me, thank you.

TABLE OF CONTENTS

Page

PUBLICATION DISSERTATION OPTION ..... iii

ABSTRACT ..... iv

ACKNOWLEDGMENTS ..... v

LIST OF ILLUSTRATIONS ..... viii

LIST OF TABLES ..... x

NOMENCLATURE ..... xi

SECTION 1. INTRODUCTION ..... 1
1.1 OBJECTIVES ..... 1
1.2 OVERVIEW OF MEMBRANES ..... 1
1.3 GEOLOGIC MEMBRANE MECHANISMS ..... 2
1.3.1 Ion Exchange. ..... 2
1.3.2 Electrical Restrictions. ..... 4
1.3.3 Pore Size Restriction ..... 4
1.4 MEMBRANE PROCESSES. ..... 5
1.5 MATHEMATICS OF MEMBRANES ..... 8
1.6 MODELLING HYPERFILTRATION ..... 10

PAPER 1. LOW HEAD HYPERFILTRATION THROUGH INTACT BURLINTON LIMESTONE AND JEFFERSON CITY DOLOMITE ..... 17
1.1 ABSTRACT ..... 17
1.2 INTRODUCTION ..... 18
1.3 GEOLOGIC BACKGROUND ..... 19
1.4 METHODS ..... 21
1.5 RESULTS ..... 24
1.6 DISCUSSION ..... 27
1.7 CONCLUSIONS ..... 33
1.8 REFERENCES ..... 35

PAPER 2. MEMBRANE PROPERTIES OF LOW PERMEABILITY CONCRETE 53
2.1 ABSTRACT ..... 53
2.2 INTRODUCTION ..... 53

2.3 METHODS ..... 55
2.4 RESULTS ..... 57
2.5 DISCUSSION ..... 60
2.6 CONCLUSIONS ..... 63
2.7 REFERENCES ..... 64
PAPER 3. LOW HEAD HYPERFILTRATION THROUGH INTACT DARRINGTON PHYLLITE CORES ..... 74
3.1 ABSTRACT ..... 74
3.2 INTRODUCTION ..... 74
3.3 GEOLOGIC BACKGROUND ..... 77
3.4 METHODS ..... 78
3.5 RESULTS ..... 80
3.6 DISCUSSION ..... 82
3.7 CONCLUSIONS ..... 85
3.8 REFERENCES ..... 87
SECTION 2. OVERALL EXPERIMENTAL CONCLUSIONS ..... 99
2.1 SUMMARY ..... 99
2.2 CONCLUSIONS ..... 100
REFERENCES ..... 102
VITA ..... 108

# LIST OF ILLUSTRATIONS

Figure Page

SECTION 1

Figure 1.1 Electric restrictions on pore throats. 4

Figure 1.2. Diagram showing osmotic flow 5

Figure 1.3. Diagram showing flows during reverse osmosis 6

Figure 1.4. Conceptual CPL development 7

PAPER 1

Figure 1.1. Conceptual CPL development. 41

Figure 1.2: Experimental Apparatus Schematic 42

Figure 1.3: Experimental Testing Schematic 43

Figure 1.4: Effluent Concentration and Flux versus Time for Limestone Experiment 1. 44

Figure 1.5: Effluent Concentration and Flux versus Time for Limestone Experiment 2 . 45

Figure 1.6: Effluent Concentration and Flux versus Time for Limestone Experiment 3. 46

Figure 1.7: Effluent Concentration and Flux versus Time for Limestone Experiment 4. 47

Figure 1.8: Effluent Concentration and Flux versus Time for Dolomite Experiment 1… 48

Figure 1.9: Effluent Concentration and Flux versus Time for Dolomite Experiment 2… 49

Figure 1.10: Effluent Concentration and Flux versus Time for Dolomite Experiment 3. 50

Figure 1.11: Effluent Concentration and Flux versus Time for Dolomite Experiment 4. 51

Figure 1.12: Effluent Concentration and Flux versus Time for Silica Experiment with Limestone. 52

PAPER 2

Figure 2.1. Conceptual CPL development 67

Figure 2.2: Experimental Apparatus Schematic 68

Figure 2.4: Experimental Testing Schematic 69

Figure 2.5: Effluent Concentration and Flux versus Time for Experiment 1. 70

Figure 2.6: Effluent Concentration and Flux versus Time for Experiment 2. 71

Figure 2.7: Effluent Concentration and Flux versus Time for Experiment 3. 72

Figure 2.8: Effluent Concentration and Flux versus Time for Experiment 4. 73

PAPER 3

Figure 3.1. Conceptual CPL development. 91

Figure 3.2: Thin Section Photo of Darrington Phyllite at 40X magnification. ..... 92
Figure 3.3: Experimental Apparatus Schematic. ..... 93
Figure 3.4: Experimental Testing Schematic. ..... 94
Figure 3.5: Effluent Concentration and Flux versus Time for Experiment 1. ..... 95
Figure 3.6: Effluent Concentration and Flux versus Time for Experiment 2. ..... 96
Figure 3.7: Effluent Concentration and Flux versus Time for Experiment 3. ..... 97
Figure 3.8: Effluent Concentration and Flux versus Time for Experiment 4. ..... 98

# LIST OF TABLES

Table Page

PAPER 1

Table 1.1: Experimental Parameters and Calculated Results. ..... 38

Table 1.2: Experimental Parameters and Calculated Results. ..... 39

Table 1.3: Experimental Parameters and Calculated Results. ..... 40

PAPER 2

Table 2.1: Experimental Parameters and Calculated Results ..... 66

PAPER 3

Table 3.1: Experimental Parameters and Calculated Results. ..... 90

# NOMENCLATURE

| Symbol | Description |
|---|---|
| $J_v$ | Solution flux through membrane (cm/s) |
| $L_p$ | Permeability coefficient ($cm^3$/dyne s) |
| $J_s$ | Solute flux through membrane (mole/cm s) |
| $\sigma$ | Reflection coefficient or osmotic efficiency coefficient |
| $\Delta P$ | Pressure difference across membrane (dyne/$cm^2$) |
| $\Delta\pi$ | Theoretical osmotic pressure difference across membrane (dyne/$cm^2$) |
| $\bar{c}_s$ | Average solute concentration across membrane (mole/$cm^3$) |
| $\omega$ | Solute permeation coefficient (mole/dyne s) |
| $c_o$ | Concentration on the high-pressure membrane face (mole/$cm^3$) |
| $c_e$ | Effluent concentration (mole/$cm^3$) |
| $c_i$ | Influent concentration (mole/$cm^3$) |
| v | Number of particles correction factor |
| R | Gas constant (dyne cm/mole °K) |
| $\rho$ | Fluid density (g/$cm^3$) |
| g | Gravitation constant ($cm^2$/s) |
| $\phi$ | Porosity (%) |
| D | Diffusion constant of solute ($cm^2$/s) |
| D* | Diffusion constant of solute relative to lithologic interactions ($cm^2$/s) |
| A | Membrane area ($cm^2$) |
| T | Temperature (˚K) |
| $p_{sample}$ | Density of the sample membrane (g/$cm^3$) |
| $\zeta$ | Tortuosity of membrane |

# INTRODUCTION

## 1.1 OBJECTIVES

The primary objective of this dissertation was to experimentally determine whether intact rock discs taken from cores could behave as membranes through chemical osmosis and hyperfiltration.

This dissertation is divided into three papers and two sections. This, the first section, serves as an introduction to the membrane properties of geologic materials. The first paper presents the results of a series of hyperfiltration experiments on Burlington Limestone and Jefferson Dolomite. The second paper presents the results of a series of membrane experiments on low permeability concrete. The third paper describes the results of a series of membrane experiments on Darrington Phyllite. Papers 1-3 are in publication format for separate journals as stated in the publication format disclosure. The final section presents an overall summary and conclusions based on the experimental results and theoretical investigation.

## 1.2 OVERVIEW OF MEMBRANES

To introduce the reader to the topic of geologic membranes it is first necessary to establish some general concepts pertaining to the subject. Geologic materials, such as clays, shales, siltstone, and river mud have been demonstrated to behave as semi-permeable membranes (Milne et al. 1963, Young and Low 1965, Kemper 1966, Olsen 1972, Kharaka and Berry 1973, Magara 1974, Kharaka and Smalley 1976, Benzel and Graf 1984, Fritz and Marine 1983, Fritz and Eady 1985, Haydon and Graf 1986, Fritz 1986, Demir 1988, Fritz and Whitworth 1994, Whitworth and Fritz 1994, Ishiguro et al. 1995, Whitworth and DeRosa 1997, Whitworth et al. 1999, Neuzil 2000, Sherwood and

Craster 2000, Malusis and Shackelford 2002, Liangxiong et al. 2003a, b, Saindon, 2005). A semi-permeable membrane is defined as a material which will permit the passage of some molecules but not others (Noggle, 1984). A perfect membrane would absolutely preclude the passage of certain molecular species; however, such perfect membranes probably do not exist in nature (Fritz, 1986).

A working definition of a geological membrane is any lithology which allows one solution component to pass through more easily than another. Two such semi-permeable membrane processes are believed to occur in the subsurface: osmosis and hyperfiltration (which is also called reverse osmosis or solute sieving, Graf 1982).

Membrane processes include *osmosis* and *reverse osmosis*. *Osmosis* is chemical concentration gradient-driven migration, or attempted migration, of particles through a membrane (Alexander 1990). *Reverse osmosis* is physical pressure driven migration of particles through a membrane, also known as *hyperfiltration* (Alexander 1990). Reverse osmosis occurs when hydraulic pressure is applied in excess of the osmotic pressure present on the inflow side of the membrane. During reverse osmosis, water flows across the membrane from the high to low solute concentration side. These processes will be discussed in further detail in section 1.4.

## 1.3 GEOLOGIC MEMBRANE MECHANISMS

Selectivity of geologic membranes occurs through one of three main mechanisms: ion exchange, electrical restrictions, and pore size restrictions.

**1.3.1 Ion Exchange.** Ion exchange is the stoichiometric substitution of an ion or a series of ions for another ion or series of ions of equal net ionic charge from free solution (Drever, 1997). Ion substitutions occur on the edges of the crystal lattice,

effectively changing the particle charge potential (Weaver, 1989 Whitworth, 1999). Ion affinity is proportional to the valence charge of the ion; lower valent ions from the crystal lattice are preferentially exchanged for higher valent free solution ions. Ion exchange is a finite process in that ion exchange will only continue as long as vacancies or exchange potential exists. A constant solution composition will eventually expend this exchange potential and ion exchange will cease. Ion exchange is directly correlated to the cation exchange capacity (CEC) of a material. The CEC is a quantitative measurement of the ability of a substance to exchange cations. Cation exchange potential varies with pH and the nature of the ions occupying the exchange sites (Drever, 1997). Most charged clays typically have high CEC potential. Most of the lithologies tested in these experiments would probably exhibit low to moderate CEC potential.

**1.3.2 Electrical Restrictions.** Electrical restrictions occur for any charged membrane. For geologic membranes, especially clays, the surface charges are usually negative when the membrane is immersed in a solution. For clays this negatively charged surface is surrounded by a layer of fixed cations, known as the Stern layer, which offsets a majority of the negative charge for the individual clay platelet. The negative charge of the Stern layer results from broken bonds on the edges of the crystal structure and cation substitutions within the crystal lattice. The diffuse layer of cations beyond the Stern layer that surrounds the clay particle is known as the Guoy layer (Figure 1.1) (Grim 1968). Ions are more easily exchanged in the Guoy layer due to the lesser electrical charge holding those particles near the surface. Collectively, these Stern and Guoy layers fulfill the electrical potential of the particle. If negatively charged particles have large pore spaces, the electrical fields may not overlap within the pore, but may still reduce the

effective size of the pore space to charged species. If clay platelets have been compacted such as in a shale to the point where the electrical fields overlap significantly, ionic species would be repelled by the electrical field in the pore or pore throat, thus reducing or inhibiting movement of ions through the pore spaces (Figure 1.1) (Fritz 1986). The electrical restrictions of the lithologies tested in these experiments are presumed to be relatively low due to the small percentage of clay content measured.

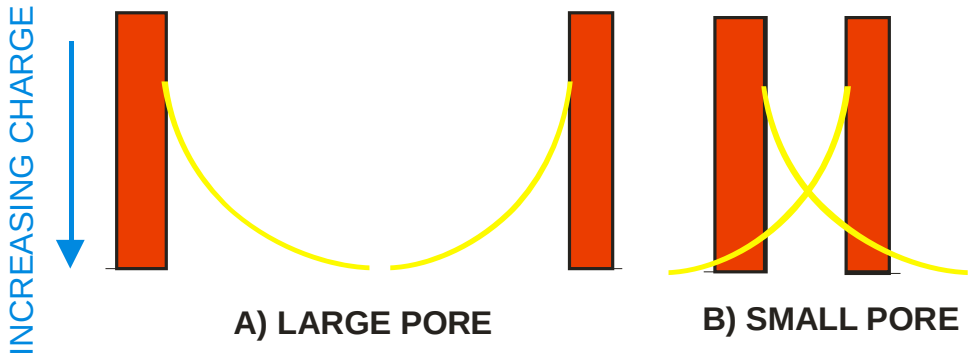


*Figure 1.1 Electric restrictions on pore throats. The yellow line denotes the extent to which the electrical charge reduces the pore throat. As the extent of the electrical charge increases, the reduction in pore throat is noted, especially in smaller pores.*

**1.3.3 Pore Size Restriction**. Pore size restrictions occur based on the size of the hydrated ionic species and the pore throat size (Figure 1.1). If the solutes are larger than the smallest pore throat within the flow pathway, the solute will prohibited from passing unless an alternate flow pathway is obtained. Solutes larger than the smallest pore along the path would also effectively block off potential paths for the smaller ions, a process referred to as fouling (Tchobanoglous et al. 2003). If the pore diameter is just slightly larger than the species trying to pass, it is likely that the velocity of the species traveling through it will be slowed due to frictional effects (Gregor and Gregor, 1968). Larger particles that are slowed down due to frictional effects will in turn reduce the potential

maximum speed of any smaller ions taking the same flow path. This would occur due to a reduced effective pore size because the larger ion takes up a portion of the pore volume. Any smaller particles that could not fit past the larger particle and the flow path boundaries would be slowed to speed of the larger particle. Even if the smaller particle can pass the larger particle, the effective pore space would be smaller. Thus increasing the boundary frictional effect and reducing the velocity of the smaller particle. The primary restriction of the lithologies tested in these experiments was pore size restrictions. The lithologies were selected due to their relatively low permeability.

**1.4 MEMBRANE PROCESSES.**

Reverse osmosis (hyperfiltration) and osmosis are the two commonly discussed clay membrane processes (Fritz 1986). Osmosis occurs when a concentration difference exists across the membrane. In this case the flow of the dissolved solute and the solvent is a function of their respective concentration gradients across the membrane (Figure 1.2).

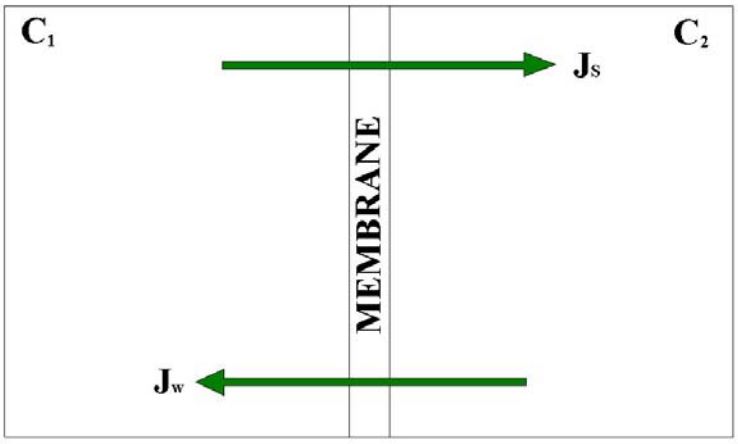


*Figure 1.2. Diagram showing osmotic flows where $C_1$ and $C_2$ are solute concentrations, $J_s$ is solute flux, and $J_w$ is water flux across the membrane. Since $C_1>C_2$, solute flux is from the high concentration to the low concentration of solute, while the water flux is*

*from the high concentration of water (low solute concentration) to the low concentration of water (high solute concentration).*

Reverse osmosis occurs when a hydraulic head difference greater than the osmotic pressure exists across a semi-permeable membrane (Figure 1.3) When the solution is forced through the membrane by the hydraulic head, some of the solute is rejected by the membrane. The solute that is rejected starts to form a zone of increased concentration on the high pressure side of the membrane directly adjacent to the membrane. This zone of increased solute concentration is called the concentration polarization layer (CPL). Since solute rejection of a membrane is based on the solute concentration at the upgradient face of the membrane, as the CPL develops the solute concentration of the fluid that has passed through the membrane will increase. This process continues until the CPL is fully developed and the solute concentration of the effluent is equal to the original feed solution (Figure 1.4).

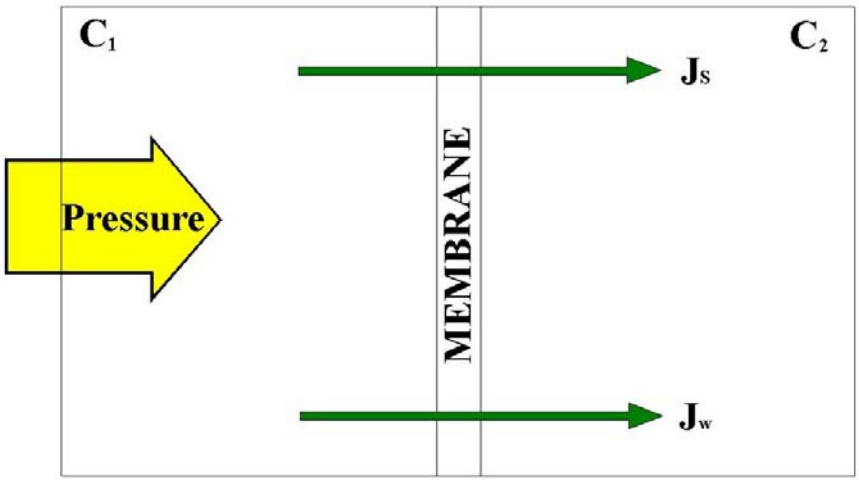


*Figure 1.3. Diagram showing flows during reverse osmosis or hyperfiltration where $C_1$ and $C_2$ are solute concentrations, $J_s$ is solute flux, and $J_w$ is water flux across the membrane. Since $C_1>C_2$, solute flux is from the high concentration to the low*

*concentration of solute; while the water flux is from the high pressure side of the membrane to the low pressure side. Diagram shows a static flow configuration for simplicity.*

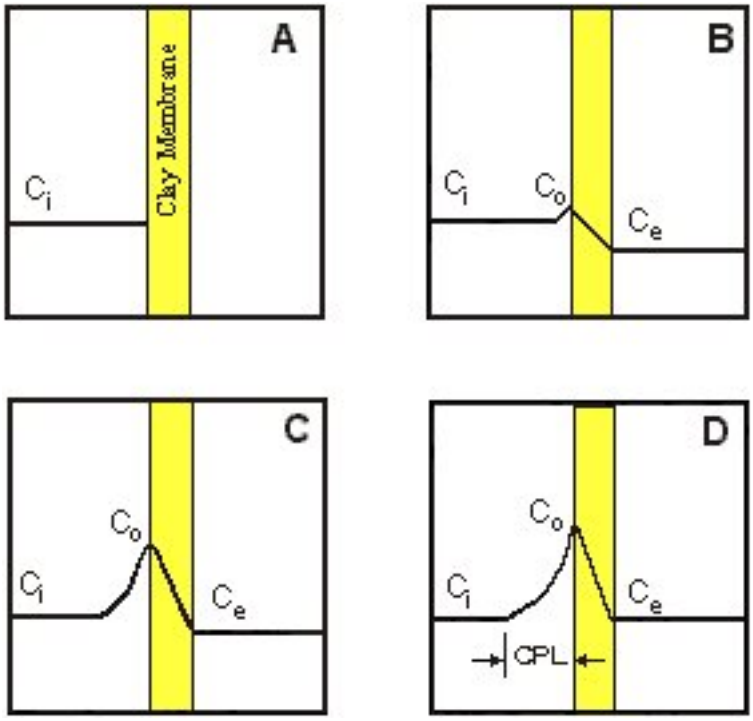


*Figure 1.4. Conceptual CPL development assuming that the solute is conservative and no ion exchange or biological processes are occurring. Initially, (A) the solute is all on the high-pressure side of the membrane and no solute is contained within the pore fluids within the membrane. After solute flux across the membrane begins, (B) the concentration at the high-pressure membrane face $c_o$ increases due to solute rejection, and the effluent has lower concentrations of solute than the original solution. (C) CPL continues to develop. At steady-state (D) the input concentration $c_i$ is now equal to the output $c_e$ and the value of $c_o$ is constant. (Redrawn from Fritz and Marine 1983).*

Reverse osmosis processes occur in a variety of flow configurations. The two most common flow configurations for reverse osmosis are static and cross-flow. In a static flow configuration, all the feed solution passes through the membrane and becomes effluent. The static flow configuration permits the CPL to develop. In a cross-flow configuration, the feed solution enters the system and flows parallel to the membrane in such a matter that turbulent flow is achieved and reduces the likelihood that a CPL will

form next to the membrane. A portion of the feed solution, the concentrate, exits the system without passing through the membrane. The concentrate serves to remove any increase in solute concentrations that form on the upgradient side of the membrane. The remaining solution passes through the membrane and exits as the effluent or permeant. Cross-flow configurations are often utilized to purify water, recover metals and water in the electroplating industry, and the removal or concentration of organic or inorganic hazardous waste species (LaGrega et al. 1994).

## 1.5 MATHEMATICS OF MEMBRANES

Non-equilibrium thermodynamics was used to derive Equations 1.1 and 1.2, which describe the flux of solution and solute through membranes (Kedem and Katchalsky 1962). Non-electrolytes served as the basis for the development of these equations, but both equations have been successfully applied to electrolytes (Spiegler and Kedem 1966, Harris et al. 1976; Fritz and Marine 1983, Fritz 1986, Mariñas and Selleck 1992, Whitworth et al. 1994). Describing a conservative, single solute system, the two equations are:

$$J_v = L_p(\Delta P - \sigma\Delta\pi) \tag{1.1}$$

and

$$J_s = \bar{c}_s(1-\sigma)J_v + \omega\Delta\pi \tag{1.2}$$

where $L_p$ = water permeation coefficient (m/Pa·s), $\Delta P$ = pressure difference across the membrane (Pa), $J_v$ = experimental solution flux (m/s) through the membrane, $J_s$= solute flux (m/s) through the membrane, $\Delta x$ is membrane thickness (m), $\sigma$ = reflection

coefficient (dimensionless), $\Delta\pi$ = theoretical osmotic pressure difference across the membrane ($Pa/m^2$), $\omega$ = solute permeation coefficient (mole/Pa·s), and $\bar{c}_s$ = average solute concentration across the membrane ($mole/m^3$) where:

$$\bar{c}_s = \frac{c_o + c_e}{2} \tag{1.3}$$

where $c_o$ = concentration at the high-pressure membrane face ($mole/m^3$) and $c_e$ = effluent concentration ($mole/m^3$).

The equation for $\Delta\pi$ for a dilute single solute is:

$$\Delta\pi = vRT(c_o - c_e) \tag{1.4}$$

where v is a factor that corrects for the number of particles due to ion formation. For example, since $KNO_3$ forms two ions in solution, $K^+$ and $NO_3^-$, then for $KNO_3$, v = 2. However, for $MgCl_2$, which forms one $Mg^{++}$ ion and two $Cl^-$ ions for each molecule of $MgCl_2$, v = 3. In Equation 1.4, R is the gas constant (8.314 N·m/mole), and T is the temperature in °K.

Of the phenomenological coefficients of Kedem and Katchalsky (1962), Fritz (1986) found that $\sigma$, $\omega$, and $L_p$ describe the behavior of non-ideal, geologic membrane systems. Values of the reflection coefficient ($\sigma$) range from zero to one. If $\sigma = 0$, then there is no membrane effect. If $\sigma = 1$, the osmotic efficiency is 100%, all solute is retarded and the membrane is perfect. In the case of $\sigma = 0$, Equation 1.1 reduces to a one-dimensional form of Darcy's Law. No known perfect membranes exist in nature and therefore values of $\sigma$ for non-ideal geological membranes should be greater than zero, but less than one. The reflection coefficient ($\sigma$) is important because it is a measure of

osmotic efficiency (Fritz and Marine 1983). Therefore, a membrane with a $\sigma = 0.90$ would exhibit 90% of the theoretically predicted osmotic pressure. For solutes such as $KNO_3$, with identical anion and cation concentrations, $\sigma_{anion} = \sigma_{cation}$. However, for systems such as $CuCl_2$, where the dissolved anion concentration is twice that of the cation concentration, the anion and the cation have differing values of $\sigma$.

The solute permeation coefficient $\omega$ describes the diffusion of solute through the membrane. For ideal membranes, $\omega = 0$ and no solute can pass through the membrane. For typically non-ideal geologic membranes $\omega$ should be greater than zero. For systems where the anion concentration is not equal to the cation concentration, $\omega_{anion} \neq \omega_{cation}$.

## 1.6 MODELLING HYPERFILTRATION

Whitworth (1998) developed a steady state analytical mathematical model of hyperfiltration membrane effects in shallow aquifers based on the irreversible thermodynamic approach of Kedem and Katchalsky (1962) and subsequent work by Marine and Fritz (1981), Fritz and Marine (1983), Fritz (1986), and Fritz and Whitworth (1994) that quantitatively describe membrane effects of non-ideal geologic membranes. Whitworth's (1998) model is capable of handling multi-solute groundwaters. In 1999, Whitworth et al. published a steady state method for predicting experimental parameters without advanced knowledge of cell solution. The development of this steady state 1999 method is shown below:

Fritz and Marine (1983) derived a steady-state solution that describes the CPL profile within the free solution adjacent to the membrane. Their equation is:

$$c_x = (c_o - c_i)\left[\exp(\frac{-J_v x}{D}) - \exp(\frac{-J_v x_i}{D})\right] + c_i \qquad (1.5)$$

where $c_x$ is the concentration in moles/$m^3$ at distance x (m) from the membrane, and $x_i$ is the distance from the membrane where $c_x = c_i$, D is the diffusion constant of the solute ($m^2$/s). In Equation 1.6, $J_v$ represents the flux toward the membrane. Fritz and Whitworth (1994) state that the term -exp ($-J_v x_i/D$) in Equation 1.5 can be ignored if the length of the test cell is large relative to the ratio $D/J_v$.

Due to interaction of the diffusing solute with mineral grains, diffusion in free solution occurs quicker than diffusion in porous media (Fetter 1988; Domenico and Schwartz 1990). The effective solute diffusion coefficient for porous media is typically represented by D* (Freeze and Cherry 1979; Fetter 1988). D* is defined by the relation D* = wD, where w is a unitless empirical constant determined from laboratory experiments (Fetter, 1988). Freeze and Cherry (1988) reported that w ranges from 0.01 to 0.5. The lower end of this range is for clayey sediments (Berner 1971). For porous media, Equation 1.5 reduces to

$$c_x = (c_o - c_i)\left[\exp\left(\frac{-J_v x}{D^*}\right)\right] + c_i \qquad (1.6)$$

Fritz and Marine (1983) stated that because ω tends to be very small, the ωΔπ term in Equation 1.2 can often be ignored. By omitting the ωΔπ term and by substituting Equation 1.3 into Equation 1.2, they derived the following relationship

$$\sigma \approx \frac{c_o - c_e}{c_o + c_e} \qquad (1.7)$$

At equilibrium, $c_e = c_i$ by definition. By substituting $c_i$ for $c_e$ into Equation 1.7 and solving for $c_o$ we can develop the following approximate relationship between σ, $c_i$, and $c_o$

$$c_o \approx \frac{-(\sigma c_i + c_i)}{\sigma - 1} \tag{1.8}$$

Equation 1.1 shows that the total solution flux through the membrane increases as the differential pressure across the membrane increases and decreases with increasing osmotic pressure. In order to model multiple-solutes in the groundwater, Whitworth (1998) derived several steady-state equations describing the behavior of non-ideal geologic membranes. If the osmotic pressure is zero, then Equation 1.1 reduces to a one-dimensional form of Darcy's Law. On the other hand, if osmotic pressure is significant, $J_v$ will be less than would be predicted by Darcy's Law (Whitworth et al., 1999):

$$J_v = \frac{K\Delta P}{\rho g \Delta x} \tag{1.9}$$

Whitworth (1998) found that substituting Equation 1.5 and Equation 1.6 into Equation 1.1 yields:

$$J_v = \frac{K}{\rho g \Delta x}(\Delta P - \sigma v RT(c_o - c_e) \tag{1.10}$$

The only unknown parameter in this equation is $c_o$. Solving Equation 1.8 for $c_o$ and substituting the steady-state relationship $c_e = c_i$ as described in Equation 1.8. Substituting Equation 1.9 into 1.10 yields:

$$J_v = \frac{K}{\rho g \Delta x}(\Delta P - \sigma v RT(\frac{-(\sigma c_i + c_i)}{\sigma - 1} - c_i)) \tag{1.11}$$

Whitworth (1998) derived an analytical expression for $c_o$ by substituting Equations 1.2, 1.3, 1.11, and the following expression for ω

$$\omega = \frac{D}{RT\Delta x \zeta} \tag{1.12}$$

where $\zeta$ is tortuosity and is defined here as the ratio of the actual path length through the membrane to the membrane thickness and the steady-state relationships $J_s = J_{v,}$ $c_e$, and $c_i = c_e$, into Equation 1.2. This expression is:

$$c_o = -c_i \cdot \frac{J_v \Delta x \zeta (1+\sigma) + 2Dv}{J_v \Delta x \zeta (\sigma - 1) - 2Dv} \tag{1.13}$$

Moreover, this equation is suitable for free solution. For porous media, Equation 1.13 becomes:

$$c_o = -c_i \cdot \frac{J_v \Delta x \zeta (1+\sigma) + 2D^* v}{J_v \Delta x \zeta (\sigma - 1) - 2D^* v} \tag{1.14}$$

Using equations 1.6, 1.12, and 1.14, Whitworth (1998) modeled steady-state membrane effects for single solute systems in natural groundwater systems.

For multi-component solutions, Katchalsky and Curran (1965), stated

$$J_v = L_P(\Delta P - \sum_{j=1}^{n} \sigma_j \Delta \pi_j) \tag{1.15}$$

By substituting equations 1.3, 1.4 1.7 and 1.12 into Equation 1.15, Whitworth (1998) derived:

$$J_v = \frac{K}{\rho g \Delta x}\left[\Delta P - \sum_{j=1}^{n}\left(\sigma_j \nu_j RT\left(\frac{-\left(\sigma_j c_{i_j} + c_{i_j}\right)}{\sigma_j - 1} - c_{i_j}\right)\right)\right] \tag{1.16}$$

The value of $\sigma$ is dependent upon both the properties of the solution as well as the properties of the membrane. A value for the reflection coefficient will be needed for each ion pair, or non-ionic solute in order to model membrane effects for multi-solute solutions.

Not all clays have significant electrical charge and most lithologies that are not greater than 12% clay, or clay rich, do not exhibit significant electrical charges. For example, kaolinite is essentially uncharged at typical groundwater pH (Grim, 1968) and for carbonates which contain kaolinite as a trace mineral there is essentially no charge as well. Whitworth et al. (1999) have shown that compacted, essentially uncharged clay-sized quartz particles act as membranes when undersaturated solution is hyperfiltrated through thin layers of these particles. In fact, this process is capable of precipitating calcite. Additionally, Saindon (2005) found that compacted and resedimented mixtures of quartz sand and uncharged kaolinites as well as smectites exhibited membrane properties.

A model having broad application needs to effectively deal with charged and uncharged membranes in order to calculate values of $\sigma$, as most lithologies which are reflective of natural situations and confined or unconfined aquifers will be in the majority uncharged.

A model for describing hyperfiltration capable of handling charged and uncharged membranes is that of Fritz and Whitworth (1994). The transient solution describing hyperfiltration developed by Fritz and Whitworth (1994) provides a means of calculating experimental parameters such as:

$$c_{x,t} = \left[\left(c_{o(t)} - \frac{c_i}{2}\right)\right]\left\{\begin{array}{l}\left[\exp\left(\frac{-J_v x}{D}\right) - \exp\left(\frac{-J_v x_i}{D}\right)\right] \\ erfc\left(\frac{x - J_v t}{2(Dt)^{1/2}}\right) + erfc\left(\frac{x + J_v t}{2(Dt)^{1/2}}\right)\end{array}\right\} + c_i \qquad (1.17)$$

where t is time in seconds and x is the distance from the membrane in centimeters.

However, this method requires extremely accurate measurements of the solution concentration within the cell during the experiment and is cumbersome for determining steady state values of σ. As measuring the cell solution would disrupt the production of the concentration polarization layer, as well as remove mass from the mass balance equation, a simpler method for calculating the reflection coefficient is needed.

In order to calculate steady-state values of σ without advanced knowledge of the cell solution concentration, Whitworth et al. (1999) developed a method for calculating experimental parameters of membrane effects. Equations 1.15 and 1.17 are simultaneous equations, which can thereby be resolved for σ and $c_o$ according to Whitworth et al 1999. Whitworth et al. (1999) developed the following equation:

$$\begin{aligned} c_o = & \left( \frac{1}{2 \cdot L_p vRT(J_v \Delta x - 2vD)} \right) \cdot (-2L_p vRTJ_v c_i \Delta x\zeta - 4L_p v^2 RTDc_i \\ & + \Delta x\zeta J_v L_p \Delta P - \Delta x^{1/2}\zeta^{1/2} \cdot (-8\zeta \Delta x c_i J_v{}^3 TRvL_p + 8\zeta \Delta x c_i J_v{}^2 TRvL_p{}^2 + \zeta \Delta x J_v{}^4 \\ & - 2\zeta \Delta x \Delta P L_p J_v{}^3 + \zeta \Delta x \Delta P^2 L_p{}^2 J_v{}^2 - 16 J_v{}^2 c_i DTRv^2 L_p{}^2)^{1/2}) \end{aligned} \tag{1.18}$$

Additionally, Whitworth et al. (1999) derived an equation for σ that is

$$\sigma = \frac{L_p \Delta P - J_v}{L_p vRT(c_o - c_i)} \tag{1.19}$$

Using the Whitworth et al. (1999) method, in order to calculate σ, $c_o$ must first be calculated. This method does not require advanced knowledge of the average concentration within the experimental cell and therefore may more aptly model membrane effects within natural groundwater systems as well as predicts experimental parameters without disruption of the experiment. The Whitworth et al (1999) method (Equations 1.18 and 1.19) will be used throughout this dissertation as a basis for examining the steady state experimental parameters of σ in hyperfiltration.

The three following chapters address individual experiments that were conducted on intact rock discs using a static cell configuration. All experiments showed measurable membrane effects, and reflection coefficients were determined for all of the experiments using the equations in the model shown above and as derived in the literature.

# PAPER 1. LOW HEAD HYPERFILTRATION THROUGH INTACT BURLINTON LIMESTONE AND JEFFERSON CITY DOLOMITE

## 1.1 ABSTRACT

Hyperfiltration is the ability of a membrane to retard the passage of one solute under a hydraulic head in excess of osmotic pressure. Shales, mudstones, clays, and tuff have been shown to exhibit hyperfiltration-induced membrane effects in past experiments. However, limestone and dolomite have not previously been tested. Therefore, we performed eight hyperfiltration experiments on intact Burlington Limestone and Jefferson City Dolomite to assess the membrane properties of these lithologies. Four experiments were conducted on each lithology using chloride solutions of 185 and 345 ppm at heads of 0.5 and 1.0 m. Reflection coefficients, a measure of osmotic efficiency, ranged from 0.34 to 0.39 for the Burlington Limestone and 0.32 to 0.40 for the Jefferson City Dolomite. At the end of the hyperfiltration experiments, chloride was concentrated within the cell above input concentrations by 79 to 101% for the Burlington Limestone and 82 to 108% for the Jefferson City Dolomite. An additional experiment passed 120 ppm dissolved silica solution through the Burlington Limestone at a head of 0.96526 bar (14 psi). The ending concentration of silica within the cell was 256 ppm at steady-state; a concentration 113% higher than the original input solution concentration. The reflection coefficient for this experiment was calculated to be 0.33. The results of these experiments suggest that membrane properties in these lithologies may be worthy of consideration in some geologic scenarios, including: 1) shallow or perched aquifers bounded by thin limestone or dolomite strata, 2) overpressured aquifers bounded by limestone or dolomite, 3) limestone or dolomite bounded aquifers with

significant vertical components of flow, and 4) facies changes with significant lateral component of flow bounded by either lithology. Furthermore, our results suggest that silica cementation may be possible even under relatively low head conditions. Cementation due to hyperfiltration, even at shallow depths and lower pressures should be further investigated. Similarly, other low permeability lithologies such as phyllite, chalk, fault gouge, and schist are also likely candidates to be geologic membranes.

## 1.2 INTRODUCTION

Fritz and Whitworth (1994) suggested that chemical gradients may result in groundwater adjacent to membrane functioning lithologies undergoing hyperfiltration and affect groundwater sampling chemistry results. Hyperfiltration (also termed reverse osmosis or solute-sieving (Graf, 1982)) is a geologic semi-permeable membrane process by which solutes can be locally concentrated (Fritz, 1986). When an electrolyte advects towards a membrane-functioning lithology under a hydraulic head sufficient to overcome the osmotic pressure, solutes can concentrate due to partial solute-rejection at the high-pressure face of the lithology (Porter, 1979; Fritz, 1986; Fritz and Whitworth, 1994). This zone of concentrated solutes is termed the concentration polarization layer or CPL (Figure 1; Fritz, 1986).

Hyperfiltration has been shown experimentally to occur through clays, shales, and siltstones (McKelvey and Milne, 1960; Young and Low, 1965; Kharaka and Berry, 1973; Barone et al., 1992; Whitworth and DeRosa, 1997). Very few experiments have examined the ability of intact rock and “tight” lithologies to function as osmotic membranes under a chemical gradient (McKelvey and Milne, 1960; Young and Low, 1965; Kharaka and Berry, 1973; Barone et al., 1992; Whitworth and DeRosa, 1997);

though various lithologies such as phyllite, fault gouge and chalk have been suggested as potential candidates (Mackay, 1946, Alexander, 1990; Whitworth and DeRosa, 1997; Whitworth et al. 1999; Whitworth et al. 2002). The purpose of this study was to explore the hyperfiltration properties of intact Jefferson City Dolomite and Burlington Limestone using chloride solutions of 185 and 345 ppm. We experimentally tested thin (~3mm thick), intact rock core discs using constant heads of 0.5 and 1.0 m and chloride concentrations of 185 and 345 ppm to determine whether significant hyperfiltration-induced concentration build-up of chloride is possible due to solute reflection by the membrane. An additional experiment passed 120 ppm silica solution through a thin limestone disc at a constant pressure of 14 psi in order to assess the potential of silica to concentrate via hyperfiltration.

## 1.3 GEOLOGIC BACKGROUND

The Jefferson City Dolomite is early Ordovician in age and outcrops predominantly in the Ozark region of Missouri (Thompson, 1985). Jefferson City Dolomite is composed of light-brown to brown, medium to finely crystalline dolomite, and argillaceous dolomite. Lenses of orthoquartize, conglomerate, and shale are locally present in the formation. Many rock exposures exhibit a particular sequence within this formation locally called the Quarry Ledge Dolomite. This rock is massively bedded, mainly brown in color and has a well formed crystalline texture. Locally, the Quarry Ledge Dolomite is heavily favored for dimension stone due to its resistance to weather and superior competency (Thompson, 1985). Insoluble siliceous spicules commonly referred to as “spines” and a variety of oolitic chert are both noticeable at the interface between the main body of the Jefferson Dolomite and Quarry Ledge Dolomite. Hand

samples averaging 10 to 40 lbs each used in these experiments were collected from the University of Missouri–Rolla Experimental Mine located at 37° 56.23'N, 91° 47.44'W. The samples taken were from the Quarry Ledge dolomite and were composed of 64% dolomite, 26% limestone, 6% quartz, 2% smithsonite, 1% limonite, and trace amounts of marcasite, pyrite, sphalerite, barite, and greenockite as determined using x-ray diffraction.

The Burlington Limestone is Mississippian in age and outcrops across the state of Missouri in differing thickness and competency. The Burlington Limestone is a generally white to light gray, medium to coarsely crystalline limestone. Chert occurs in zones of 0.3 to 3.048 meters (1 to 10 feet) thick, separated by 9.1 to 15.24 meters (30 to 50 feet) of well crystalline, chert free limestone. The lower 6.09 to 9.1 meters (20 to 30 feet) in the St. Louis area is locally called the Lower Burlington Limestone and contains 50 percent chert, except for the bottom 0.61 to 1.5 meters (2-5 feet) which is coarsely crystalline and is virtually 98% $CaCO_3$ (Thompson, 1995). Samples were obtained in the chert free portion of the Lower Burlington Limestone along Highway 640 in Columbia, MO. The exact location was 38°55'53.7" N 92°17'53.1"W. Collection of samples was performed during a rainy portion of the year and multiple seeps occurred along the chert/limestone boundary. The samples used in this study were composed of 98% limestone, 1% quartz, and trace amounts of clay, chert, and organics as determined using x-ray diffraction.

Both formations are laterally extensive, nearly horizontal beds occurring regionally within Missouri (Thompson, 1995). Both formations have a shallow regional dip towards the south (Thompson, 1995). Thick residuum sediments blanket most of the

bedrock and are of dolomitic and sandstone origin. Immature karst features are noticed in the predominantly carbonate bedrock structures with caves, dolines, springs, and seeps the major geomorphic features (Orndorff et al. 2002; 2003).

## 1.4 METHODS

The hand samples, averaging 4.54 to 18.1 kg (10 to 40 lbs in weight), were cored to obtain 6.35 cm (2.5 inch) diameter cylinders. These were then sliced into discs and the discs ground down using silicon carbide paste on glass until the slices were approximately 3 mm thick. Thin discs were used instead of thicker columns of core in order to shorten the experimental duration.

The discs were placed into a custom-made hyperfiltration cell consisting of a transparent acrylic cylinder with an internal area of 15 $cm^2$ and wall thickness of 0.64 cm similar to those used by Hart and Whitworth, 2005 (Figures 1.2 and 1.3). The acrylic cylinders were fitted to two O-ringed, 3.80 cm thick, Garlite™ caps. The caps were held in place by eight threaded rods, which pass through both caps parallel to the cylinder. The hyperfiltration cell components were thoroughly washed and then rinsed multiple times with deionized water before each experiment.

A Marriotte flask suspended at either 0.5 or 1.0 m of height supplied a constant head. Initially deionized water was passed through the assembled experimental cells in order to determine water permeation ($L_p$) (Fritz and Whitworth, 1994; Figure 1.3). The deionized water was removed from the experimental cell and replaced with 185 and 345 ppm chloride solutions (Table 1.1 and Table l.2). The experiments began immediately after insertion of stock solution to the cell in order to observe the entirety of the reverse

osmotic process. Effluent samples were collected at intervals during the experiment. At the end of the experiment the concentration within the cell was measured.

Reagent grade chemicals were used to make the solutions. NaCl concentrations were measured with a Dionex DX-120 ion chromatograph and compared against standard concentrations. Analytical precision was computed by calculating the two standard deviation of triplicate testing of effluent samples. Each sample passed through the ion chromatograph was tested in triplicate; the average of each triplicate is reported in Figures 1.4 through 1.11 where the two standard deviation errors bars in these figures were calculated from this triplicate analysis.

Charge balance error was calculated for every chemical analysis but is only reported as the average of all analyses for a given experimental run. Charge balance error is based on the concept that the sum of the positive charges should equal the sum of the negative charges in a solution (Freeze and Cherry, 1979). There are two versions of the charge balance equation in use, from which we chose the equation more commonly used in literature (Fritz, 1994).

$$\%CBE = \frac{\sum z * m_c - \sum z * m_a}{\sum z * m_c + \sum z * m_a} * 100\% \qquad (1.1)$$

According to Fritz (1994), a %CBE less than 5% is considered adequate for most applications. With more dilute samples as with these experiments, less than 10% charge balance error is acceptable. All calculated charge balance errors were less than 5%. Since the measurements of nine ions were performed to examine the charge balance error, ion exchange of $Na^+$ for $K^+$, $Mg^{+2}$, and $Ca^{+2}$ could be observed. Ion exchange was slight but measurable in the first few effluent samples for these experiments, but never

exceeded 1 ppm of $K^+$, $Mg^{+2}$, or $Ca^{+2}$. Ion exchange was negligible by steady-state conditions for each run. Steady state concentrations of $Cl^-$ were used to determinate membrane properties (Table 1.1 and 1.2).

In order to study the potential membrane effects of silica passing through pure limestone, a pump was used to deliver a higher pressure than was obtainable by the Marriotte Flask alone. A gravity-fed piston pump similar to that used by Saindon (2004) was used to supply approximately 14 psi of hydraulic pressure to the same experimental cell in Figure 1.2. Deionized water was first placed within the pump to obtain a control reaction of the limestone to pressurized fluid flow and to calculate $L_p$. The deionized water was then replaced with a solution of 120 ppm silicic acid at a pH of 5.2 (90% solubility). The entire experiment took approximately 30 hours to obtain steady-state (Figure 1.12).

Colorimetry analysis was used to determine the concentration of silica. Samples were diluted 10 to 1 in order to obtain concentrations in the working range of the colorimeter. At the end of the experiment the solution in the cell was stirred carefully and decanted into a clean sample bottle. Triplicate analyses were performed on each effluent and cell sample in order to obtain the average silica concentration and pH of effluent samples collected over time (Figure 1.12). Additionally, each diluted effluent and cell sample were passed through the ion chromatograph in the manner as the previous eight experiments. Since the measurements of nine ions were performed to examine the charge balance error, ion exchange of $Na^+$ for $K^+$, $Mg^{+2}$, and $Ca^{+2}$ could be observed. This was performed in order to obtain a charge balance error and to determine if ion exchange was occurring using Equation 1.1. Ion exchange was noticeable in the first

effluent samples but never exceeded 0.5 ppm of $K^{+}$, $Mg^{+2}$, or $Ca^{+2}$ and was negligible by steady-state conditions. The steady-state concentrations of silica are used in determining the membrane coefficients reported in the silica experiment portion of this paper.

At the end of the experiment the limestone disc was removed from the cell and examined via a scanning electron microscope (SEM) in order to determine if precipitation of silica occurred. Amorphous blobs of some substance were found on the surface of the limestone; however, the substance was unidentifiable by the SEM method or any method available at that time.

## 1.5 RESULTS

Tabulated results for the individual experiments can be found in Table 1.1, 1.2, and 1.3. $J_v$, the steady-state volumetric solution flux was calculated by Equation 1.2.

$$J_v = \frac{V}{A \cdot s} \tag{1.2}$$

where V is the volume of effluent aliquot ($cm^3$), A is the area of the membrane ($cm^2$), and s is the total time elapsed during collection of each aliquot (seconds). $J_v$ decreases as the osmotic pressure increases within the cell until a steady-state flux is established. $J_v$ reported in Table 1.1 and 1.2 are the averages of the last three samples taken once steady-state was established. $J_v$ ranged from $4.852 \times 10^{-9}$ to $9.981 \times 10^{-9}$ (m/s) for the limestone and $1.050 \times 10^{-9}$ to $8.720 \times 10^{-9}$ (m/s) for dolomite.

A mass balance approach was used to predict the expected concentration within the cell at the end of the experiment. The total moles input into the cell were calculated based upon stock solution concentrations. This value was then compared to the total moles that were collected during the experiment within the cell. Equation 1.3 yields the calculated accumulation at the end of the experiment ($c_{predicted}$). This value was then

compared to the measured cell concentration within the cell at the end of the experiment (Table 1.1 and 1.2).

$$\sum Moles_{in} - \sum Moles_{out} = Accumulation \quad (1.3)$$

For the dolomite Equation 1.3 predicted accumulations of 718 and 616 ppm $Cl^-$ for the 345 ppm initial concentration experiments and 326 and 334 ppm $Cl^-$ for the 185 ppm initial concentration experiments. For the limestone predicted concentrations were 348 and 688 ppm $Cl^-$ for the 345 pm initial concentration experiments and 322 and 323 ppm $Cl^-$ for the 185 ppm $Cl^-$ initial concentration experiments. Comparison of the predicted ($c_{predicted}$) and measured ($c_{final}$) concentration values resulted in a less than 5% difference for all experiments (Table 1.1 and 1.2).

All experiments resulted in significant increases in chloride concentration within the experimental cell. Final cell concentrations ranged from 331 to 692 ppm $Cl^-$ for the limestone experiments (Table 1.1) and 337 and 725 ppm $Cl^-$ for the dolomite experiments (Table 1.2). Ending cell concentrations of chloride increased within the cell by 79 to 101 % over the input concentration for the limestone experiment (Table 1.1) and 82.2 to 108% over input concentration for the dolomite experiments (Table 1.2). During all experiments, volumetric solution flux ($J_v$) decreased until it reached a steady-state minimum (Figures 1.4 - 1.11). This decrease in $J_v$ is attributed to the buildup of osmotic pressure within the cell (Fritz and Whitworth, 1994).

One measure of membrane efficiency is the reflection coefficient, $\sigma$, a unitless measure of osmotic efficiency (Staverman, 1952). If $\sigma = 1.0$, the membrane is perfect and rejects all dissolved solute. If $\sigma = 0$, there is no solute rejection. For intermediate values, rejection is partial and proportional to the value of $\sigma$. The steady-state reflection

coefficient can be calculated from the experimental data without prior knowledge of the concentration at the membrane interface via Equations 1.4 through 1.6 (Whitworth, 1998).

$$L_P = \frac{J_{v_{DI}}}{\Delta P} \tag{1.4}$$

$$\begin{aligned} c_o = {} & \frac{1}{2L_P vRT(J_v \Delta x - 2vD)} \cdot (-2L_P vRTJ_v c_i \Delta x\zeta - 4L_P v^2 RTDc_i \\ & + \Delta x\zeta J_v L_P \Delta P - \Delta x^{1/2}\zeta^{1/2}(-8\zeta\Delta x c_i J_v{}^3 TRvL_P + 8\zeta\Delta x c_i J_v{}^2 TRvL_P{}^2 \\ & + \zeta\Delta x J_v{}^4 - 2\zeta\Delta x\Delta P L_P J_v{}^3 + \zeta\Delta x\Delta P^2 L_P{}^2 J_v{}^2 - 16J_v{}^2 c_i DTRv^2 L_P{}^2)^{1/2}) \end{aligned} \tag{1.5}$$

$$\sigma = L_P\Delta P - J_v / L_P vRT(c_o - c_i) \tag{1.6}$$

where $L_p$ = water permeation coefficient (m/Pa·s), $J_{v_{DI}}$ = deionized water flux through the membrane (m/s), $\Delta P$ = pressure difference across the membrane (Pa), $c_o$ = concentration at the high-pressure membrane face (M), v is a factor that corrects for the number of particles due to ion formation, R is the gas constant (8.314 N·m/mole), T is the temperature in °K, $J_v$ = experimental solution flux (m/s) through the membrane, $\Delta x$ is membrane thickness (m), D = diffusion coefficient for free solution (1.89 x $10^{-9}$ $m^2/s$), $c_i$ = the input solute concentration (M), and $\zeta$ is the tortuosity and is defined here as the ratio of the actual path length through the membrane to the membrane thickness and was used as 3.5 for all calculations. This value of tortuosity is an average value obtained from experimental results obtained from similar limestone lithologies (Wang et al., 2005).

The values of $\sigma$ calculated from Equation 2.6 for the experiments reported herein ranged between 0.34 to 0.39 for limestone (Table 1.1) and 0.32 to 0.40 for dolomite (Table 1.2). These values indicate that the limestone and dolomite discs exhibited significant membrane properties. Values of $L_p$, calculated from Equation 1.4, ranged

from $1.041 \cdot 10^{-12}$ to $1.37 \cdot 10^{-12}$ (m/Pa·s) for limestone (Table 1.1) and $1.621 \cdot 10^{-13}$ to $8.901 \cdot 10^{-13}$ (m/Pa·s) for dolomite (Table 1.2). The steady-state values of maximum concentrations in the cells, located at the membrane face ($c_o$), were calculated from Equation 1.5 to be between 190 and 361 ppm $Cl^-$ for limestone (Table 1.1) and 192 to 361 ppm $Cl^-$ for dolomite (Table 1.2).

The average time to reach steady-state for all eight chloride experiments was approximately 110 days. Additionally, the silica experiment took approximately 30 hours to reach steady-state and achieved a reflection coefficient of 0.33. All experiments demonstrated membrane properties and achieved moderate efficiencies, similar to the reflection coefficients of approximately 0.33 found in kaolinites tested in previous experiments (Hart and Whitworth, 2005; Derrington et al., 2006).

## 1.6 DISCUSSION

The main purpose of this study was to experimentally determine if dolomite and limestone can behave as semi-permeable geologic membranes under relatively low head conditions using a conservative solute. Each experiment ended with significant concentration of sodium chloride within the cell above input concentrations (79-108% increase; Tables 1.1 and 1.2). Total solution flux decreased significantly during all eight experiments. The concentration increase in the cells is attributed to membrane ion rejection and the flux decrease is attributed to the build-up of osmotic pressure within the experimental cell (Fritz and Whitworth, 1994). Calculated osmotic efficiencies ranged between 0.32 and 0.40. The results of this study indicate that at least some limestones and dolomites can act as membranes under applied heads. Dolomite and limestone bounded aquifers which might exhibit membrane behavior include perched aquifers and

artesian aquifers in which a downward component of groundwater flow exists. In these cases the limestone and dolomites may act to naturally concentrate some solutes adjacent to the high-pressure membrane face in a concentration polarization layer or CPL.

One method of determining whether a particular facies is functioning as a membrane would be through geochemical sampling adjacent to the high-pressure face of the potential membrane within the CPL. Geochemical sampling of a water well screened within the interval of the CPL could result in anomalously high readings of some ions (Fritz and Whitworth, 1994). Multi-level water sampling and chemical analysis across an aquifer thickness would be required to determine if a CPL is present. Otherwise, anomalous chemical analyses, especially for chloride or some metals, might be misinterpreted as a contaminant plume as opposed to a naturally occurring process and unnecessary remediation undertaken. A recent geochemical study of the regional Ogalala aquifer found through multi-layer sampling solute concentrations did indeed increase with proximity to a clay bounding layer (Schulmeister et al., 2004). This evidence is strongly suggestive of the presence of a CPL in the Ogalala aquifer.

Perched aquifers bounded by a membrane-functioning aquitard may be affected by hyperfiltration as well as regional artesian aquifers (Hart et al., 2005). While lower hydrostatic heads are often found in perched aquifers, and these heads are dependant upon seasonal precipitation and infiltration, modeling has shown that a concentration polarization layer may be vertically more extensive at lower heads (Whitworth et al., 2002). Perched aquifers are subject to other seasonal functions such as influent concentrations of solutes and types of solute flux which may affect the ability of the membrane to concentrate ions by changing the hydraulic or chemical gradients. If the

hydraulic gradient is not in excess of osmotic pressure year-round seasonal fluctuations in the CPL can occur in shallow systems such as perched aquifers. Seasonal increases of water in shallow systems such as during the spring and fall, would likely coincide with hyperfiltration; while hyperfiltration might not occur when water input and hydraulic pressure are lower. As these seasons also correspond to the highest overland flow times, the total dissolved load will also commensurately increase. Increasing the total dissolved load would potentially increase the geochemical gradient within shallow aquifers. Because precipitation is often variable throughout the year, membrane processes at shallow depths may never reach equilibrium. Aquifer chemistry studies sampled on a quarterly basis often average the results over a year. Perhaps a better method would be to examine the data seasonally, in addition to annually, in order to detect possible seasonal CPL formation.

When hydraulic head in a fractured system exceeds osmotic pressure ($\sigma\Delta\pi$) , especially in crystalline aquifers such as the Jefferson Dolomite and Burlington Limestone, flow is not only along the fracture, but outwards into the rock matrix. As solutes contained within these fractures are driven outwards through the matrix, the limestone or dolomite may act as a membrane and retard solute flow into the rock matrix, resulting in a solute concentration increase in the fracture. Both the Burlington Limestone and Jefferson Dolomite act as aquifers for the Ozark region of Missouri and the majority of groundwater movement is via fracture flow (Overstreet, 1989).

Flow through a fracture is obviously not unidirectional. The termination of the fracture into the rock matrix functions as a flow focusing point (White and White, 2005) (Figure 1.14). The matrix rock boundary of a fracture termination might function as a

static hyperfiltration membrane in which CPL formation may occur. The flow-focusing concept for hyperfiltration was first presented by Lueth and Whitworth (2001) who suggested that a flow-focusing point may be partially responsible for the location of copper deposits in the Pastura District of New Mexico.

In each of the mines examined by Lueth and Whitworth (2001), mineralization was most pronounced at the sand/shale interface and decreased in intensity with distance from the contact. Lueth and Whitworth (2001) hypothesized that hyperfiltration concentrated the copper and nutrients for sulfate reducing bacteria, which then produced $H_2S$ resulting in precipitation of the sulfide ore minerals.

Fothergill (1955) found that zones of calcite cementation commonly occur in sandstones immediately adjacent to bounding shales. He attributed the formation of these calcite layers to hyperfiltration.

Laier and Nielson (1989) additionally suggested that halite cementation in the Triassic Bunter Sandstone might be the result of hyperfiltration through underlying shale. Calcite precipitation has been experimentally shown to occur as a result of hyperfiltration of a calcium solution through a clay membrane (Fritz and Eady, 1985). Heavy metals have also been precipitated by hyperfiltrating undersaturated solutions through clay layers (Whitworth and DeRosa, 1997).

Since hyperfiltration may influence solute concentration distributions in some membrane-bounded aquifers or in some fractured limestones and/or dolomites, hyperfiltration may have an effect on localization of mineral precipitation and/or other diagenetic processes (Becker, 1892; Mackay, 1946; Lueth and Whitworth, 2001). The possibility of cementation via natural hyperfiltration has been examined experimentally

in disaggregated clays, shales, and even pulverized quartz used to simulate fault gouge (Fritz and Eady, 1985, Whitworth and DeRosa, 1997, Whitworth et al., 1999).

Deposition of silica and other residues is common along joints or fractures and is noticeable along outcrops of the Burlington Limestone (Thompson, 1995). Cementation in the Burlington Limestone, especially along fracture flow, is mainly chert or varieties of silica. Natural groundwaters contain silica levels in the range of 20 to 60 mg/L with those of the California Central Valley being the most well known in the United States (USGS, 1970; Jenkins and Snoeyink 1980). Higher values of silica are found in well waters in New Mexico and throughout the American Southwest (USGS, 1970). The average well water concentration in the United States is somewhere in the range of 50 to 100 mg/L (USGS, 1970). Well waters contain silica from dissolved silica-containing rocks and for the most part this is a reactive form of silica (USGS, 1970). On the other hand, surface waters will contain a colloidal form of silica as well as a reactive form of silica (USGS, 1970).

One experiment was performed in order to determine the ability of limestone to concentrate silica via hyperfiltration to create a saturated silica solution. In our experiment silica concentrations within the cell had increased by 113% over background, from 120 to 256 ppm. Additionally, during the experiment the pH of the effluent concentration rose from input of 5.2 to final cell pH of 7.2. A reflection coefficient of 0.33 was calculated for the silica using Eqns. 1.4 - 1.6 and a tortuosity factor of 3.5.

While we were unable to identify the amorphous material present on the membrane at the end of the experiment using the SEM, consider that at a pH of 7.2, the ending pH in the experimental cell, the solubility constant of amorphous silica is

approximately $2X10^{-3}$ at 25 °C (Drever, 1997; Iller, 1979; Lerman and Scheerer, 1988). For a pH of 7.2, the solubility of silica is only 120 ppm at 25°C (77°F). The average cell concentration at the end of the experiment was then supersaturated at 256 ppm and precipitation of amorphous silica could potentially have occurred.

The capability of limestone to concentrate silica to a supersaturated state under hyperfiltration suggests that some silica cementation of limestone may be due to hyperfiltration. For silica cementation to occur in limestone or dolomite during hyperfiltration three conditions must be met: First, the rock matrix must be membrane-functioning. Second, a hydraulic head in excess of the osmotic pressure ($\sigma\Delta\pi$) must be available. And third, dissolved silica must be present, suggesting a nearby silica source. In Missouri, the St. Francois Mountains are mainly composed of granitic rocks and the decomposition of feldspars could serve as a likely source of dissolved silica (Thompson, 1995). Regional silica concentrations in Missouri well waters are 50 ppm (Thompson, 1995).

As an example, using a regional silica concentration of 50 ppm, a hydraulic applied head 14 psi, and a reflection coefficient of 0.33, the concentration of silica adjacent to a limestone membrane face is calculated by Eqn. 1.5 to be 125 ppm. Thus the regional input concentration of silica would be sufficient to form a supersaturated solution of silica under hydraulic heads of about 3.2 feet. If a shallow, fractured, non-membrane functioning limestone aquifer with sufficient hydraulic head is bounded by a less fractured, low permeability limestone, membrane effects might be sufficient to cause precipitation of silica at the interface between the two limestones. Cementation of the less crystallized limestone could then occur along the interface and throughout the

fractures as concentrations reach supersaturation as the CPL grows in both extent and concentrations. This scenario might explain the increased concentration of silica reported within the lower Burlington Limestone. At very least our dissolved silica experiment demonstrates the ability of some limestone to act as a membrane and suggests it should be possible under some conditions to concentrate dissolved silica from below saturation to supersaturation.

## 1.7 CONCLUSIONS

Sodium chloride solutions of 185 and 345 ppm $Cl^-$ were passed through thin, intact discs of Burlington Limestone and Jefferson City Dolomite at heads of 0.5 and 1.0 m. These are the first experiments in which intact cores of limestone and dolomite were tested for hyperfiltration effects. Calculated hyperfiltration reflection coefficients (osmotic efficiencies) ranged from 0.34 to 0.39 for the Burlington Limestone and 0.32 to 0.40 for the Jefferson City Dolomite. During the hyperfiltration experiments, chloride was concentrated within the cell over the background concentrations by 79 to 101% for the Burlington Limestone and 82 to 108% for the Jefferson City Dolomite.

Additionally, a 120 ppm dissolved silica solution was passed through the Burlington Limestone at a head of 14 psi. Concentrations of silica within the cell were 256 ppm at steady-state; 113% higher than the original input solution. A reflection coefficient of 0.33 was calculated. This value is comparable to those achieved when passing chloride through limestone. This experiment is the first geologic membrane experiment performed using dissolved silica and the first to describe the membrane behavior of limestone with respect to dissolved silica.

These experiments have shown that Jefferson City Dolomite and Burlington Limestone are capable of hyperfiltration effects at relatively low heads such as might be found in shallow aquifers. Consequently, membrane effects may be more significant in intact rocks and at shallower depths than previously thought. Fracture flow in limestones and dolomites may be accompanied by hyperfiltration-induced solute concentration which may cause precipitation of calcite and silica as fracture-filling veins. Additional work is needed to determine hydraulic and geochemical conditions prevalent in natural scenarios and relate these conditions to hyperfiltration. The results of our experiments suggest there may be a need to study membrane effects in a broad spectrum of subsurface groundwater processes.

## 1.8 REFERENCES


Barone, F. S.; Rowe, R. K.; and Quigley, R. M. (1990) Laboratory determination of chloride diffusion coefficient in intact shale: *Canadian Geotechnical Journal* **27**:177-184.

Becker G. F. (1892) Quicksilver ore deposits, in Day, D. D., Mineral Resources of the United States for 1892, *U.S. Geol. Survey Report*: 139-168.

Derrington D, Hart, M. and Whitworth T. (2006) Low Head Sodium Phosphate and Nitrate Hyperfiltration through thin Kaolinite and Smectite Layers – Application to Engineered Systems, *Applied Clay Science* **33**(1):52-58.

Drever, J.L. (1997) *The geochemistry of natural waters: surface and groundwater environments*. Prentice-Hall Inc., New Jersey: 197-199.

Fothergill, C.A., (1955) The cementation of oil reservoir sands and its origin, *Proc. 4th World Pet. Cong* **4**: 302-314.

Freeze, R. A. and Cherry, J. A., (1988) Groundwater, Prentice-Hall, Englewood Cliffs, N. J., : 604

Fritz S. J. and Eady C. D. (1985) Hyperfiltration-induced precipitation of calcite, *Geochim. Cosmochim. Acta* **49**: 761-768.

Fritz S. J. and Whitworth T. M. (1994) Hyperfiltration-induced fractionation of lithium isotopes: ramifications relating to representativeness of aquifer sampling. *Water Resources Research* **30**: 225-235.

Fritz, S. J., 1986, Ideality of clay membranes in osmotic processes: a review, *Clays and Clay Minerals* **34**: 214-223.

Graf, D.L., (1982) Chemical osmosis, reverse osmosis, and the origin of subsurface brines, *Geochimica et Cosmochimica Acta*. **46**: 1431-1448.

Hart, M. and Whitworth, T. M. (2006) Hyperfiltration of Potassium Nitrate through Clay Membranes under Relatively Low-Head Conditions, *Geochimica Cosmochimica et Acta* **69** (20): 4817-4823.

Iller, R.K. (1979) *The Chemistry of Silica,* John Wiley and Sons, New York, N.Y.

Jenkins, D.; Snoeyink, V.L. (1980) *Water Chemistry,* John Wiley and Sons, New York, N.Y.

Kharaka, Y. K., Berry, F.A.F., (1973) Simultaneous flow of water and solutes through geologic membranes, I. Experimental investigation. *Geochim. Cosmochim. Acta* **37:** 2577-2603.

Laier, T., Nielson, B. L., (1989) Cementing halite in Triassic Bunter Sandstone as a result of hyperfiltration of brines. *Chemical Geology* **76**: 353-363.

Lerman, S.I.; Scheerer, C.C. (1988) The Chemical Behavior of Silica. *ULTRAPURE WATER* **5**(9): 24-30.

Lueth V.W. and Whitworth T. M. (2001) *A Geologic Membrane-Microbial Metabolism Mechanism for the Origin of the Sedimentary Copper Deposits in the Pastura District, Guadalupe County, New Mexico*. New Mexico Geological Society, 52nd Field Conference Guidebook.

Mackay R. A. (1946) The control of impounding structures on ore deposition, *Economic Geology* **61**: 13-46.

McKelvey, J. G. and Milne, I. H. (1960) The flow of salt solutions through compacted clay, *Clays and Clay Minerals* **9**: 248-259.

Milne, I. H., McKelvey, J. G., and Trump, R. P. (1963) Permeability and salt-filtering properties of compacted clay, Clays and Clay Minerals, Monograph No. 13, The MacMillan Company, New York, 250-251.

Orndorff, R.C., Weary, D.J., and Harrison, R.W., (2003) The role of sandstone in the development of an Ozark karst system, southeastern Missouri - *Geological Society of America Abstracts with Programs* **35**(6): 19-5.

Orndorff, R.C., Weary, D.J., and Šebela, S. (2002) Geologic framework of the Ozarks of south-central Missouri; contributions to a conceptual model of karst - Missouri *Speleology*, **42** (1-2):1-8.

Porter, M.C., (1979) Membrane filtration, in *Handbook of Separation Techniques for Chemical Engineers*, edited by P.A. Schweitzer, McGraw-Hill, New York.

Saindon R.M. and Whitworth T.M., (2005) Hyperfiltration of Nacl Solutions Using a Simulated Clay/Sand Mixture at Low Compaction Pressures. *Aquatic Geochemistry*, 11(4): 433-444.

Staverman A. J. (1952) Non-equilibrium thermodynamics of membrane processes. *Trans. Faraday Soc*. **48**, 176-185.

Thompson, T.L. (1995) The stratigraphic succession in Missouri: Missouri Department of Natural Resources, Division of Geology and Land Survey, **40**, 2d ser.: 189.

U.S. Geological Survey (1970) "Study and Interpretation of the Chemical Characteristics of Natural Water," Supply Paper 1473, U.S. Government Printing Office, Washington, D.C.

Wang R., Pavlin T., Rosen T. M. S. , Mair R.W., Cory D.G., Walsworth R.L. (2005) Xenon NMR measurements of permeability and tortuosity in reservoir rocks. *Magnetic Resonance Imaging* **23**: 329–331

White W.B. and White E.L. (2005) Ground water flux distribution between matrix, fractures, and conduits: constraints on modeling / Speleogenesis and Evolution of Karst Aquifers 3 (2), www.speleogenesis.info:1-6.

Whitworth T. M. (1998) Steady-State Mathematical Modeling of Geological Membrane Effects in Aquifer Systems, presented at *Joint Conference on the Environment*: 37-40.

Whitworth T. M. and DeRosa G. (1997) Geologic Membrane Controls on Saturated Zone Heavy Metal Transport. *New Mexico Water Resources Research Institute Report No. 303*, Las Cruces, New Mexico: 88.

Whitworth T. M., Haneberg W. C., Mozley P. S. and Goodwin L. B. (1999) Solute Sieving on Pulverized Quartz Sand—Experimental Results and Implications for the Membrane Behavior of Fault Gouge, presented at Special Penrose Conference, *American Geophysical Union Monography Series* **113**, 149-158.

Young A. and P.F. Low (1965) Osmosis in argillaceous rocks. *American Assoc. of Pet. Geol. Bull.* **46**:1004-1008.

Table 1.1: Experimental Parameters and Calculated Results.

| **Parameter** | **Experiment** | | | |
|---|---|---|---|---|
| | **Limestone 1** | **Limestone 2** | **Limestone 3** | **Limestone 4** |
| Head (m) | 1.00 | 0.5 | 1.0 | 0.5 |
| Membrane Thickness (mm) | 3.10 | 3.05 | 3.01 | 3.02 |
| Membrane Area ($m^2$) | 0.0015 | 0.0015 | 0.0015 | 0.0015 |
| Solution Flux, $J_v$ (m/s) | $9.950 \times 10^{-9}$ | $5.955 \times 10^{-9}$ | $9.981 \times 10^{-9}$ | $4.852 \times 10^{-9}$ |
| Analytical Chemical Precision at Two Standard Deviations (%) | ±2.27 | ±2.05 | ±2.19 | ±2.32 |
| Initial Conc., $c_i$, ppm $Cl^-$ | 345 | 345 | 185 | 185 |
| Final Conc., $c_{final}$, ppm $Cl^-$ | 692 | 656 | 331 | 336 |
| Predicted Conc., $c_{predicted}$, ppm $Cl^-$ | 688 | 648 | 323 | 322 |
| Change in Cell Conc. (%) | 101 | 90.1 | 79.0 | 81.6 |
| $L_p$, Permeation Coefficient (m/Pa·s) | $1.105 \times 10^{-12}$ | $1.37 \times 10^{-12}$ | $1.072 \times 10^{-12}$ | $1.041 \times 10^{-12}$ |
| Calculated Steady-State, $c_o$ | 361 | 356 | 196 | 190 |
| Calculated Steady-State σ | 0.34 | 0.37 | 0.39 | 0.37 |
| Charge Balance Error | -1.25 | 2.30 | -1.94 | 0.45 |

Note: Measurements recorded at 21 °C.

Table 1.2: Experimental Parameters and Calculated Results.

| **Parameter** | **Experiment** | | | |
|---|---|---|---|---|
| | **Dolomite 1** | **Dolomite 2** | **Dolomite 3** | **Dolomite 4** |
| Head (m) | 1.00 | 0.50 | 1.00 | 0.50 |
| Membrane Thickness (mm) | 3.75 | 3.50 | 3.67 | 3.72 |
| Membrane Area ($m^2$) | 0.0015 | 0.0015 | 0.0015 | 0.0015 |
| Solution Flux, $J_v$ (m/s) | $8.720 \times 10^{-9}$ | $6.71 \times 10^{-9}$ | $1.05 \times 10^{-9}$ | $6.05 \times 10^{-9}$ |
| Analytical Chemical Precision at Two Standard Deviations (%) | ±2.51 | ±2.07 | ±2.19 | ±2.86 |
| Initial Conc., $c_i$, ppm $Cl^-$ | 345 | 345 | 185 | 185 |
| Final Conc., $c_{final}$, ppm $Cl^-$ | 725 | 636 | 337 | 345 |
| Predicted Conc., $c_{predicted}$, ppm $Cl^-$ | 718 | 616 | 326 | 334 |
| Change in Cell Conc. (%) | 108 | 84.3 | 82.2 | 86.5 |
| $L_p$, Pearmeation Coefficient (m/Pa·s) | $8.901 \times 10^{-14}$ | $1.621 \times 10^{-13}$ | $2.959 \times 10^{-13}$ | $1.825 \times 10^{-13}$ |
| Calculated Steady-State, $c_o$ | 361 | 356 | 192 | 192 |
| Calculated Steady-State $\sigma$ | 0.32 | 0.34 | 0.36 | 0.40 |
| Charge Balance Error | -0.32 | 0.02 | 2.25 | 0.17 |

Note: Measurements recorded at 21 °C.

Table 1.3: Experimental Parameters and Calculated Results.

| **Parameter** | **Experiment** |
|---|---|
| | **Silica Experiment** |
| Head (m) | 9.843 |
| Membrane Thickness (mm) | 3.45 |
| Membrane Area ($m^2$) | 0.001496 |
| Solution Flux, $J_v$ (m/s) | $1.4978 \times 10^{-5}$ |
| Analytical Chemical Precision at Two Standard Deviations (%) | ±2.51 |
| Initial Conc., $c_i$, ppm | 120 |
| Final Conc., $c_{final}$, ppm | 256 |
| Predicted Conc., $c_{predicted}$, ppm $Cl^-$ | 261 |
| Change in Cell Conc. (%) | 113 |
| $L_p$, Permeation Coefficient (m/Pa·s) | $4.509 \times 10^{-10}$ |
| Calculated Steady-State, $c_o$ | 389 |
| Calculated Steady-State σ | 0.33 |
| Charge Balance Error | -0.04 |

Note: Measurements recorded at 21 °C.

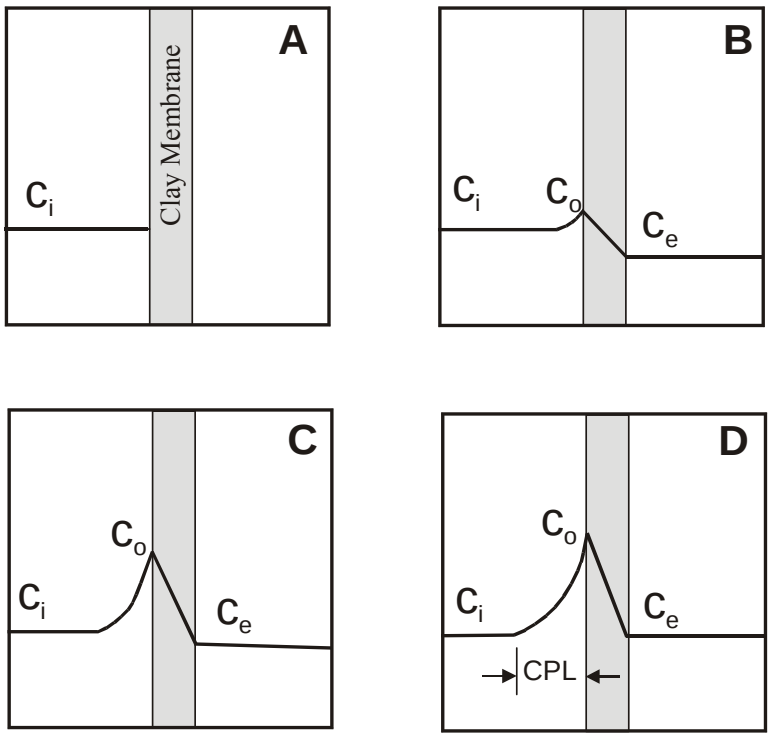


*Figure 1.1. Conceptual CPL development.* This assumes that the solute is conservative and no ion exchange is occurring. Initially, (A) the solute is all on the high-pressure side of the membrane and no solute is contained within the pore fluids within the membrane. After flux commences, (B) the concentration at the high-pressure membrane face $c_o$ increases due to solute rejection. Effluent samples contain some solute now. (C) $C_o$ has increased further as has the effluent concentration $c_e$. At steady-state (D) the input concentration $c_i$ is now equal to the output $c_e$ and the value of $c_o$ is constant. (Redrawn from Fritz and Marine, 1983).

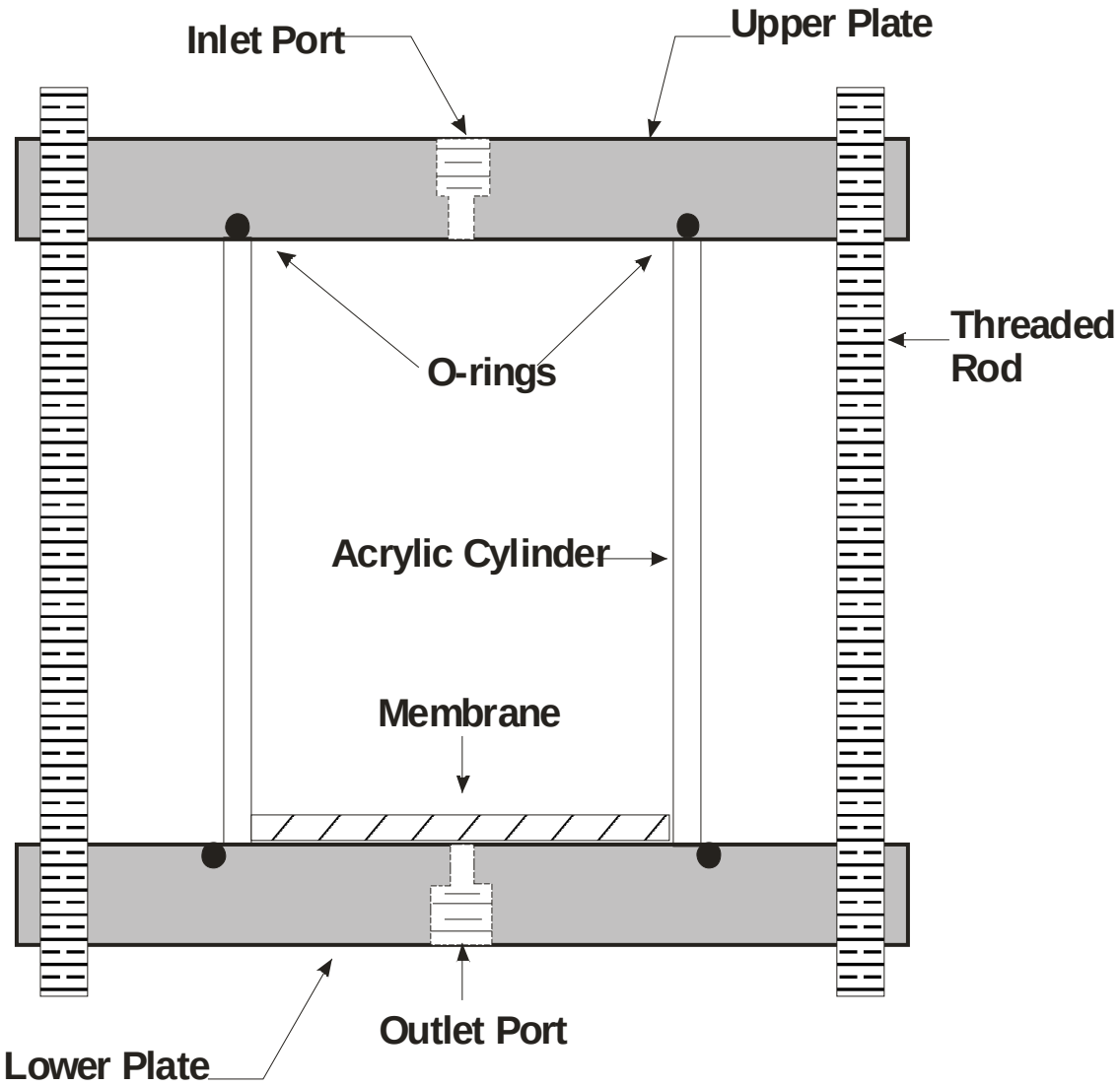


*Figure 1.2: Experimental Apparatus Schematic*

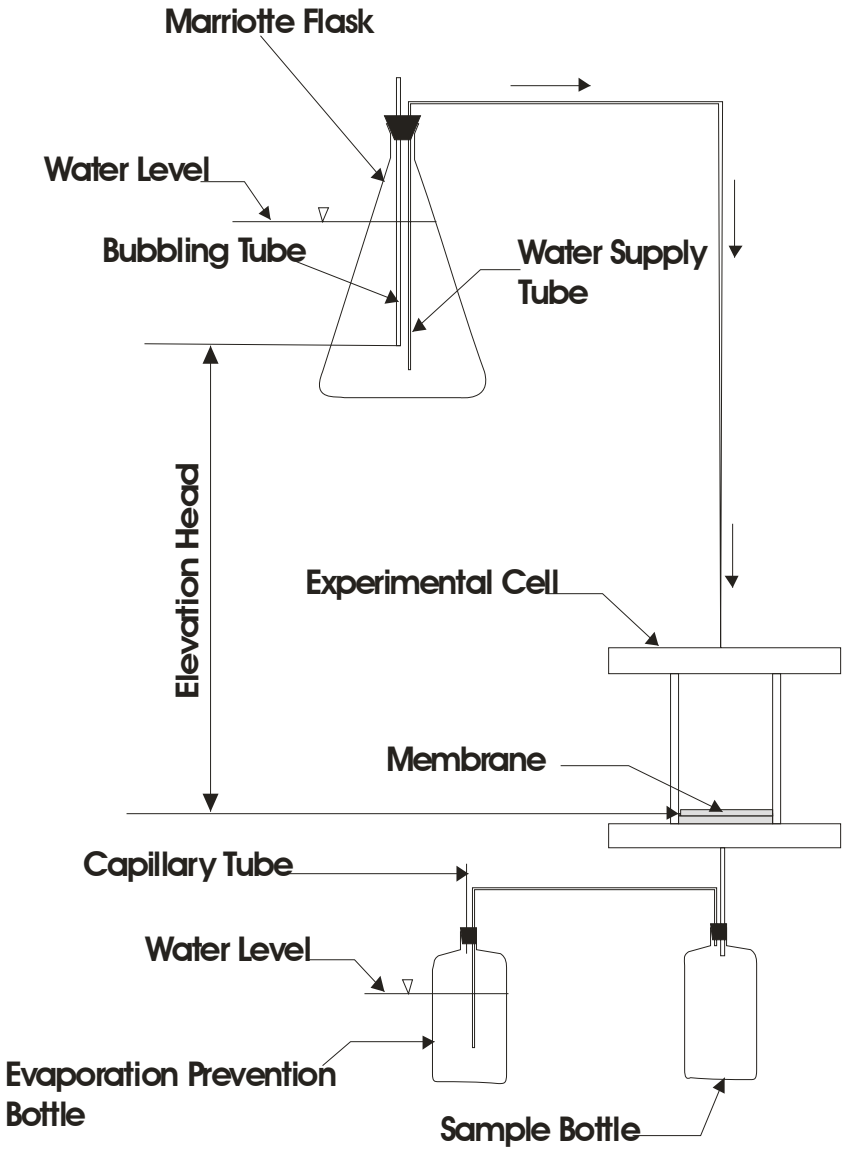


*Figure 1.3: Experimental Testing Schematic*

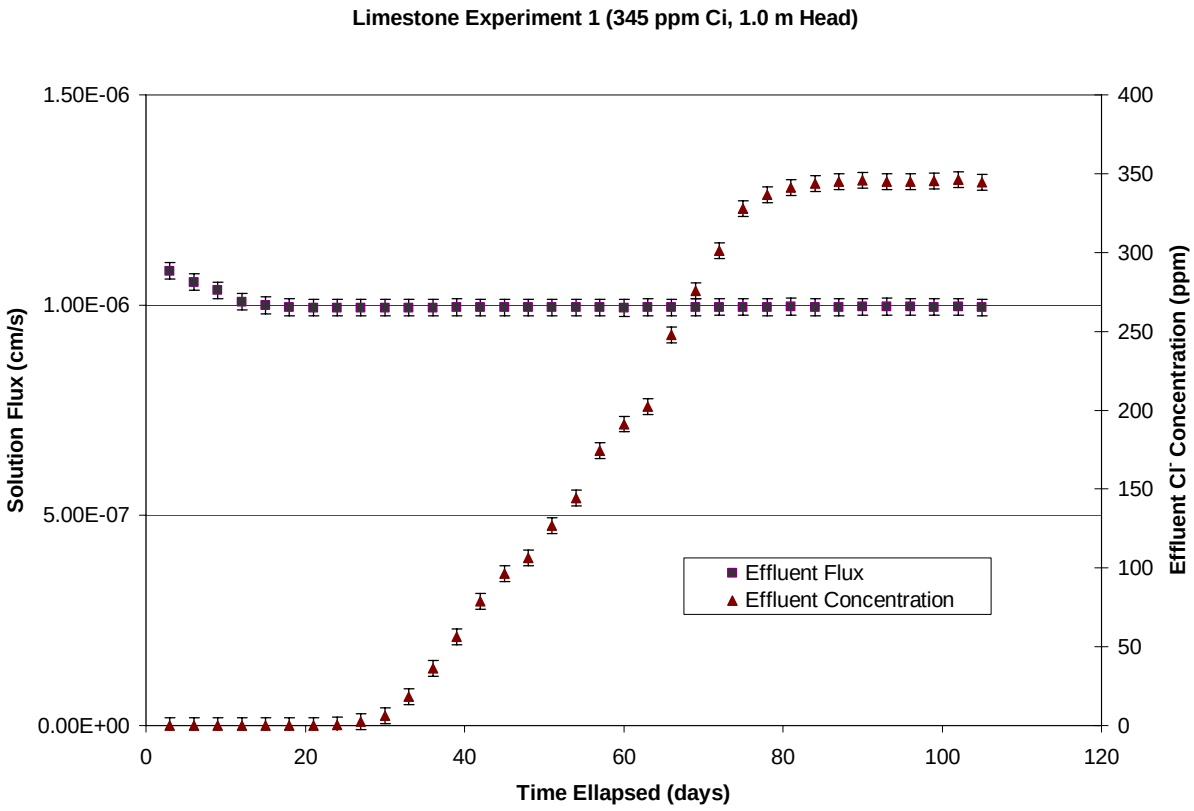


*Figure 1.4: Effluent Concentration and Flux versus Time for Limestone Experiment 1.*

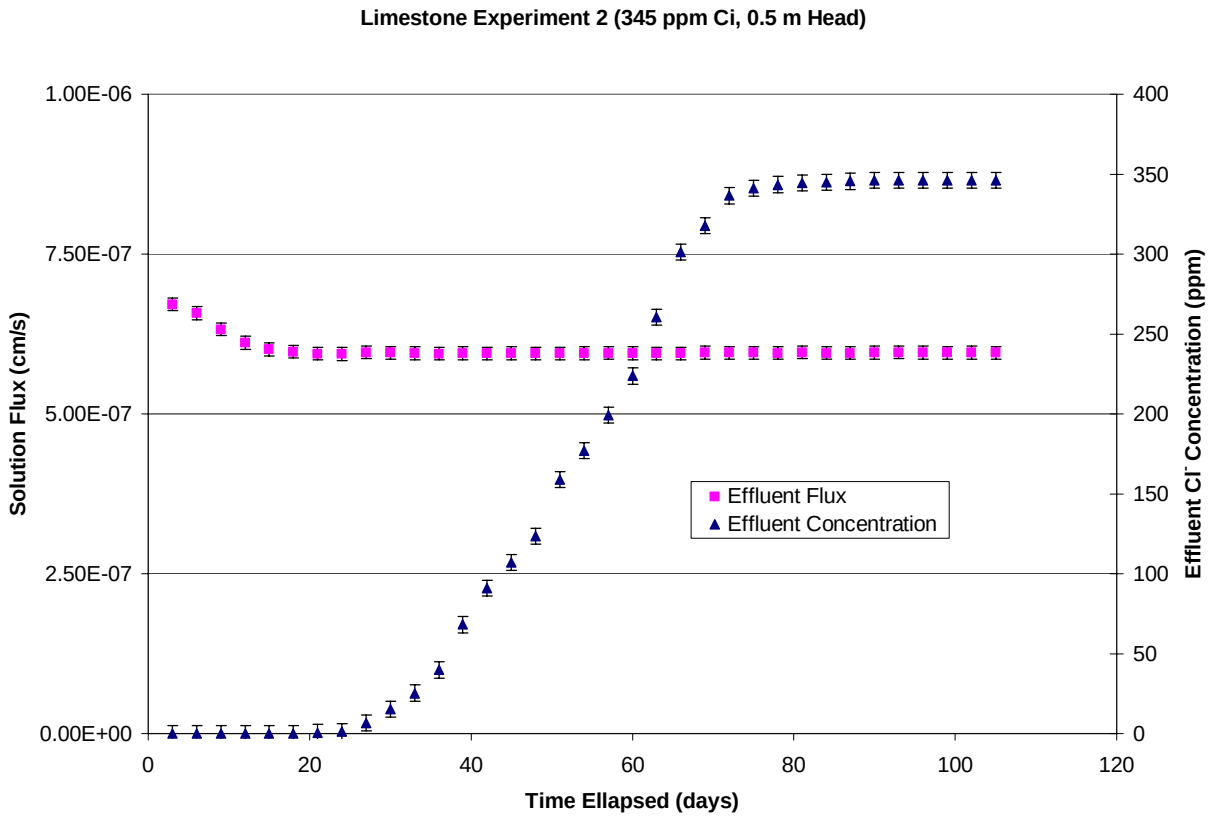


*Figure 1.5: Effluent Concentration and Flux versus Time for Limestone Experiment 2.*

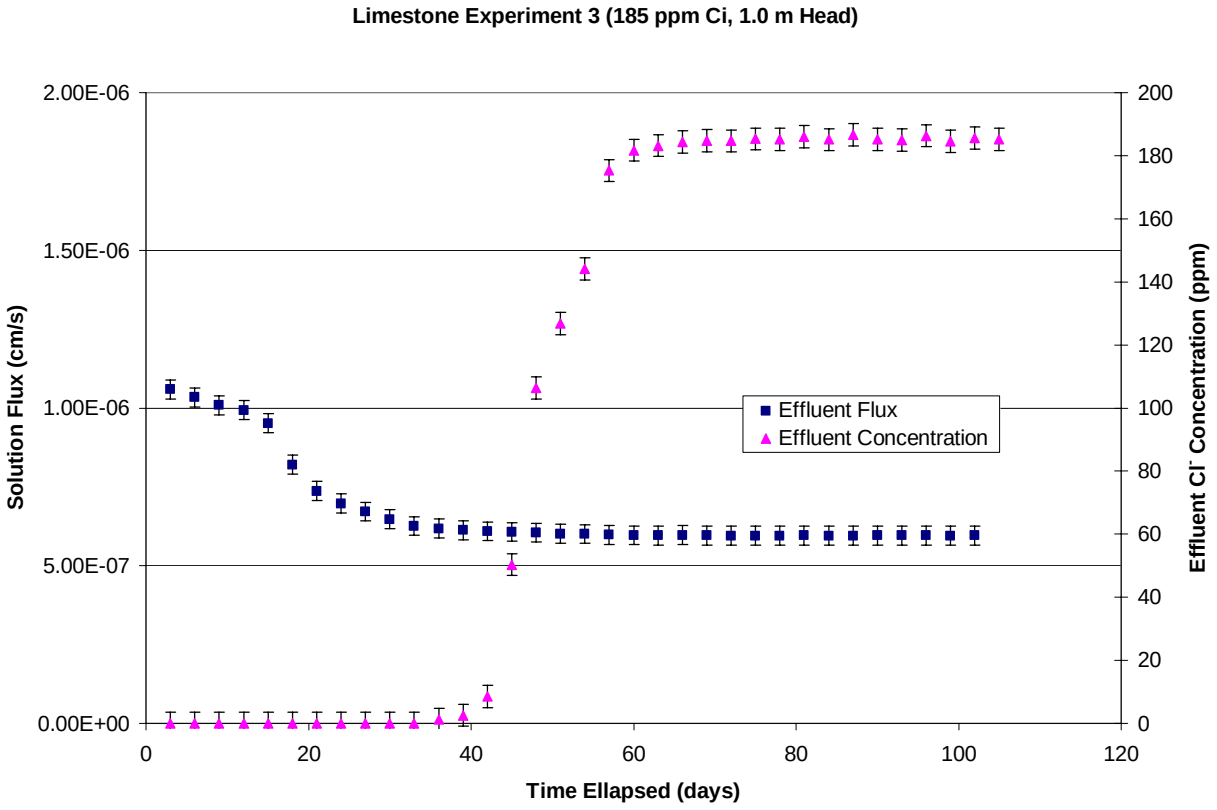


*Figure 1.6: Effluent Concentration and Flux versus Time for Limestone Experiment 3.*

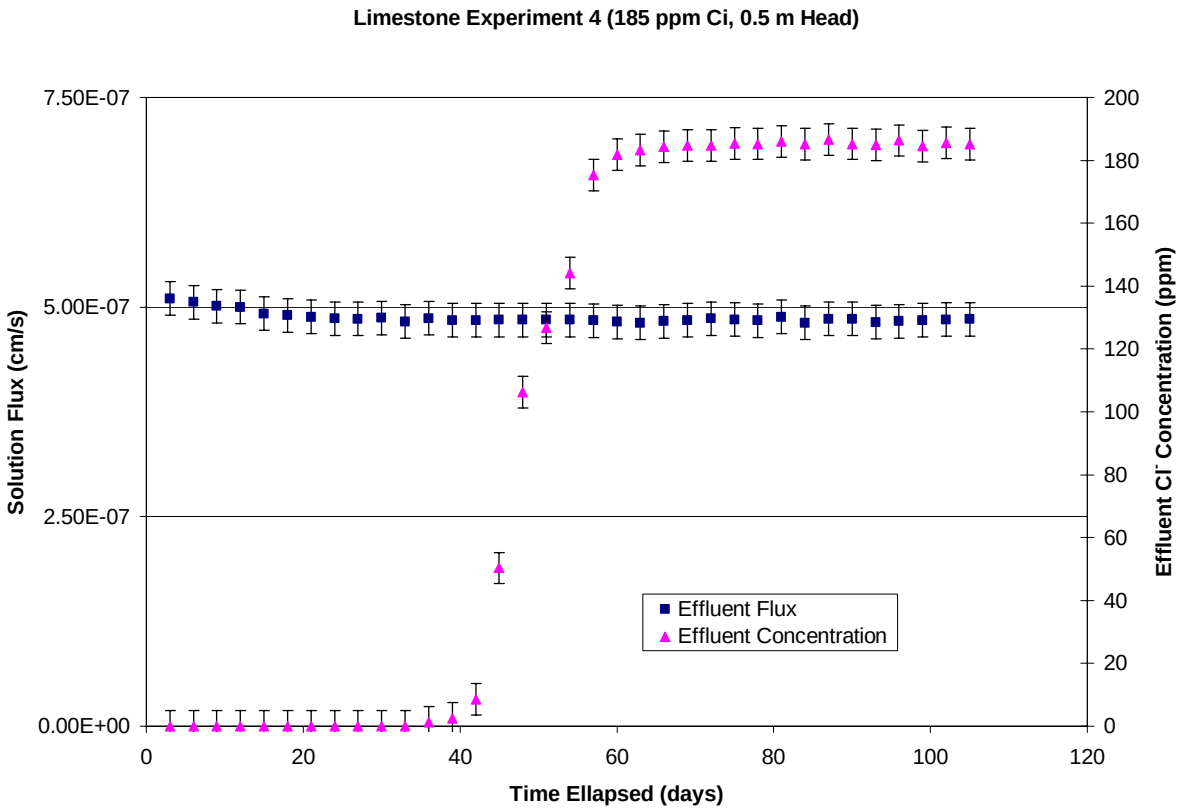


*Figure 1.7: Effluent Concentration and Flux versus Time for Limestone Experiment 4.*

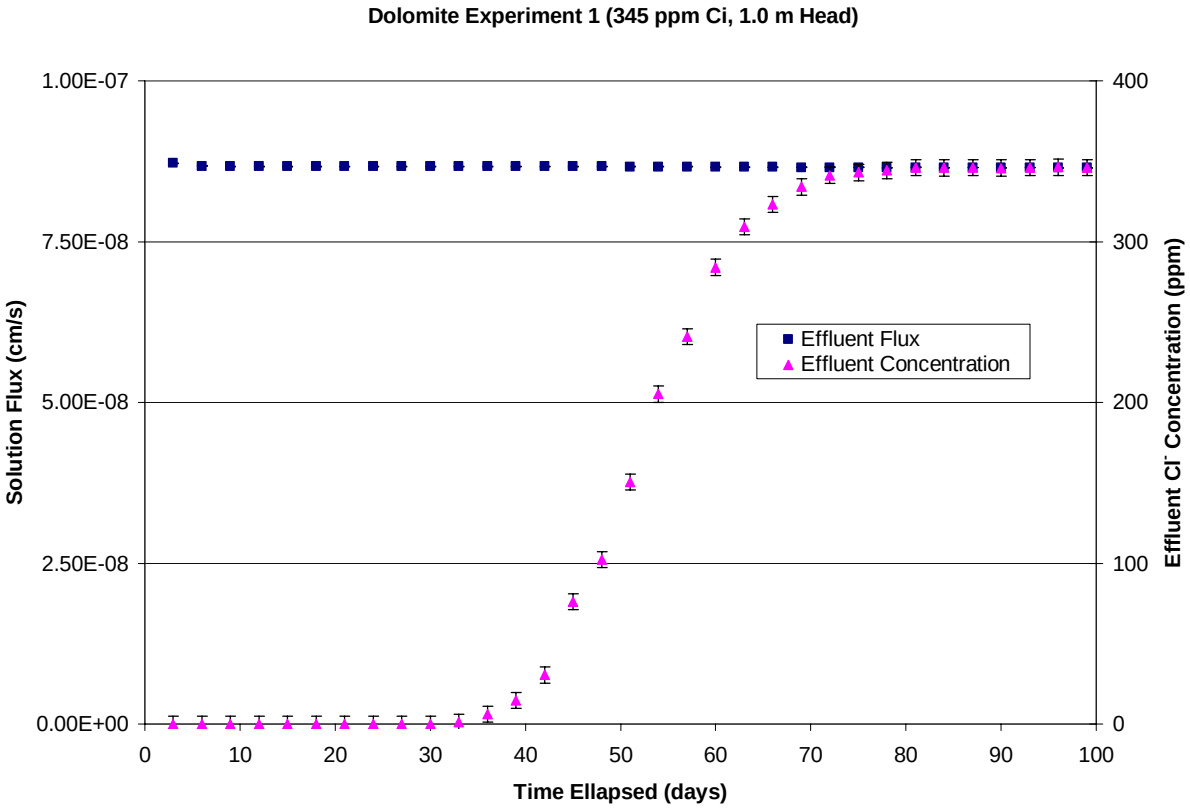


*Figure 1.8: Effluent Concentration and Flux versus Time for Dolomite Experiment 1.*

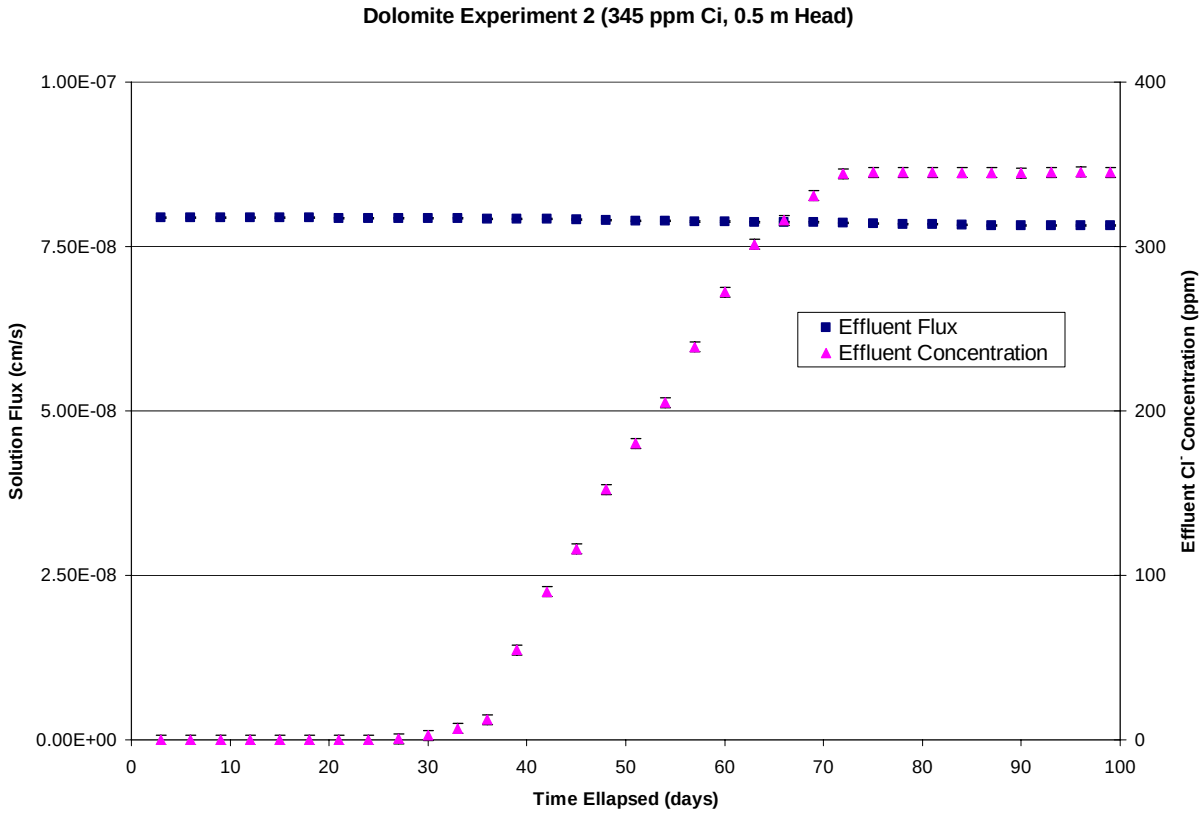


*Figure 1.9: Effluent Concentration and Flux versus Time for Dolomite Experiment 2.*

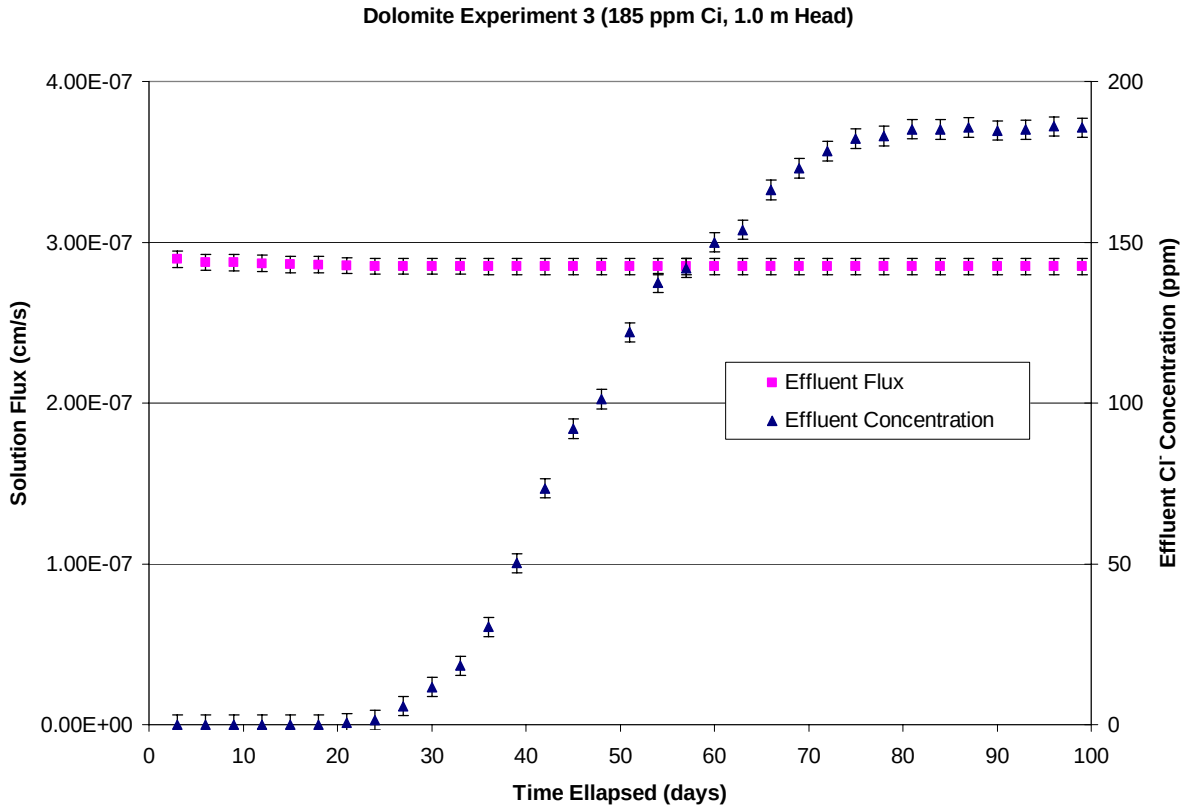


*Figure 1.10: Effluent Concentration and Flux versus Time for Dolomite Experiment 3.*

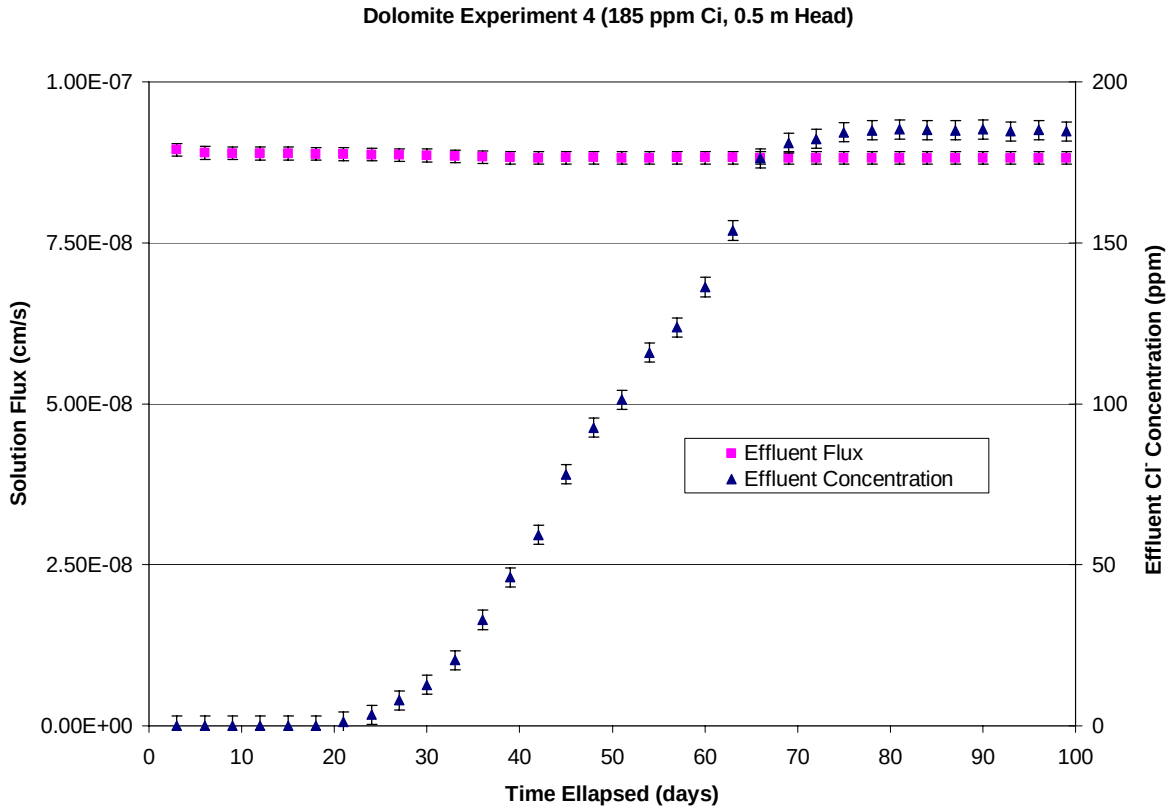


*Figure 1.11: Effluent Concentration and Flux versus Time for Dolomite Experiment 4.*

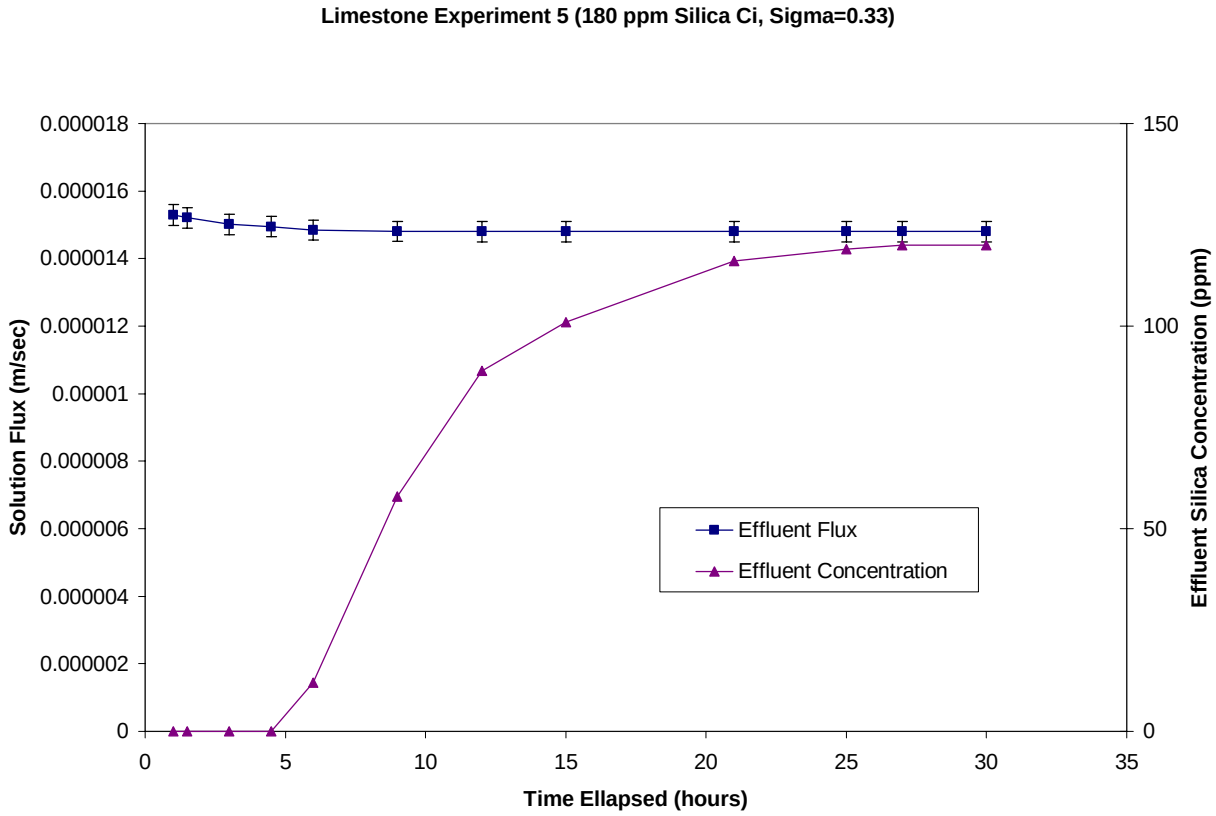


*Figure 1.12: Effluent Concentration and Flux versus Time for Silica Experiment with Limestone.*

# PAPER 2. MEMBRANE PROPERTIES OF LOW PERMEABILITY CONCRETE

## 2.1 ABSTRACT

Hyperfiltration is the ability of a membrane to retard the passage of one solute under a hydraulic head in excess of osmotic pressure. Shales, mudstones, clays, and tuff have been shown to exhibit hyperfiltration-induced membrane effects in past experiments. However, low permeability concrete has not previously been tested. Therefore, we performed four hyperfiltration experiments on intact low permeability concrete discs to assess the potential for membrane properties. Four experiments were conducted solutions of 185 and 345 ppm at heads of 0.5 and 1.0 m. Concentration increases within the cell were between 126% and 152% above input concentrations. Calculated values of the reflection coefficient ranged from 0.15 and 0.19, suggesting that these thin, low permeability concrete discs exhibited significant membrane effects. The results of these experiments suggest that membrane properties under some conditions membrane-functioning concrete may contribute to deterioration of steel reinforcements within concrete structures by increasing the salt ($Cl^-$) concentration gradient in the pores of the low permeability concrete significantly above background solute concentrations. Additional experiments should be conducted to determine the significance of deterioration of steel reinforcements related to hyperfiltration effects.

## 2.2 INTRODUCTION

Many low permeability geologic lithologies have been shown to function as membranes, including shale, clay, and tuff (McKelvey and Milne, 1960; Young and Low, 1965; Kharaka and Berry, 1973; Barone et al., 1992; Whitworth and DeRosa, 1997).

Four samples of low permeability concrete were tested to determine if it is capable of functioning as a membrane. Membrane processes include osmosis and hyperfiltration . Hyperfiltration was examined in this study as it appears the most pertinent to concrete structures. For further information on osmosis in low permeability lithologies and on the basic mathematics describing membrane processes, both osmosis and hyperfiltration, please see Fritz (1986).

Hyperfiltration, often called solute-sieving, occurs when a solute is partially rejected from a solution passing through a membrane (Graf, 1982). When hydraulic head in excess of osmotic pressure exists across a membrane, hyperfiltration can occur. The rejected solute concentrates adjacent to the higher pressure face of the membrane, forming a zone of increased concentration called a concentration polarization layer, or CPL (Fritz, 1986) (Figure 2.1). The maximum solute concentration ($C_o$) is immediately adjacent to the higher pressure membrane. As solute concentrates on the high-pressure membrane face, solute also diffuses into the membrane and creases a chemical concentration gradient across the membrane. Eventually, a steady state is reached in which the influent concentration is equivalent to the effluent concentration. The CPL and chemical concentration gradient across the membrane remain at steady state.

Permeability is a measure of how easily water or other liquids penetrate concrete (AASHTO, 2000). Concrete, in all forms, contains pores that allow entry of these liquids. Low permeability concrete is created by reducing this pore volume by addition of polymers, decreasing the water/cement ratio, addition of fly ash, and other various substances (AASHTO, 2000; API, 1956; Whiting, 1988). Typical concrete has

permeability values in the range of $1x10^{-6}$ m/s, while lower permeability concrete has values closer to $1x10^{-8}$ m/s (Whiting, 1988).

There are several methods for determining the permeability of concrete to chloride. Resistance to chloride-ion penetration, for example, can be determined by ponding chloride solution on a concrete surface and, at a later stage, determining the chloride content of the concrete at particular depths (AASHTO T 259). Various absorption methods, including ASTM C 642, are also used. Direct water permeability data can be obtained by using the U.S. Army Corp of Engineers CRC C 163-92 test method for water permeability of concrete using a triaxial cell. None of the above test methods were designed to measure the membrane efficiency of concrete.

The experiments reported in this paper are intended only to be a first look to see if the investigation of membrane properties of low permeability concrete might yield positive results. More complete research will need to be undertaken to characterize the membrane properties, or lack thereof, of the various types of low permeability concrete.

## 2.3 METHODS

Multiple samples, weighing between 4.5 to 13.6 kg (10 to 30 lbs) each, of low permeability concrete were randomly chosen from low permeability concrete slabs used in the Missouri University of Science and Technology – Rolla Rock Mechanics testing facility. Low permeability concretes are routinely used in the water jet laboratory facility, as well as various testing for infrastructure uses. The samples were cored to obtain 6.35 cm (2.5 inch) diameter cores. The core ends were discarded and the middle of the core was sliced and kept at identical atmospheric pressure, temperature, and water saturation content as per AASHTO T 259. These discs were then ground down using

silica carbide paste on glass until each was approximately 3 mm thick and washed thoroughly to remove loose material. Thin discs were used instead of thicker columns of core in order to shorten the time needed to perform the experiments.

The discs were placed into a custom-made hyperfiltration cell consisted of a transparent acrylic cylinder with an internal area of 15 $cm^2$ and wall thickness of 0.64 cm similar to those used by Hart and Whitworth, 2005 (Figure 2.4). The 2.75 cm long acrylic cylinders were fitted to two O-ringed, 3.80 cm thick, Garlite™ caps. The caps were held in place by eight threaded rods, which pass through both caps parallel to the cylinder. The hyperfiltration cell components were thoroughly washed and then rinsed multiple times with deionized water before each experiment.

A Marriotte flask suspended at 0.5 and 1.0 m of height supplied a constant head. Initially, deionized water was passed through the concrete in order to determine the water permeation coefficient ($L_p$) (Fritz and Whitworth, 1994) (Figure 2.2). The deionized water was then removed from the experimental cell and replaced with 185 and 345 ppm sodium chloride solutions (Table 2.1). The experiments began immediately after insertion of stock solution into the cell. Effluent samples were collected at intervals during the experiment (Figures 2.3, 2.4, 2.5, and 2.6). At the end of the experiment the cell solution was collected and the $Cl^-$ concentration within the cell was measured. Reagent grade chemicals were used to make the solutions. NaCl concentrations were measured with a Dionex DX-120 ion chromatograph and compared against standards. Analytical precision was calculated by finding the standard deviation of triplicate testing of effluent samples (Table 2.1) and ranged between 2.0 and 2.7% for different experimental runs.

## 2.4 RESULTS

Tabulated results for individual experiments can be found in Table 3.1. $J_v$, the steady-state volumetric solution flux was calculated using

$$J_v = \frac{V}{A \cdot s} \tag{3.1}$$

where, V is the volume of effluent, A is the area of the membrane, and s is the total time elapsed for a specific sample. $J_v$ decreases as the osmotic pressure increases within the cell until a steady-state flux is established. $J_v$ reported in Table 3.1 for each experiment is the average of the last 3 samples taken once steady-state was established.

A mass balance approach was used to predict the expected concentration within the cell at the end of the experiment. The total moles of $Cl^-$ input into the cell were calculated. This value was then compared to the total moles of $Cl^-$ that were collected during the experiment within the cell. From this data we calculated the predicted concentration in the cell at the end of the experiment ($c_{predicted}$). This value was then compared to the measured cell concentration within the cell at the end of the experiment ($c_{final}$) (Table 2.1).

This approach predicted ending $Cl^-$ cell chloride concentrations of 431 and 434 ppm for the experiments using a 345 ppm $Cl^-$ input solution. The actual ending cell concentration was 436 and 438 ppm $Cl^-$, respectively. Similarly, for the experiments using a 185 ppm $Cl^-$ input solution, the predicted ending concentrations were 278 and 234 ppm $Cl^-$. The actual concentrations were 281 and 239 ppm $Cl^-$. Comparison of the predicted ($c_{predicted}$) and measured ($c_{final}$) values resulted in a less than 5% difference between predicted and actual values for all experiments (individual experimental comparisons are presented in Table 2.1). During each experiment the volumetric solution

flux ($J_v$) decreased until it reached a steady-state minimum (Table 2.1). In each experiment the final cell concentrations were much higher than the input concentration.

One measure of membrane efficiency is the reflection coefficient σ, a unitless measure of osmotic efficiency (Staverman, 1952). If σ = 1.0, the membrane is perfect and rejects all dissolved solute. If σ = 0, there is no solute rejection. For intermediate values, rejection is partial and proportional to the value of σ. The steady-state reflection coefficient can be calculated from the experimental data without prior knowledge of the concentration at the membrane interface via Eqns. 2.2 through 2.5 (Whitworth, 1998).

$$L_P = \frac{J_{v_{DI}}}{\Delta P} \tag{2.2}$$

$$\begin{aligned} c_o = {} & \frac{1}{2L_P vRT(J_v \Delta x - 2vD)} \cdot (-2L_P vRTJ_v c_i \Delta x\zeta - 4L_P v^2 RTDc_i \\ & + \Delta x\zeta J_v L_P \Delta P - \Delta x^{1/2}\zeta^{1/2}(-8\zeta\Delta x c_i J_v{}^3 TRvL_P + 8\zeta\Delta x c_i J_v{}^2 TRvL_P{}^2 \\ & + \zeta\Delta x J_v{}^4 - 2\zeta\Delta x\Delta P L_P J_v{}^3 + \zeta\Delta x\Delta P^2 L_P{}^2 J_v{}^2 - 16J_v{}^2 c_i DTRv^2 L_P{}^2)^{1/2}) \end{aligned} \tag{2.3}$$

$$\sigma = L_P\Delta P - J_v / L_P vRT(c_o - c_i) \tag{2.4}$$

$$\Delta\pi = vRT(c_o - c_e) \tag{2.5}$$

where $L_p$ = water permeation coefficient (m/Pa·s), $J_{v_{DI}}$ = deionized water flux through the membrane (m/s), ΔP = pressure difference across the membrane (Pa), $c_o$ = concentration at the high-pressure membrane face (M), v is a factor that corrects for the number of particles due to ion formation, R is the gas constant (8.314 N·m/mole), T is the temperature in °K, $J_v$ = experimental solution flux (m/s) through the membrane, Δx is membrane thickness (m), D = diffusion coefficient for free solution (1.89 x $10^{-7}$ $m^2$/sec), ζ is the tortuosity and is defined here as the ratio of the actual path length through the disc to the concrete disk thickness and for low permeability concrete is 2.05 (Yang and

Su, 2002), $c_i$ = the input solute concentration (M), $\Delta\pi$ = theoretical osmotic pressure difference across the membrane (dyne/cm$^2$), and $c_e$ = effluent concentration (mole/cm$^3$). For a full derivation of these equations, please refer to Whitworth and DeRosa (1997).

The steady-state maximum concentrations of $Cl^-$ in the cells, located at the membrane face ($c_o$), were calculated from Eqn. 2.3 to be between 216-395 ppm $Cl^-$ indicating concentration increases at the membrane between 115 to 119% greater the initial concentration (Table 2.1). The reason that the ending cell concentrations were greater than the calculated values of $C_o$ is attributed to the fact that the cell length was significantly less than the CPL length for experimental conditions resulting in higher ending cell concentrations than would have occurred if the cell had been longer. Calculations performed after the experiments were completed suggest the experimental cells would have needed to be in excess of 21 to 83 cm instead of the 2.75 cm length allowed by restriction of the experimental device, depending on the experiment, to be longer than the CPL lengths in these experiments. The CPL length can be approximated by $10D/J_v$ (Fritz, 1986). Since the experiments were designed to test low permeability concrete for the presence of membrane parameters and not to accurately determine the values of $C_o$, the cell length discrepancies are unimportant for the experiments. Future work should carefully adjust cell length to experimental conditions if values of $C_o$ are important. The data from these experiments will provide a starting point for more precise experimental design.

The values of $\sigma$ calculated from Eqn. 2.4 for the experiments reported herein ranged between 0.15 to 0.19 for chloride (Table 2.1). These values indicate that the

concrete discs exhibited significant membrane properties. Values of $L_p$, calculated from Eqn. 2.2, ranged from $1.107 \cdot 10^{-11}$ to $2.033 \cdot 10^{-11}$ (m/Pa·s).

## 2.5 DISCUSSION

The purpose of this paper was to experimentally determine if low permeability concrete could behave as a membrane under relatively low head conditions using a conservative solute. We conducted four experiments and each showed a significant increase in chloride concentrations above the input solution concentration within the experimental cell at the end of the experiment (112 - 134% increase; Table 3.1). This increase is attributed to partial rejection of solute by the membrane-functioning concrete. Total solution flux decreased significantly during all four experiments. The solution flux decrease is attributed to the build-up of osmotic pressure within the experimental cell (Fritz and Whitworth, 1994). Calculated reflection coefficients ($\sigma$) ranged between 0.15 and 0.19. Reflection coefficients of 0.19 have been reported at 35 ppm NaCl for lightly compacted smectite membranes (Saindon, 2005). Milne et al. (1963) found reflection coefficients of 0.14 -0.60 for mixtures of bentonites and silica silt sized particles using 0.1 N sodium chloride solutions. Additionally, Fritz and Marine found reflection coefficients of 0.04 to 0.89 for bentonites under static head conditions using 0.01, 0.096, and 0.094 molar sodium chloride solutions. The reflection coefficients reported herein for concrete are on the lower end of those reported from hyperfiltration testing of remolded and compacted smectite membranes with chloride solutions. While low permeability concrete may not be as efficient a membrane as smectite, low permeability concrete does exhibit membrane effects. A brief description of a few scenarios in which low permeability concrete membrane properties might prove important follows.

Low permeability concrete is traditionally used to help reduce the potential for reinforcing steel to corrode when exposed to chlorides by limiting the permeation of those chlorides into concrete. When reinforcing steel comes into contact with plastic concrete, a chemical reaction occurs between the steel and the concrete that causes a protective layer to develop around the reinforcing steel. This passive layer protects against corrosion of the reinforcing steel. If the concrete is exposed to de-icing salts, these salts can migrate down to the reinforcing steel through small pores in the concrete. The deterioration of both the concrete and reinforcing steel compromises the integrity of the structure. For engineered structures that are routinely exposed to salts and water infiltration, low permeability concretes are selected to reduce the ability of salt penetration. Low permeability concrete is commonly used in many engineering applications such as a water barrier for dams, retaining walls, deep basements, swimming pools, major bridges, and other infrastructure features such as culverts and tunnels. As transportation and water barrier infrastructure ages, many of these structures are not providing the service life that was intended (Whiting, 1988) and this could be in part due to potential membrane effects acting on the steel reinforcements.

While low permeability concrete reduces the flow of water through the concrete itself, it may increase the hydraulic head the concrete is exposed to by pooling water behind the structure itself. This water pressure would increase even more if the concrete structure were functioning as a membrane because the solute flux is being retarded and therefore causing a buildup of hydraulic pressure in addition to normal water retention. Designing a concrete structure to withstand pooling hydraulic heads is routine. However, increasing the hydraulic head on the feature itself can create a hydraulic gradient and

perhaps an additional chemical gradient, specifically $Cl^-$, through the concrete structure if the structure is functioning as a membrane. If a low permeability concrete structure is acting as a membrane, and there is a head difference across the structure greater than the osmotic pressure, it is possible that membrane effects could occur. If membrane effects were occurring the leading edge steel reinforced bar (bar nearest the outside edge on the high pressure face of the concrete) would undergo corrosion first (Figure 2.1) because this is where the $Cl^-$ concentration would be the greatest. This would be typical in most applications without membrane effects occurring; however, in this situation the corrosion would be accelerated relative to a concrete that is not acting as a membrane. In part, this would be due to the potential development of a concentration polarization layer developing on the high pressure face of the concrete structure (Figure 2.1).

In a scenario such as this, hydraulic heads in excess of the osmotic pressure would develop on the outside face low permeability concrete structure acting as a water barrier. Initially, no solute is passing through the concrete structure, just as any other concrete structure would pass solution. After flux initiates through the concrete membrane, the concentration ($c_o$) at the high-pressure membrane face increases due to partial solute rejection. Samples of water adjacent to the high-pressure face of the concrete membrane would exhibit higher concentration of solute than background. At steady-state the input concentration ($c_i$) would match the output concentration ($c_o$) and the leading edge steel reinforced bar would be experiencing abnormally high concentration of chloride within the diffusion gradient through the concrete structure (Figure 2.1). This would be reflected in accelerated deterioration of the reinforcing in this area.

Our experiments were not designed to test steel rebar deterioration. Therefore, we suggest additional testing and modeling to determine if membrane effects in low permeability concrete have a significant effect on steel reinforcement embedded in the concrete as the results of these preliminary experiments suggest.

## 2.6 CONCLUSIONS

Solutions of 185 and 345 ppm chloride were passed through thin low permeability concrete discs (~3 mm) at heads of 0.5 and 1.0 m. In each experiment, ending cell chloride concentrations significantly increased due to partial solute rejection by the low permeability concrete membranes. Concentration increases within the cell were between 126% and 152% above input concentrations. Calculated values of the reflection coefficient ranged from 0.15 and 0.19, suggesting that these thin, low permeability concrete discs exhibited significant membrane effects. These are the first known hyperfiltration experiments performed on intact concrete cores.

Additionally, under some conditions membrane-functioning concrete may contribute to deterioration of steel reinforcements within concrete structures by increasing the salt ($Cl^-$) concentration gradient in the pores of the low permeability concrete significantly above background solute concentrations. Additional experiments should be conducted to determine the significance of deterioration of steel reinforcements related to hyperfiltration effects.

## 2.7 REFERENCES

AASHTO, Resistance of Concrete to Chloride Ion Penetration, AASHTO T259-80 American Association of State Highway and Transportation Officials, Washington D.C., 2000.

American Petroleum Institute, Recommended Practice for Determining Permeability of Porous Media, API RP 27 American Petroleum Institute, Washington D.C., 1956

Barone, F. S.; Rowe, R. K.; and Quigley, R. M. (1990) Laboratory determination of chloride diffusion coefficient in intact shale: *Canadian Geotechnical Journal* **27**:177-184.

Fritz, S. J. (1986) Ideality of clay membranes in osmotic processes: a review, *Clays and Clay Minerals* **34**: 214-223.

Fritz S. J. and Whitworth T. M. (1994,) Hyperfiltration-induced fractionation of lithium isotopes: ramifications relating to representativeness of aquifer sampling. *Water Resources Research* **30**: 225-235.

Graf, D.L. (1982) Chemical osmosis, reverse osmosis, and the origin of subsurface brines, *Geochimica et Cosmochimica Acta* **46:** 1431-1448.

Hart, M. and Whitworth, T. M., (2005) Hyperfiltration of Potassium Nitrate through Clay Membranes under Relatively Low-Head Conditions, *Geochimica Cosmochimica et Acta:* **69**, *20*, p. 4817-4823.

Kharaka, Y. K., Berry, F.A.F., (1973) Simultaneous flow of water and solutes through geologic membranes, I. Experimental investigation. *Geochim. Cosmochim. Acta* **37:** 2577-2603.

McKelvey, J. G. and Milne, I. H. (1960) The flow of salt solutions through compacted clay, *Clays and Clay Minerals* **9**: 248-259.

Milne, I. H., McKelvey, J. G., and Trump, R. P., (1963) Permeability and salt-filtering properties of compacted clay, Clays and Clay Minerals, Monograph No. 13, The MacMillan Company, New York, 250-251.

Saindon R.M. (2005) *Relevance of clay membrane properties of clay-rich geologic materials to water-related engineering issues*. PhD thesis, University of Missouri at Rolla.

Staverman A. J. (1952) Non-equilibrium thermodynamics of membrane processes. *Trans. Faraday Soc*. **48**, 176-185.

Tyler, I.L. and Erlin, Benard, A Proposed Simple Test Method for Determining the Permeability of Concrete, Research Department Bulletin RX133, Portland Cement Association, 1961.

Whiting, D., Rapid Determination of the Chloride Permeability of Concrete, FHWA-RD-81-119, Federal Highway Administration, Springfield, Virginia, 1981

Whitworth T. M. (1998) Steady-State Mathematical Modeling of Geological Membrane Effects in Aquifer Systems, presented at *Joint Conference on the Environment*, 37-40.

Whitworth T. M. and DeRosa G. (1997) Geologic Membrane Controls on Saturated Zone Heavy Metal Transport. *New Mexico Water Resources Research Institute Report No. 303*, Las Cruces, New Mexico, 88.

Yang, C.C., and Su, J. K., (2002) Approximate migration coefficient of interfacial transition zone and the effect of aggregate content on the migration coefficient of mortar. *Cement and Concrete Research* **32**(10): 1507-1678.

Young A. and P.F. Low (1965) Osmosis in argillaceous rocks. *American Assoc. of Pet. Geol. Bull.* **46**:1004-1008.

Table 2.1: Experimental Parameters and Calculated Results.

| Parameter | Concrete 1 | Concrete 2 | Concrete 3 | Concrete 4 |
|---|---|---|---|---|
| Head (m) | 1.00 | 0.50 | 1.00 | 0.50 |
| Membrane Thickness (m) | 0.00375 | 0.00375 | 0.00375 | 0.00375 |
| Membrane Area ($m^2$) | 0.0015 | 0.0015 | 0.0015 | 0.0015 |
| $J_v$ (m/s) | $1.909 \times 10^{-8}$ | $5.351 \times 10^{-8}$ | $9.185 \times 10^{-8}$ | $7.581 \times 10^{-8}$ |
| Analytical Precision (2SD) | ±2.62 | ±2.71 | ±2.36 | ±2.04 |
| $c_i$ (ppm $Cl^-$) | 345 | 345 | 185 | 185 |
| $c_{final}$ (ppm $Cl^-$) | 436 | 438 | 281 | 239 |
| $c_{predicted}$ (ppm $Cl^-$) | 431 | 434 | 278 | 234 |
| Change in Cell Conc. (%) | 126 | 127 | 152 | 129 |
| $L_p$ (m/Pa·s) | $2.014 \times 10^{-12}$ | $2.033 \times 10^{-11}$ | $1.107 \times 10^{-11}$ | $1.869 \times 10^{-11}$ |
| $c_o$ (ppm $Cl^-$) | 360 | 395 | 216 | 216 |
| Calculated Steady-State $\sigma$ | 0.15 | 0.16 | 0.17 | 0.19 |
| CBE | -1.23 | -2.25 | 0.75 | 1.20 |

Note: Measurements recorded at 21 °C.

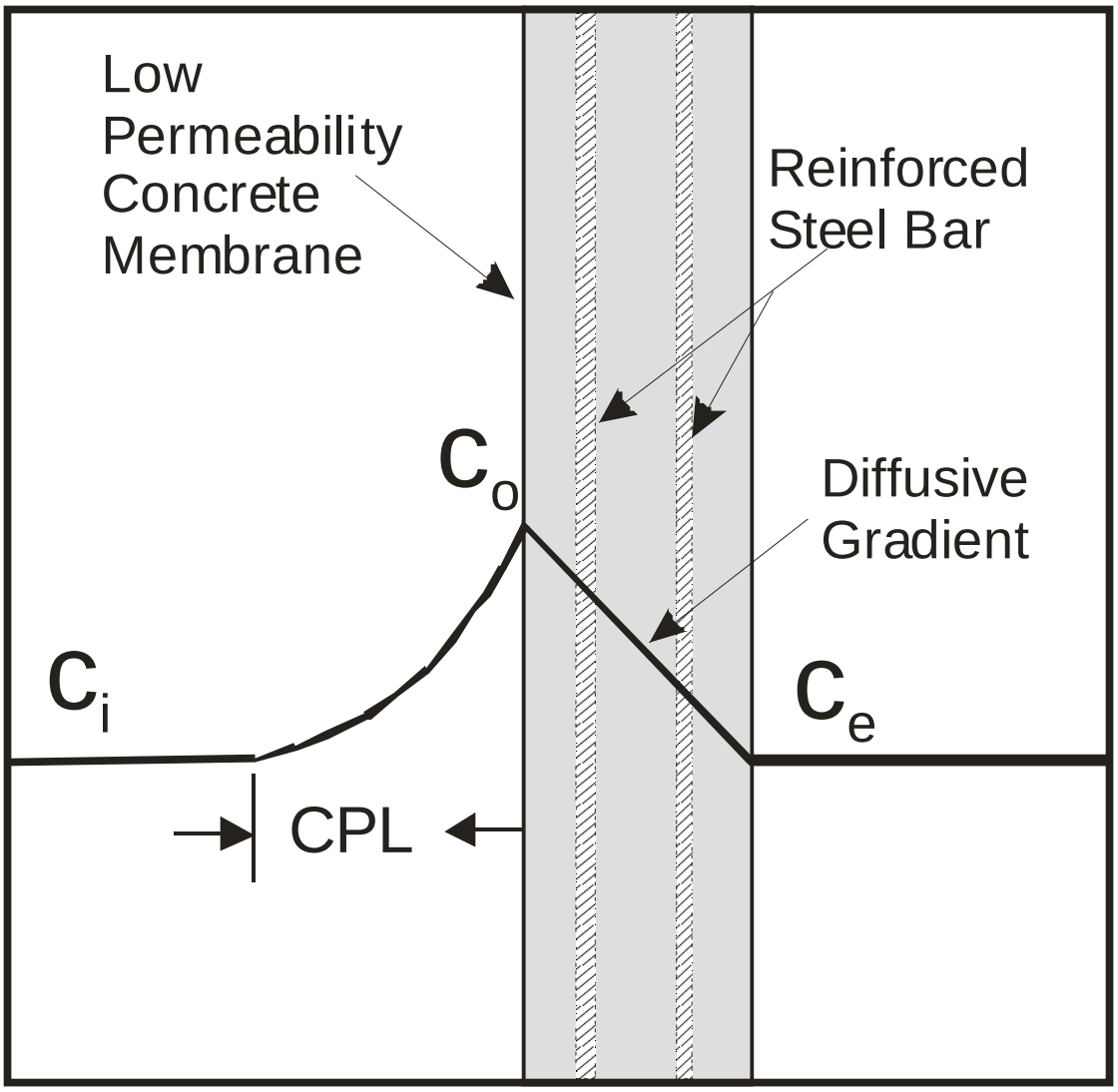


*Figure 2.1. Conceptual CPL development of low permeability concrete acting as a hyperfiltration membrane. (Redrawn from Fritz and Marine, 1983).*

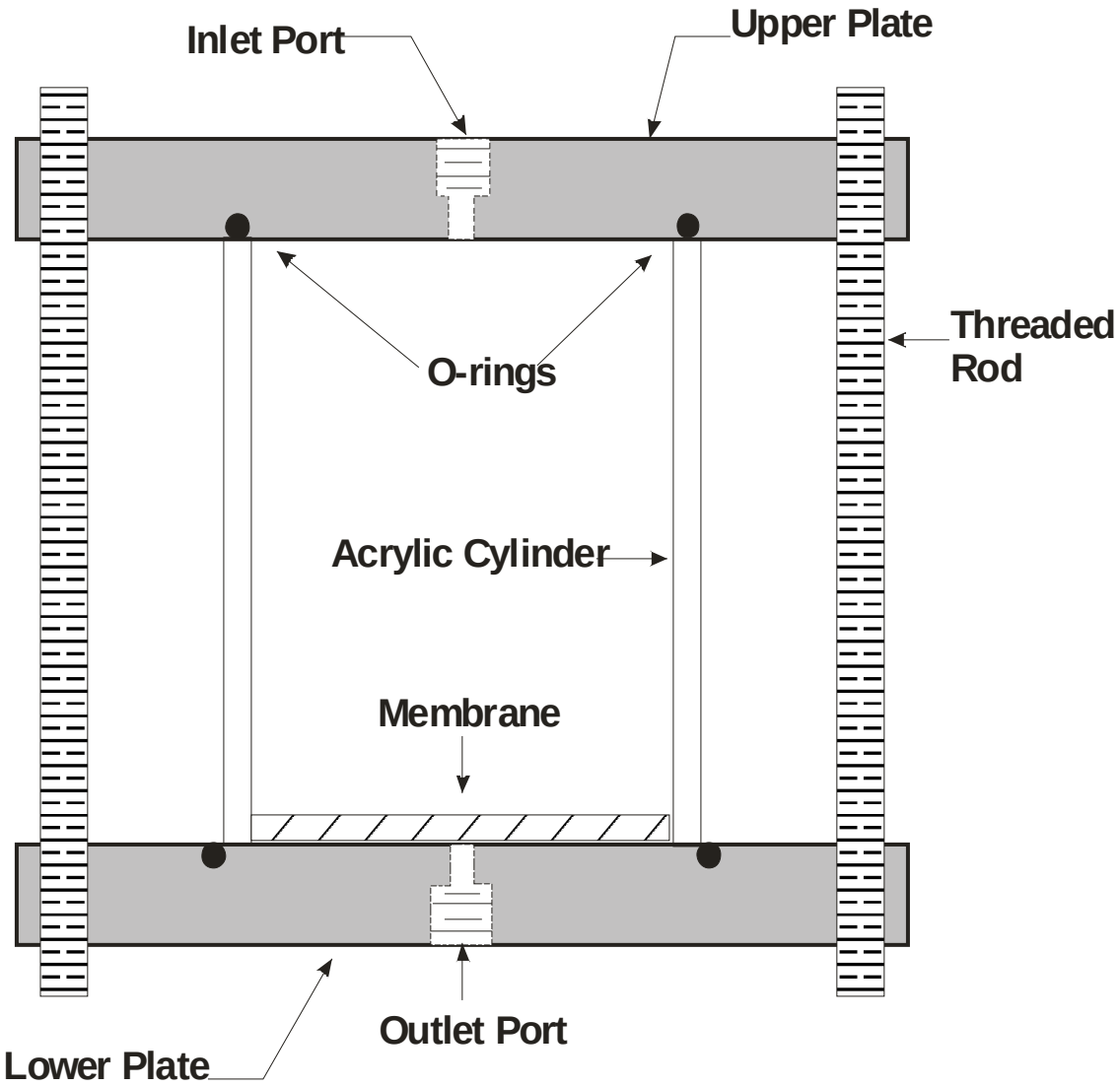


*Figure 2.2: Experimental Apparatus Schematic*

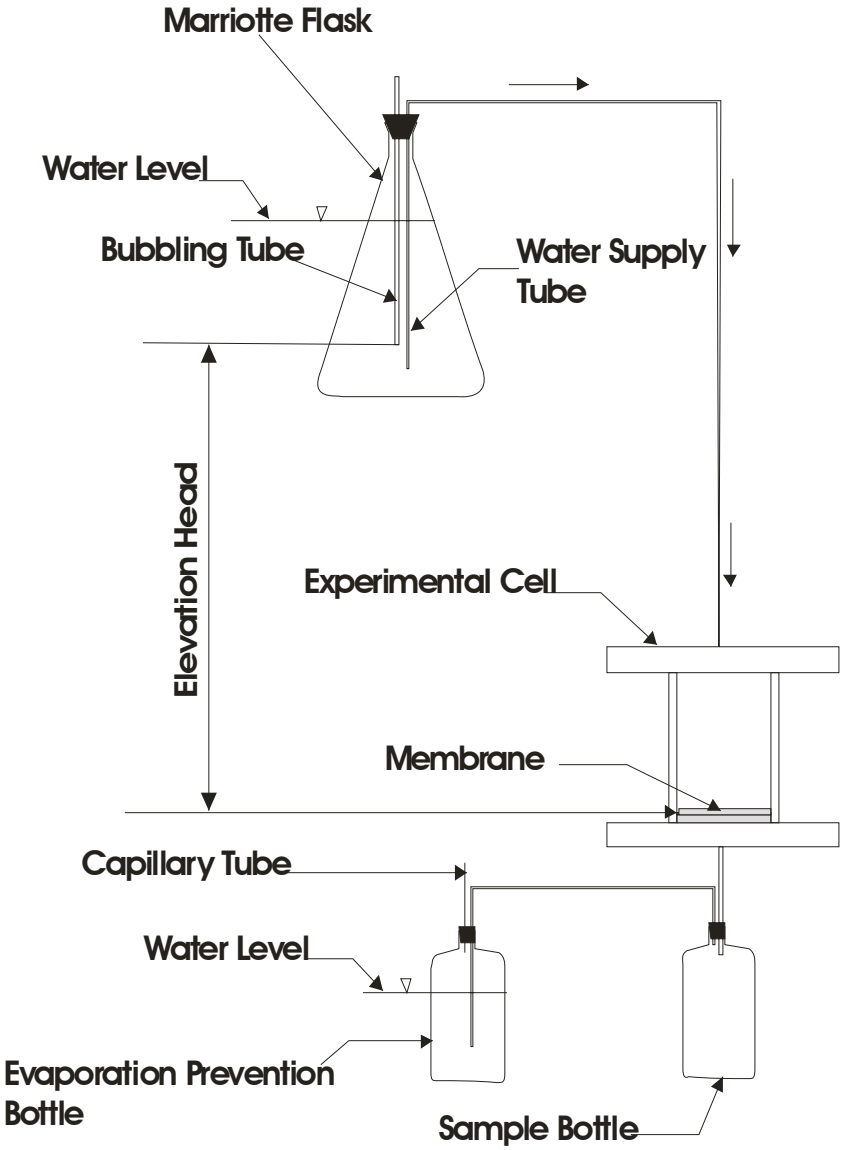


*Figure 2.3: Experimental Testing Schematic*

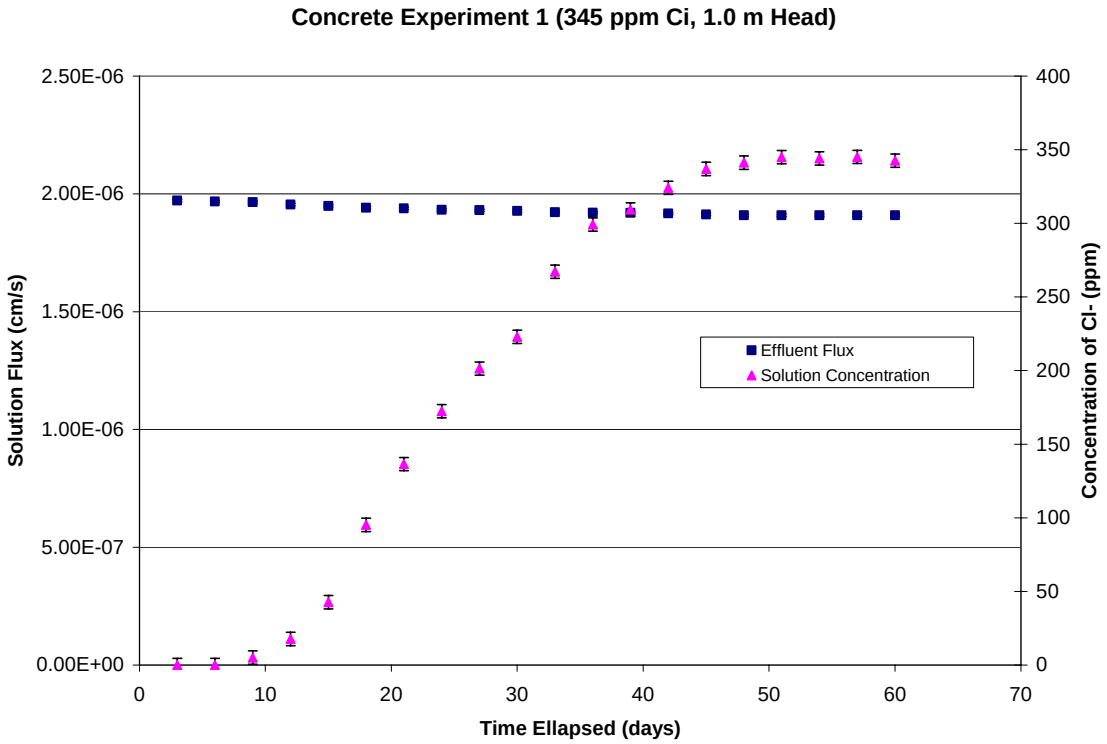


*Figure 2.4: Effluent Concentration and Flux versus Time for Experiment 1.*

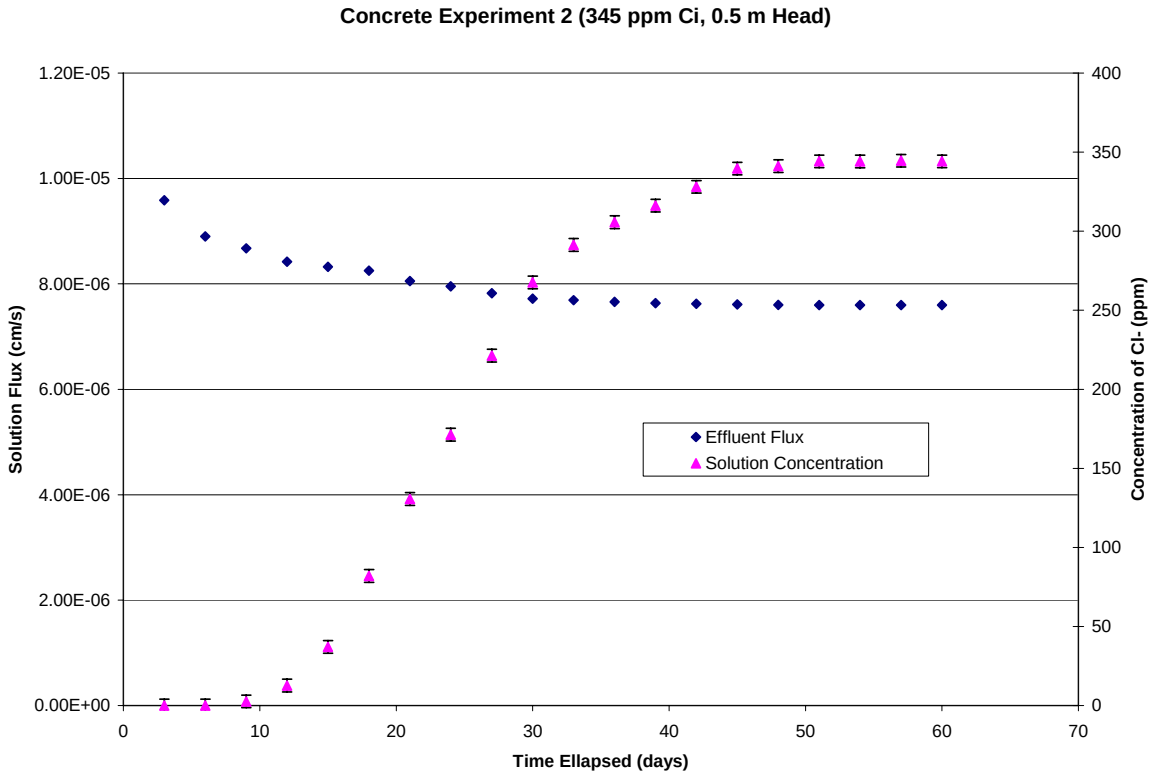


*Figure 2.5: Effluent Concentration and Flux versus Time for Experiment 2.*

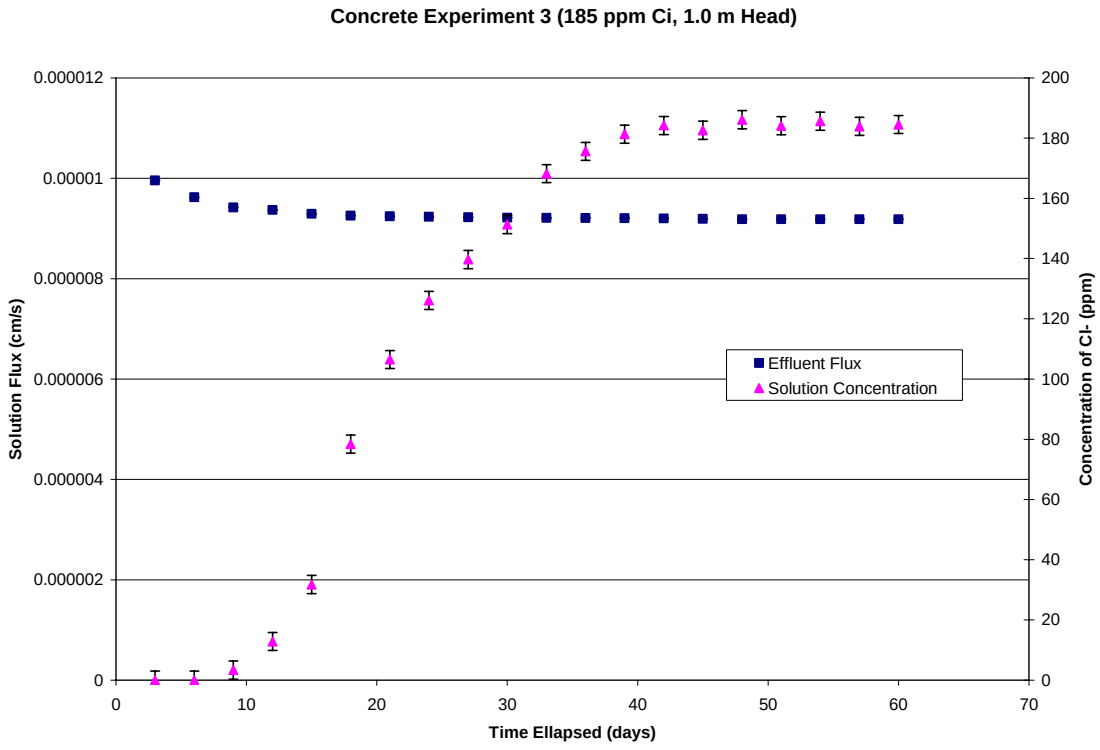


*Figure 2.6: Effluent Concentration and Flux versus Time for Experiment 3.*

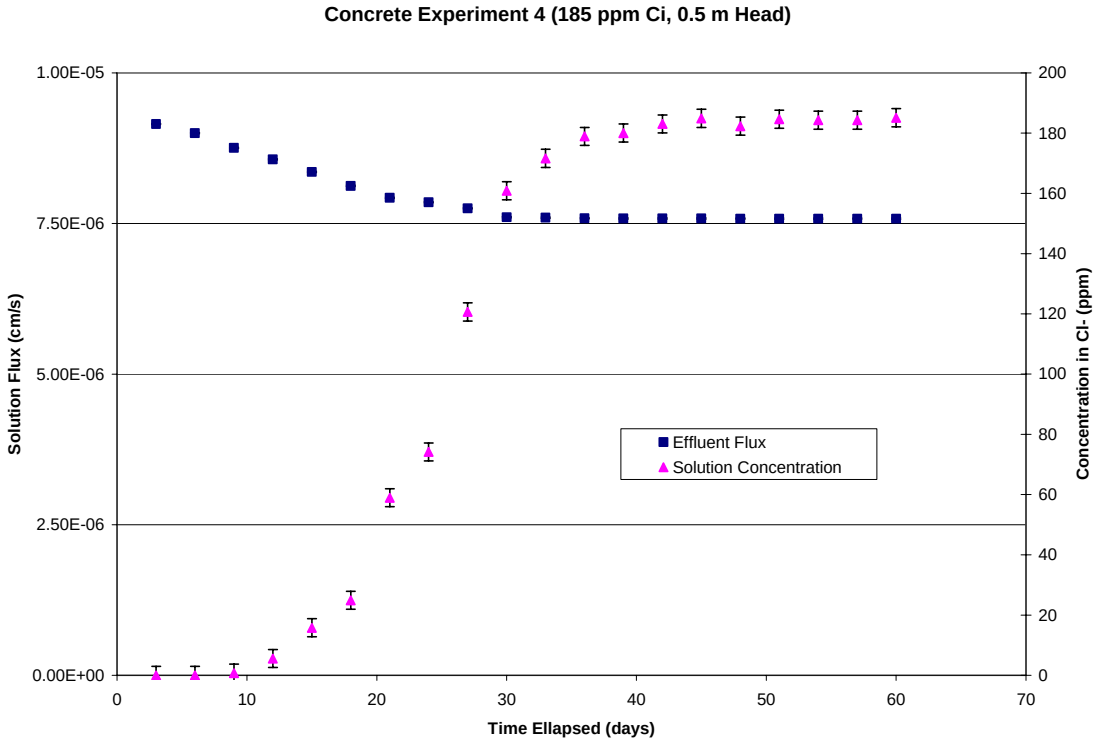


*Figure 2.7: Effluent Concentration and Flux versus Time for Experiment 4.*

# PAPER 3. LOW HEAD HYPERFILTRATION THROUGH INTACT DARRINGTON PHYLLITE CORES

## 3.1 ABSTRACT

Hyperfiltration is a process in which a membrane retards the passage of one solute relative to another under a hydraulic head in excess of osmotic pressure. Experiments have shown that clay membranes containing layered fabric have higher separation efficiencies than clay membranes with a house-of-cards fabric. Low-permeability metamorphic rocks with a foliated fabric might exhibit membrane properties. To test this hypothesis, four hyperfiltration experiments were conducted on samples of Darrington Phyllite. Chloride solutions were passed through thin, intact discs of Darrington Phyllite at relatively low heads. At the end of the experiments, dissolved chloride concentrations in the experimental cells had increased between 112 and 134%. This is attributed to partial solute rejection by the phyllite. Calculated values of the reflection coefficient ranged from 0.87 to 0.88 which correspond well to measurements in highly compacted bentonites. Natural scenarios in which phyllite might exhibit membrane properties include 1) shallow perched aquifers bounded below by phyllite, 2) overpressured aquifers bounded by phyllite, and 3) phyllite bounded aquifers with significant vertical groundwater flows. Membrane processes in phyllite may also contribute to the formation of some low temperature ore bodies, some of which exist in the area where the phyllite samples were obtained.

## 3.2 INTRODUCTION

There are two major membrane processes that are believed to occur in the subsurface: osmosis and hyperfiltration (Fritz, 1986). Osmosis occurs when two

solutions of differing concentrations are separated by a semi-permeable membrane. The flux of water and solute are then a function of the respective concentration gradients. The result is a net flux of solute from the more concentrated solution across the membrane into the less concentrated solution. The net flux of water molecules opposes this flow since the water is less concentrated in the solution which contains the highest concentration of dissolved solids. Flux across the membrane induces a pressure on the membrane termed the osmotic pressure, which is defined as the pressure necessary to stop the flow of solute from high to low concentration across the membrane (Martin, 1964).

Hyperfiltration, often called solute-sieving, is also a naturally-occurring geologic phenomenon in which a solute is partially rejected when groundwater passes through a membrane-functioning lithology (Graf, 1982). When hydraulic head in excess of osmotic pressure exists across a membrane-functioning lithology, hyperfiltration can occur. Rejected solutes concentrate adjacent to the high pressure face of the membrane, forming a zone of increased concentration called a concentration polarization layer, or CPL (Fritz, 1986) (Figure 3.1).

The purpose of the experiments reported here were to determine the membrane potential of intact Darrington Phyllite cores at room temperature under relatively low hydraulic heads of 0.5 and 1.0 m using chloride solutions of 185 and 365 ppm. To the best knowledge of the authors, phyllite has never been previously tested for membrane effects. Relatively few published laboratory studies have examined the ability of intact rock to act as geologic membranes. Young and Low (1965) tested siltstones and claystones to determine if osmosis was possible at natural compaction pressures under a

very high sodium chloride concentration gradient. Very low calculated osmotic efficiencies were determined from these experiments. Walter (1982) found that fractured tuffs demonstrated osmotic effects while studying matrix diffusion of solutes through pores. Barone et al. (1992) looked at the diffusive properties of salts in mudstones and concluded; membrane efficiencies were not calculated for these experiments but a diffusive gradient was found. Whitworth and DeRosa (1997) and Oduor (2004) performed experiments to determine the osmotic potential of shales and siltstones. In these experiments, shale separated solutions of differing chemical concentration.

Osmotic pressure was measured and recorded over time for all experiments measuring the change in water level in a litho-osmometer. These experiments found that shales displayed relatively significant osmotic efficiencies, even at low chemical concentration differences.

Remolded clays such as illites, smectites and kaolinites have all demonstrated membrane properties in laboratory settings (Marshall, 1948; McKelvey and Milne, 1963; Kemper and Rollins, 1966; Kharaka and Berry, 1973; Fritz and Marine, 1983; Benzel and Graf, 1984; Haydon and Graf, 1986; Demir, 1988; Whitworth and Fritz, 1994, Whitworth and DeRosa, 1997, among others). Furthermore, layered fabric has been determined to increase membrane efficiency (Benzel and Graf, 1984). Benzel and Graf (1984) created two random and two oriented bentonite fabrics, and determined the membrane filtration efficiency of each sample. Membrane filtration efficiency is defined as the ability of a membrane to selectively pass one substance relative to another. Benzel and Graf (1984) found that the hydraulic conductivity of oriented fabrics is higher than for random fabrics and that steady state occurred more quickly for thinner samples than thicker ones. They

also found that the filtration efficiency almost doubled for oriented fabrics than random fabrics and filtration efficiency was better for $Na^{+}$ than $Ca^{++}$ in three of the four samples tested.

It would stand to reason that low permeability rocks with layered fabric, such as some low-grade metamorphic rocks, might also exhibit measurable membrane properties. Therefore, we tested thin, intact phyllite discs exhibiting significant layered metamorphic fabric for membrane properties using an experimental hyperfiltration setup with NaCl solutions (185 and 365 ppm $Cl^{-}$) and relatively low constant heads of 0.5 and 1.0 m, similar to what might be found under natural conditions.

## 3.3 GEOLOGIC BACKGROUND

The Darrington Phyllite is a micaeous Jurassic-Cretaceous metamorphic rock found in the Easton Metamorphic Suite of the Northwest Cascades in Washington State (Figure 3.2). The Easton Metamorphic Suite comprises the Shuksan Greenschist and Darrington Phyllite with the Shuksan underlying the Darrington. The Darrington Phyllite was metamorphosed in the Early Cretaceous and formed from oceanic shale and sandstone protolith. Most of the Darrington is graphitic in nature with quartz-albite-sericite phyllite predominant throughout the unit. Some localized well-recrystallized fine-grained muscovite schist is found commonly in association with albite porphyroblasts and well-developed lawonsite (Brown, 1987). Darrington Phyllite is variable in its hardness and resistance to weathering. Exposure of the phyllite terrain yields a smooth topographic expression with some scattered evidence for mass-wasting.

The Eocene Chuckanut Sandstone unconformably overlays the Darrington Phyllite and consists of thin-to-medium bedded sandstone. The Chuckanut Formation is

a fluvial deposit of mostly feldspathic arenites that developed in a faulted, down-dropped basin post terrain emplacement (Easterbrook, 1971). Subsequent displacement along the Straight Creek fault (approximately 95 kilometers (60 miles) to the west), uplift of the lowland basins, and changes in regional tectonics led to intense folding and faulting of the Chuckanut. Fine-scale stratigraphic sequences that are fining-upwards are significant throughout the entire Chuckanut aquifer, and reduce the overall hydraulic conductivity of this member. The Chuckanut formation is bounded by glacial drift and Darrington Phyllite, forming a confined, low head aquifer (EPA, 2004). Deformation is related to subduction of the San Juans under the North Olympics. Jointing, slickensides, heavy metal deposits, and coal are all present in this formation.

Low-temperature, sulfide-bearing gold, pyrite, and oxide mines exist locally in the Darrington Phyllite and Chuckanut Sandstone contact area, including the area where the samples for these experiments were collected (Brown, 1987, Derkey et al, 1990). Several mechanisms have been postulated for formation of these sulfide-bearing ores including low-temperature epithermal alteration along shear zones (Derkey et al., 1990) and percolation of heated waters during metamorphosis (Brown, 1987). The ores are not regional in extent (Brown, 1987; Derkey, et al. 1990).

## 3.4 METHODS

Multiple samples, weighing between 4.5 to 13.6 kg (10 to 30 lbs) each, were obtained in a shear zone at 48°54'28"N, 121°37'48"W near the Silver Tip Mine close to Mount Larrabee, WA. The hand samples were competent and strongly foliated (Figure 3.3). The samples were cored to obtain 6.35 cm (2.5 inch) diameter slices perpendicular to foliation. These discs were then ground down using silica carbide paste on glass until

each was approximately 3 mm thick. Thin discs were used instead of thicker columns of core in order to shorten the time needed to perform the experiments.

The discs were placed into a custom-made hyperfiltration cell consisted of a transparent acrylic cylinder with an internal area of 15 $cm^2$ and wall thickness of 0.64 cm similar to those used by Hart and Whitworth, 2005 (Figure 3.5). The acrylic cylinders were fitted to two O-ringed, 3.80 cm thick, Garlite™ caps. The caps were held in place by eight threaded rods, which pass through both caps parallel to the cylinder. The cylinder measured 2.6 cm in length. The hyperfiltration cell components were thoroughly washed and then rinsed multiple times with deionized water before each experiment.

A Marriotte flask suspended at 0.5 and 1.0 m of height supplied a constant head. Initially deionized water was passed through the phyllite in order to determine the water permeation coefficient ($L_p$) (Fritz and Whitworth, 1994) (Figure 3.6). The deionized water was then removed from the experimental cell and replaced with 185 and 345 ppm sodium chloride solutions (Table 3.1). The experiments began immediately after insertion of stock solution into the cell. Effluent samples were collected at intervals during the experiment (Figures 4.5, 4.6, 4.7, 4.8). At the end of the experiment the cell solution was collected and the $Cl^-$ concentration within the cell was measured.

Reagent grade chemicals were used to make the solutions. NaCl concentrations were measured with a Dionex DX-120 ion chromatograph and compared against standards. Chemical analysis precision was calculated by finding the standard deviation of triplicate testing of effluent samples (Table3.1).

## 3.5 RESULTS

Tabulated results for individual experiments can be found in Table 3.1. $J_v$, the steady-state volumetric solution flux was calculated by using

$$J_v = \frac{V}{A \cdot s} \tag{3.1}$$

where, V is the volume of effluent, A is the area of the membrane, and s is the total time elapsed during a specific sample. $J_v$ decreases as the osmotic pressure increases within the cell until a steady-state flux is established. $J_v$ reported in Table 3.1 for each experiment is the average of the last 3 samples taken once steady-state was established.

A mass balance approach was used to predict the expected concentration within the cell at the end of the experiment. The total moles input into the cell were calculated. This value was then compared to the total moles that were collected during the experiment within the cell. Equation 3.2 yields an estimated accumulation at the end of the experiment ($c_{predicted}$). This value was then compared to the measured cell concentration within the cell at the end of the experiment (Table 3.1).

$$\sum Moles_{in} - \sum Moles_{out} = Accumulation \tag{3.2}$$

This approach predicted $Cl^-$ accumulations between 379-415 ppm for the 345 ppm initial concentration experiments and 219-234 ppm $Cl^-$ for the 185 ppm initial concentration experiments. Comparison of the predicted ($c_{predicted}$) and measured ($c_{final}$) concentration values resulted in a less than 5% difference for all experiments (individual experimental comparisons are presented in Table 3.1).

All experiments resulted in significant increases in chloride concentrations within the experimental cells. Final cell concentrations ranged from 421-777 ppm $Cl^-$ (Table 4.1). During the hyperfiltration experiments on the Darrington Phyllite, sodium chloride

concentrated within the cell by 112 to 134 % above the background concentration (Table 3.1). During each experiment, volumetric solution flux ($J_v$) decreased until it reached a steady-state minimum. This solution flux decrease can be attributed to the buildup of osmotic pressure within the cell (Fritz and Whitworth, 1994).

One measure of membrane efficiency is the reflection coefficient σ, a unitless measure of osmotic efficiency (Staverman, 1952). If σ = 1.0, the membrane is perfect and rejects all dissolved solute. If σ = 0, there is no solute rejection. For intermediate values, rejection is partial and proportional to the value of σ. The steady-state reflection coefficient can be calculated from the experimental data without prior knowledge of the concentration at the membrane interface via Eqns. 3.3 through 3.5 (Whitworth, 1998).

$$L_P = \frac{J_{v_{DI}}}{\Delta P} \tag{3.3}$$

$$\begin{aligned} c_o = {} & \frac{1}{2L_P vRT(J_v \Delta x - 2vD)} \cdot (-2L_P vRTJ_v c_i \Delta x\zeta - 4L_P v^2 RTDc_i \\ & + \Delta x\zeta J_v L_P \Delta P - \Delta x^{1/2}\zeta^{1/2}(-8\zeta\Delta x c_i J_v{}^3 TRvL_P + 8\zeta\Delta x c_i J_v{}^2 TRvL_P{}^2 \\ & + \zeta\Delta x J_v{}^4 - 2\zeta\Delta x\Delta P L_P J_v{}^3 + \zeta\Delta x\Delta P^2 L_P{}^2 J_v{}^2 - 16J_v{}^2 c_i DTRv^2 L_P{}^2)^{1/2}) \end{aligned} \tag{3.4}$$

$$\sigma = L_P\Delta P - J_v / L_P vRT(c_o - c_i) \tag{3.5}$$

where $L_p$ = water permeation coefficient (m/Pa·s), $J_{v_{DI}}$ = deionized water flux through the membrane (m/s), ΔP = pressure difference across the membrane (Pa), $c_o$ = concentration at the high-pressure membrane face (M), v is a factor that corrects for the number of particles due to ion formation, R is the gas constant (8.314 N·m/mole), T is the temperature in °K, $J_v$ = experimental solution flux (m/s) through the membrane, Δx is membrane thickness (m), D = diffusion coefficient for free solution (1.89 x $10^{-9}$ $m^2$/sec), ζ is the tortuosity and is defined here as the ratio of the actual path length through the

membrane to the membrane thickness and was equal to 1.79 (Dullien, 1979), and $c_i$ = the input solute concentration (M).

The values of $\sigma$ calculated from Eqn. 3.5 for the experiments reported herein ranged between 0.87 to 0.88 for chloride (Table 3.1). These values indicate that the phyllite discs exhibited significant membrane properties. Values of $L_p$, calculated from Eqn. 4.3, ranged from $1.59 \cdot 10^{-11}$ to $9.95 \cdot 10^{-11}$ (m/Pa·s). The steady-state values of maximum concentrations in the cells, located at the membrane face ($c_o$), were calculated from Eqn. 4.4 to be between 195-385 ppm $Cl^-$ indcating concentration increases at the membrane between 115 to 154% greater the initial concentration.

**3.6 DISCUSSION**

The purpose of this paper was to experimentally determine if phyllite could behave as a semi-permeable geologic membrane under relatively low head conditions using a conservative solute. We conducted four experiments. Each showed a significant increase in chloride concentrations above the input solution concentration within the experimental cell at the end of the experiment (112-134% increase; Table 3.1). This increase is attributed to partial rejection of solute by the membrane-functioning phyllite. Total solution flux decreased significantly during all four experiments. The solution flux decrease is attributed to the build-up of osmotic pressure within the experimental cell (Fritz and Whitworth, 1994). Calculated reflection coefficients ($\sigma$) ranged between 0.87 and 0.88. Reflection coefficients of 0.19 have been reported at 35 ppm NaCl for lightly compacted smectite membranes (Saindon, 2005). Milne et al. (1963) found reflection coefficients of 0.14 -0.60 for mixtures of bentonites and silica silt sized particles using 0.1 N sodium chloride solutions. Additionally, Fritz and Marine found reflection

coefficients of 0.04 to 0.89 for bentonites under static head conditions using 0.01, 0.096, and 0.094 molar sodium chloride solutions. The reflection coefficients reported herein for phyllite are on the higher end of those reported from hyperfiltration testing of remolded and compacted smectite membranes with chloride solutions. Thus some phyllites are highly efficient membranes. A brief description of several geologic scenarios in which phyllite membrane properties might prove important follows.

One potential role of phyllite membranes may be in the formation of some low temperature ore deposits. Mackay (1946) postulated membrane processes might play a role in hydrothermal and low temperature ore deposits by concentrating metals to supersaturation and inducing precipitation of ore minerals and offered the lead-zinc fields in Mezica, Slovenia, the lead-zinc field in Raihbl, Italy, the quicksilver deposits in Idria, Italy, a copper deposit in Cyprus, the iron, copper, gold, and zinc deposits of Noranda, Quebec, and the gold deposits of Tanganyika and Nigera as possible examples. To test the feasibility of Mackay's (1946) ideas, Whitworth and Derosa (1997) experimentally demonstrated that compacted smectite membranes can concentrate some heavy metal solutions from below saturation to above saturation and produce heavy metal precipitates including lead chloride, cobalt chloride, and copper chloride at low temperature.

Furthermore, Lueth and Whitworth (2001) examined low-temperature, sandstone-hosted copper deposits in New Mexico and found that copper sulfide concentrations are typically highest adjacent to bounding shales and diminish with increased distance from the shales in the sandstone. They hypothesized that hyperfiltration results in increased dissolved species concentration in groundwater adjacent to shale membranes for both copper and bacterial nutrients under low-temperatures. Lueth and Whitworth (2001)

postulated that the nutrients required by sulfate reducing bacteria would be in sufficient supply within a CPL, as would sufficient quantities of copper. Reduction of the sulfate by sulfate reducing bacteria within the CPL would produce $H_2S$ and lead to precipitation of copper sulfides. The fact that at least some phyllites are membrane-functioning suggests that it is possible that the membrane properties may play a role in the origin of at least some low temperature ore deposits. Deposits of low-temperature sulfide-bearing materials do exist within the axis of synclines and along fault boundaries of the Darrington Phyllite-Chuckanut Sandstone (Brown, 1987, Deskey et al. 1991. We postulate that low-temperature hyperfiltration during may have contributed to the formation of some metallic sulfide deposits seen adjacent to the Darrington Phyllite. Further experiments and field work will need to be undertaken to confirm or refute this idea.

Mackay (1946) postulated that such membrane processes are also active in high temperature ore deposits but experimental evidence is lacking to substantiate this idea. However, further high-temperature experimental work is suggested to test the concept. .

It is also possible that the ability of the phyllite to function as a hyperfiltration membrane might play a role in shallow, low temperature diagenesis in porous rocks adjacent to phyllite aquitards due to solute concentration increases in the CPL as well as exert a partial control on solute concentration distribution in some perched aquifers bounded below by membrane-functioning phyllite.

A number of studies have suggested that overpressured, shale-bounded aquifer systems may be affected by membrane processes (Bredehoeft et al., 1963). Hyperfiltration may occur in the Milk River aquifer in the western Canadian sedimentary

basin (Berry, 1960, Phillips, and others, 1986), the Illinois Basin (Bredehoeft et al., 1963, Graf et al., 1965; Graf et al., 1966), the Oxnard coastal basin, Ventura County, California (Greenberg et al., 1973), and the Saginaw aquifer system in the upper Grand River Basin, Michigan (Wood, 1976), among others. Based on our experiments, we suggest that overpressured aquifer systems bounded by phyllite should be investigated for membrane effects as well.

## 3.7 CONCLUSIONS

Solutions of 185 and 345 ppm chloride were passed through thin phyllite discs (~3 mm) at heads of 0.5 and 1.0 m. These are the first known hyperfiltration experiments performed on intact phyllite cores. In each experiment, ending cell chloride concentrations significantly increased due to partial solute rejection by the phyllite membranes. Concentration increases within the cell were between 112% and 134% over background. Calculated values of the reflection coefficient ranged from 0.87 and 0.88, suggesting that these thin phyllite discs exhibited significant membrane effects.

These experiments have shown that intact rock cores, in particular phyllite, are capable of significant hyperfiltration effects at low heads such as might be found in shallow regional or perched aquifers. Additionally, membrane-functioning phyllite may contribute to low-temperature metal sulfide deposition, as suggested by Mackay (1946). The potential for high-temperature membrane effects in foliated metamorphic rocks and other low permeability rocks should also be explored relative to ore deposit formation.

Based on these experiments on the Darrington Phyllite, membrane effects may need to be considered in a broad spectrum of low permeability lithologies and subsurface groundwater processes. Other lithologies that should be explored for potential membrane

effects include: limestone, dolomite, chalk, schist, fault gouge, and even low-permeability concrete. These experiments could be conducted at thinner disc thicknesses with similar heads in order to expedite the experimental process as well as allow for comparison in membrane properties versus thickness of membranes.

## 3.8 REFERENCES


Barone, F. S.; Rowe, R. K.; and Quigley, R. M. (1990) Laboratory determination of chloride diffusion coefficient in intact shale: *Canadian Geotechnical Journal* **27:** 177-184.

Benzel, W. M. and Graf, D. L. (1984) Studies of smectite membrane behavior: Importance of layer thickness and fabric in experiments at 20°C, *Geochimica et Cosmochimica Acta* **48**:1769-1778

Berry, F. A. F. (1960) Geologic field evidence suggesting membrane properties of shales, American Assoc. *Pet. Geologists. Bull.*, **44**: 953-954.

Bredehoeft, J. D., Blyth, C. R., White, W. A., Maxey, G. B. (1963) Possible mechanism for concentration of brines in subsurface formations. *American Assoc. Pet. Geologists Bull.* **42**: 257-269.

Brown, E.H. (1987) *Geologic map of the northwest Cascades, Washington* Boulder, Colo.: Geological Society of America, Map and chart series (Geological Society of America); MC-61.

Demir, I. (1988) Studies of smectite membrane behavior: Electrokinetic, osmotic, and isotopic fractionation processes at elevated pressures. *Geochimica et Cosmochimica Acta* **52**, 727-737.

Derkey, Robert E.; Joseph, Nancy L.; Lasmanis, Raymond, (1990) Metal mines of Washington--Preliminary report: Washington Division of Geology and Earth Resources Open File Report 90-18, 577.

Dullien, F. A. L. (1979). *Porous Media Fluid Transport and Pore Structure*. New York: Academic Press, 396.

Easterbrook, D. J. (1971) *Geology and geomorphology of western Whatcom County*, Washington: Western Washington State College Press: 68.

EPA (2004) Evaluation of Impacts to Underground Sources of Drinking Water by Hydraulic Fracturing of Coalbed Methane Reservoirs Attachment 11 The Pacific and Central Coal Region, 816-R-04-003.

Fritz S. J. and Marine I. W. (1983) Experimental support for a predictive osmotic model of clay membranes. *Geochim. Cosmochim. Acta* **47**: 1515-1522.

Fritz S. J. and Whitworth T. M. (1994,) Hyperfiltration-induced fractionation of lithium isotopes: ramifications relating to representativeness of aquifer sampling. *Water Resources Research* **30**: 225-235.

Fritz, S. J. (1986) Ideality of clay membranes in osmotic processes: a review, *Clays and Clay Minerals* **34**: 214-223.

Graf, D.L. (1982) Chemical osmosis, reverse osmosis, and the origin of subsurface brines, *Geochimica et Cosmochimica Acta* **46:** 1431-1448.

Graf, D. L., Friedman, I., Meents, W. F. (1965) The origin of saline pore waters, II: Isotopic fractionation by shale micropore systems, *Illinois State Geological Survey Circular* **393:** 32.

Graf, D. L., Meents, W. F., Friedman, I., Shimp, N. F. (1966) The origin of saline formation waters III: calcium chloride waters, *Illinois Geological Survey Circular*, **397**: 60.

Greenberg, J. A., Mitchell, J. K., Witherspoon, P. A. (1973) Coupled salt and water flows in a groundwater basin, *J. Geophy. Res.* **78**: 6341-6353.

Hart, M. and Whitworth, T. M., (2005) Hyperfiltration of Potassium Nitrate through Clay Membranes under Relatively Low-Head Conditions, *Geochimica Cosmochimica et Acta:* **69**, *20*, p. 4817-4823.

Haydon, P. R., Graf, D. L. (1986) Studies of smectite membrane behavior: Temperature dependence, 20-180°C. *Geochemica et. Cosmochemica Acta* **50**: 115-121.

Kemper, W.D., Rollins, J.B., (1966) Osmotic efficiency coefficients across compacted clays. *Soil Science Society of America* **30**: 529-534.

Kharaka, Y. K., Berry, F.A.F., 1973. Simultaneous flow of water and solutes through geologic membranes, I. Experimental investigation. *Geochim. Cosmochim. Acta* **37**: 2577-2603.

Lueth V.W. and Whitworth T. M. (2001) *A Geologic Membrane-Microbial Metabolism Mechanism for the Origin of the Sedimentary Copper Deposits in the Pastura District, Guadalupe County, New Mexico*. New Mexico Geological Society, 52nd Field Conference Guidebook.

Mackay R. A. (1946) The control of impounding structures on ore deposition, *Economic Geology* **61**:13-46.

Martin, R.B. (1964) *Introduction to biophysical chemistry.* McGray-Hill Book Company, New York. 365.

Marshall, C.E., (1948) The electrochemical properties of mineral membranes III. J. *Physical Chem*. **52**: 1284-1295.

McKelvey, J. G. and Milne, I. H., (1960) The flow of salt solutions through compacted clay, *Clays and Clay Minerals:* **9**: 248-259.

McKelvey, J. G., Milne, I. H. (1963) Permeability and salt-filtering properties of compacted clay, Presented at Clays and Clay Minerals, (extended abstract) *Monograph No. 13*, The MacMillan Company, 250-251.

Milne, I. H., McKelvey, J. G., and Trump, R. P., (1963) Permeability and salt-filtering properties of compacted clay, Clays and Clay Minerals, Monograph No. 13, The MacMillan Company, New York, 250-251.

Oduor, P.G. (2004) *Transient modeling and experimental verification of hyperfiltration effects*, PhD thesis, University of Missouri at Rolla.

Phillips, F. M., Bentley, H. M., Davis, S. N., Elmnore, D., Swanick, G. H., (1986) Chlorine 36 dating of very old groundwater 2. Milk River Aquifer, Alberta, Canada, *Water Resources Research* **22**: 2003-2016.

Saindon R.M. (2005) *Relevance of clay membrane properties of clay-rich geologic materials to water-related engineering issues*. PhD thesis, University of Missouri at Rolla.

Staverman A. J. (1952) Non-equilibrium thermodynamics of membrane processes. *Trans. Faraday Soc*. **48**, 176-185.

Walter, G.R. (1982) Theoretical and experimental determination of matrix diffusion and related solute transport properties of fractured tuffs from Nevada test site. Los Alamos National Laboratory report LA-9471-MS. 127.

Whitworth T. M. (1998) Steady-State Mathematical Modeling of Geological Membrane Effects in Aquifer Systems, presented at *Joint Conference on the Environment*, 37-40.

Whitworth T. M. and DeRosa G. (1997) Geologic Membrane Controls on Saturated Zone Heavy Metal Transport. *New Mexico Water Resources Research Institute Report No. 303*, Las Cruces, New Mexico, 88.

Whitworth, T. M. and Fritz, S. J., (1994), Interrelationship Between Solute-Induced Permeability Increase and Membrane Effect in Clays, *Applied Geochemistry:* **9:** 533-546.

Wood, W. W. (1976) A hypothesis of ion filtration in a potable-water aquifer system, *Ground Water* **14**: 233-244.

Young A. and P.F. Low (1965) Osmosis in argillaceous rocks, *American Assoc. of Pet. Geol. Bull.* **46**: 1004-1008.

Table 3.1: Experimental Parameters and Calculated Results.

| Parameter | Phyllite 1 | Phyllite 2 | Phyllite 3 | Phyllite 4 |
|---|---|---|---|---|
| Head (m) | 1.00 | 0.50 | 1.00 | 0.50 |
| Membrane thickness (mm) | 3.10 | 3.60 | 3.59 | 3.28 |
| Membrane area ($m^2$) | 0.0015 | 0.0015 | 0.0015 | 0.0015 |
| Solution flux, $J_v$ (m/s) | $9.290 \times 10^{-8}$ | $3.391 \times 10^{-8}$ | $7.405 \times 10^{-8}$ | $3.791 \times 10^{-8}$ |
| Two standard deviation (%) | ±2.01 | ±2.12 | ±2.11 | ±2.25 |
| Initial concentration, $c_i$ (ppm $Cl^-$) | 345 | 345 | 185 | 185 |
| Final cell concentration, $c_{final}$ (ppm $Cl^-$) | 777 | 730 | 432 | 421 |
| Predicated cell concentration, $c_{predicted}$ (ppm $Cl^-$) | 760 | 724 | 419 | 404 |
| Change in cell concentration (%) | 1.25 | 1.12 | 1.34 | 1.28 |
| Permeation Coefficient, $L_p$ (m/Pa·s) | $1.917 \times 10^{-12}$ | $1.229 \times 10^{-12}$ | $1.010 \times 10^{-12}$ | $1.017 \times 10^{-12}$ |
| Conc. at membrane face, $c_o$ (ppm $Cl^-$) | 385 | 363 | 204 | 195 |
| Calculated steady-state $\sigma$ | 0.87 | 0.88 | 0.87 | 0.88 |
| CBE | -1.20 | 0.95 | 0.11 | 0.02 |
| Time to steady state (days) | 115 | 112 | 117 | 118 |

Note: Measurements recorded at 21 °C.

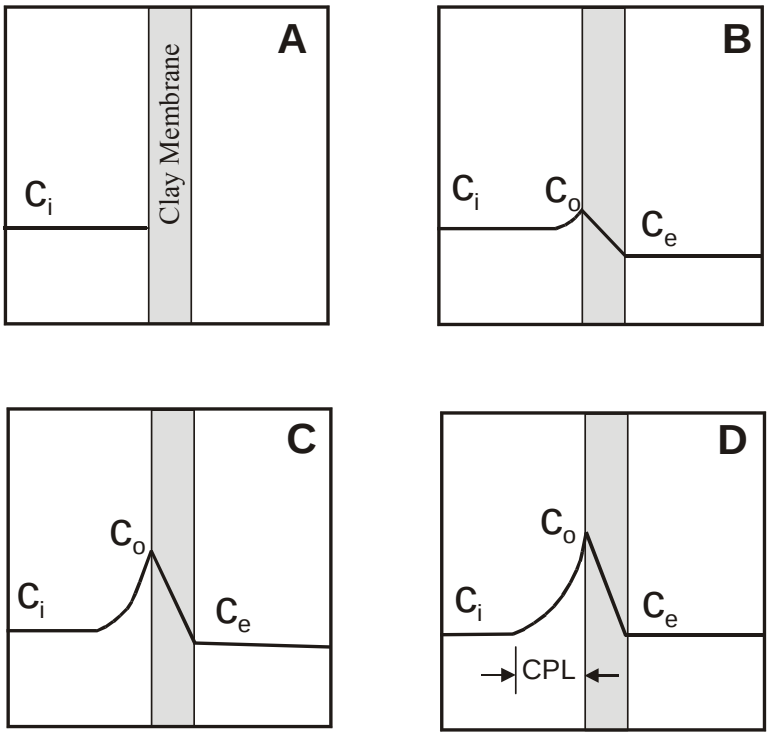


*Figure 3.1. Conceptual CPL development.* This assumes that the solute is conservative and no ion exchange is occurring. Initially, (A) the solute is all on the high-pressure side of the membrane and no solute is contained within the pore fluids within the membrane. After flux commences, (B) the concentration at the high-pressure membrane face $c_o$ increases due to solute rejection. Effluent samples contain some solute now. (C) $C_o$ has increased further as has the effluent concentration $c_e$. At steady-state (D) the input concentration $c_i$ is now equal to the output $c_e$ and the value of $c_o$ is constant. (Redrawn from Fritz and Marine, 1983).

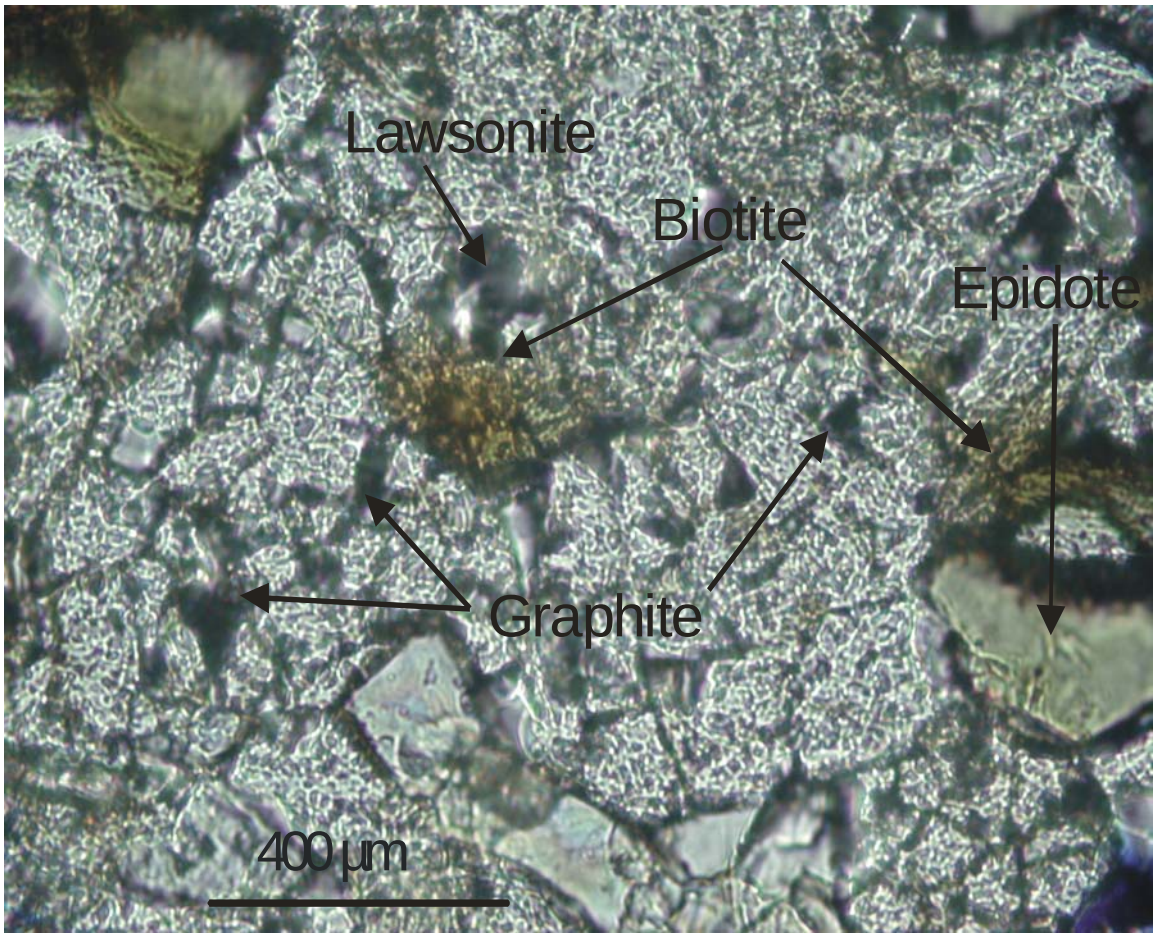


*Figure 3.2: Thin Section Photo of Darrington Phyllite at 40X magnification.*

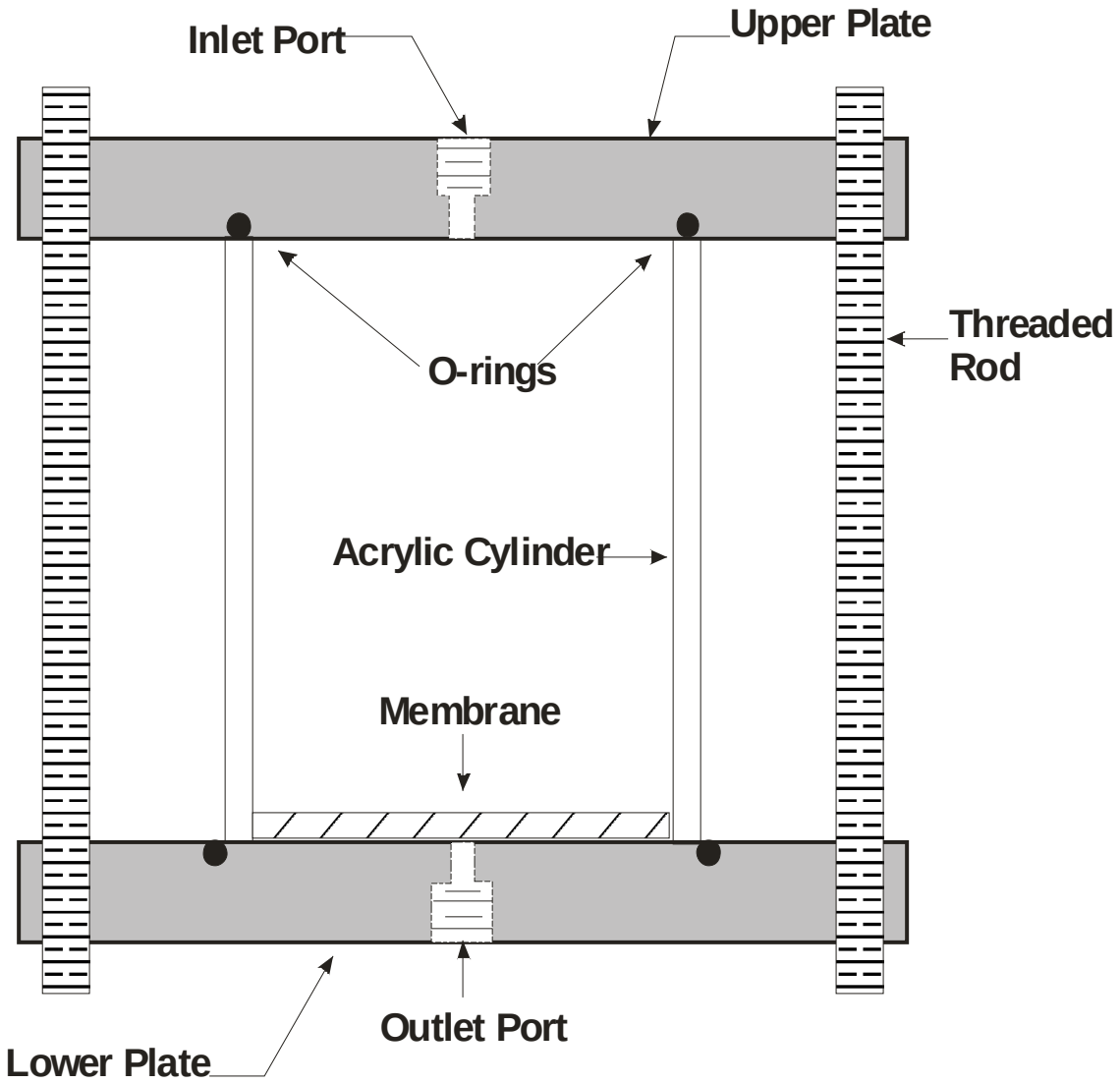


*Figure 3.3: Experimental Apparatus Schematic.*

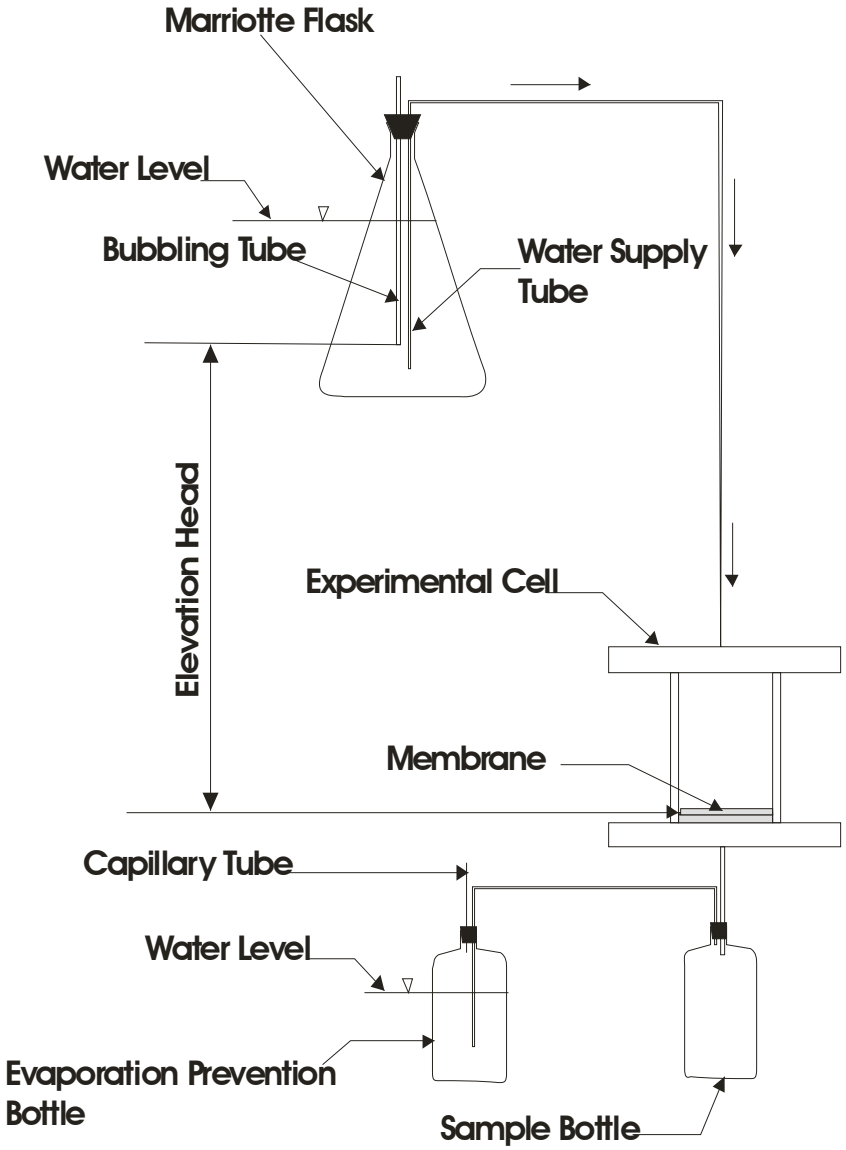


*Figure 3.4: Experimental Testing Schematic.*

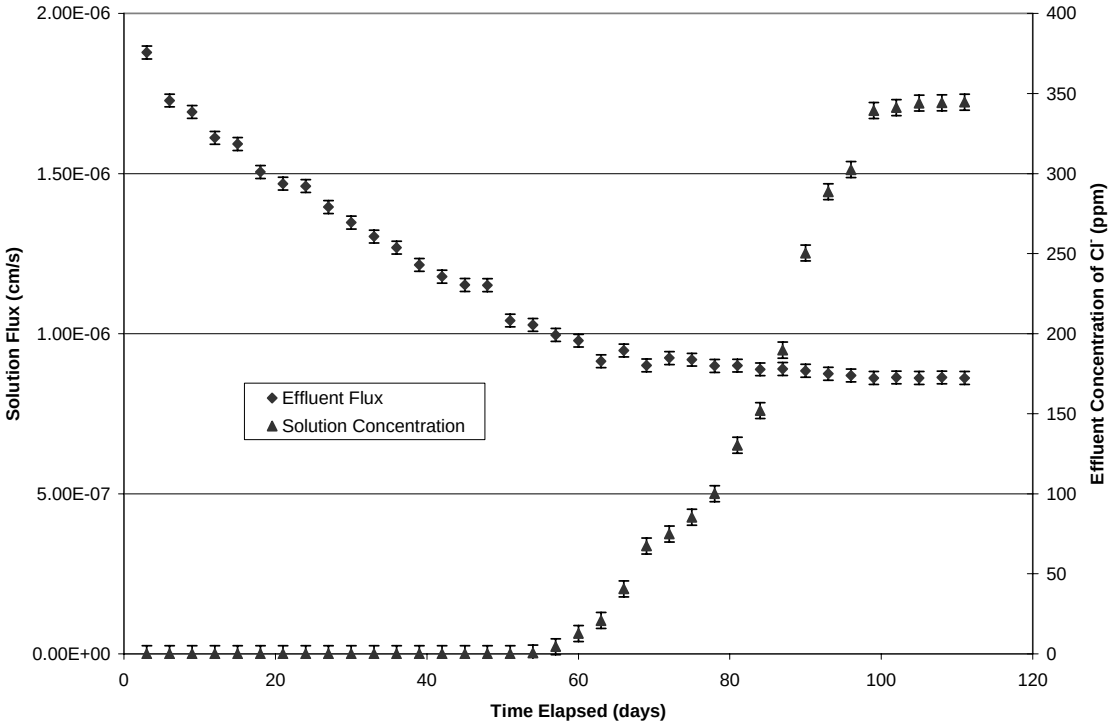


*Figure 3.5: Effluent Concentration and Flux versus Time for Experiment 1.*

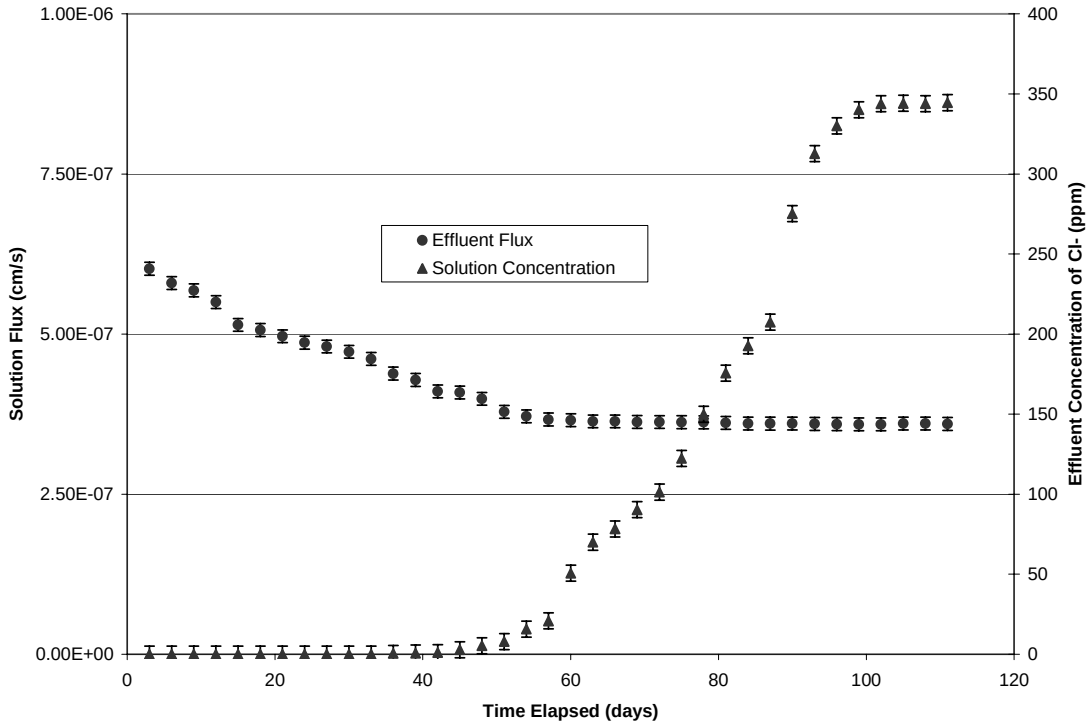


*Figure 3.6: Effluent Concentration and Flux versus Time for Experiment 2.*

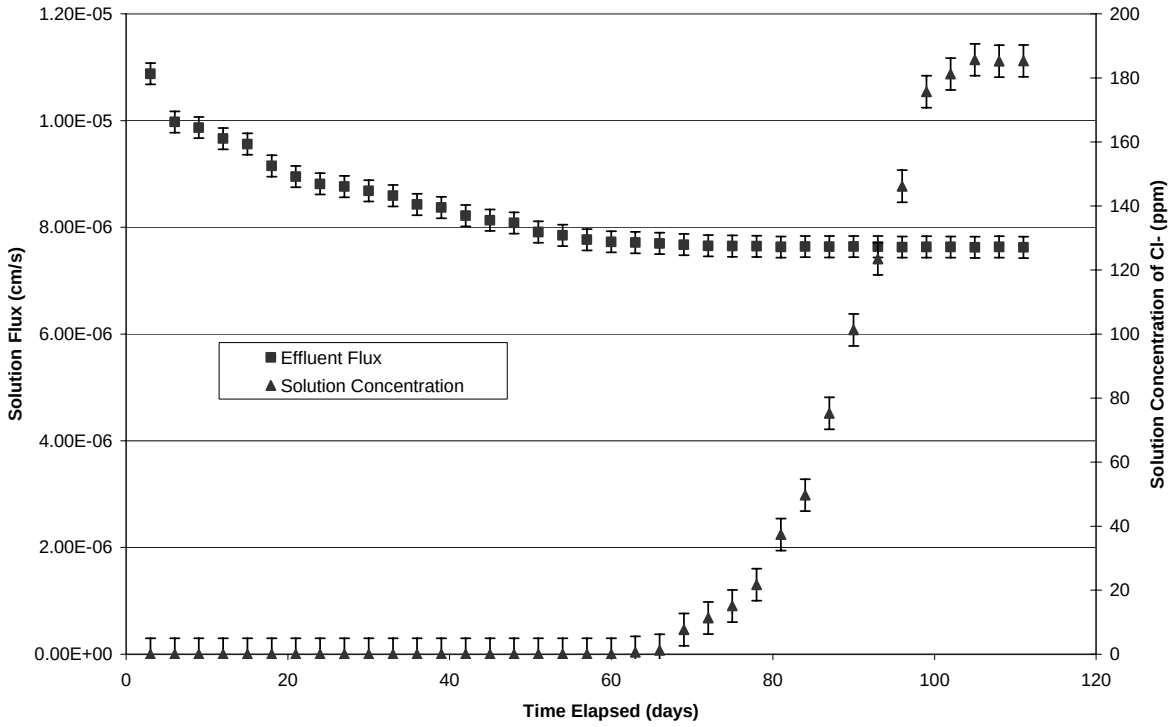


*Figure 3.7: Effluent Concentration and Flux versus Time for Experiment 3.*

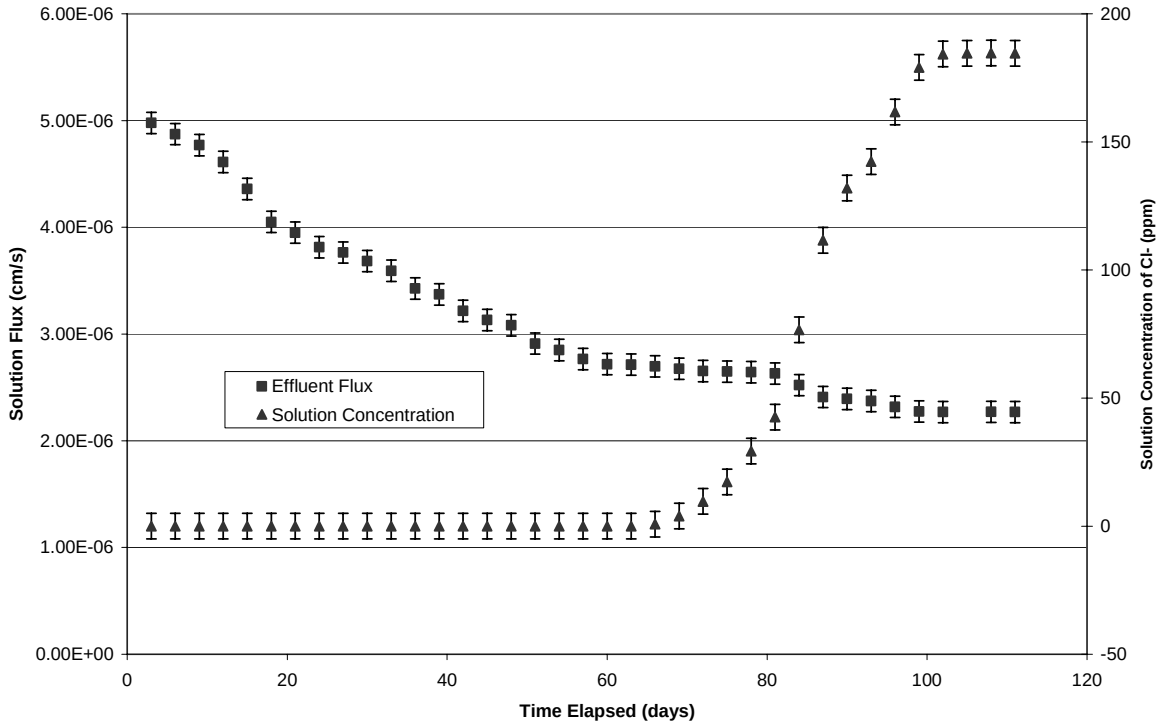


*Figure 3.8: Effluent Concentration and Flux versus Time for Experiment 4.*

# SECTION 2. OVERALL EXPERIMENTAL CONCLUSIONS

## 2.1 SUMMARY

Previous investigators have demonstrated that clays exhibit membrane properties when groundwaters are hydraulically forced through them at pressures in excess of the osmotic pressure. However, very little literature examines the capacity of an intact lithology to function as a membrane. Most experiments performed in literature examine disaggregated, recompacted shales or clay membranes and the experiments are performed at head differentials greater than what might be expected to occur in natural systems. Some investigators have therefore questioned if other lithologies without a significant clay component could exhibit significant membrane properties at the much lower gradients available in natural groundwater systems and on intact rock. Therefore, sixteen experiments were performed using a conservative chloride tracer and one experiment using silica acid on intact lower permeability lithologies including the Quarry Ridge Jefferson Dolomite, Darrington Phyllite, Lower Burlington Limestone, and low permeability concrete.

All experiments used heads of either 0.5 or 1.0 m and solute concentrations of 185 and 345 ppm $Cl^-$. All experiments exhibited membrane responses to the applied hydraulic gradients in varying amounts seen in the previous chapters. None of the lithologies tested included clay components, charged or otherwise, equal to the 12% clay rich designation. This would tend to preclude the two major methods of membrane functionality ion exchange and electrical charge. In past experiments membrane selectivity associated with ion exchange and electrical charge restrictions of negatively charged clay particles have been identified as the major mechanism for hyperfiltration;

however, the lithologies tested generally have no charged surface or clay component for which these selectivities can function. The membrane functions exhibited in these seventeen experiments therefore point to mechanical filtration (solute-sieving based upon size restrictions and dead-end pore throats alone) and deposition of cementation in pore throats as the predominant restriction causing membrane effects. These effects were not measured during the course of the experiments that were completed; however, documentation of cementation due to calcite in pore throats has been shown to occur and the restrictions measured in previous literature. In the case of the phyllite discs, the reflection coefficients were similar to those of charged smectites. There are many potential sources for the cause of this high reflection coefficient including multiple foliations and folding causing a higher percentage of close pore throats, multiple episodes of metamorphism causing cementation and perhaps even that the high graphite volume contributes some electrical component of charge previously unidentified.

Overall, the data for suggests that membrane effects may be more prevalent in natural groundwater systems than previously thought and that these effects may contribute to, accelerate or alter various naturally functioning processes such as cementation, low or high temperature ore deposition, concrete deterioration due to accelerated chloride infiltration, and misinterpretation of retarded solutes as contaminant plumes among many others.

## 2.2 CONCLUSIONS

- Low, constant, hydraulic heads in laboratory settings can induce significant CPL development through intact, lower permeability membrane-functioning lithologies including phyllite, dolomite, limestone and lower permeability concrete.

- These membrane effects may be more significant in the subsurface than previously thought.
- Experimental data reported in this dissertation provides detailed substantiation of low head differentials producing significant membrane effects through lower permeability intact rock discs which have previously never been documented.

# REFERENCES

Alexander, J., 1990, A Review of Osmotic Processes in Sedimentary Basins, British Geological Survey Technical Report WE/90/12.

American Academy of Pediatrics. Committee on Environmental Health, 1999, Handbook of Pediatric Environmental Health, American Academy of Pediatrics, Elk Grove Village, Ill.

Assembly of Life Sciences (U.S.) Committee on Nitrate and Alternative Curing Agents in Food, 1981, The Health Effects of Nitrate, Nitrite, and N-nitroso compounds: part 1 of a 2-part study., Washington, D.C., National Academy Press.

Benzel, W. M. and Graf, D. L., 1984, Studies of smectite membrane behavior: Importance of layer thickness and fabric in experiments at 20°C, Geochimica et Cosmochimica Acta, v 48, p. 1769-1778.

Bernstein, F., 1960, Distribution of water and electrolyte between homoionic clays and saturating NaCl solutions, in Clays and Clay Minerals: Proc. 8th Natl. Clay Conference., p. 122-149, Pergamon Press, Inc.

Berry, F. A. F., 1967, Role of membrane hyperfiltration on origin of thermal brines, Imperial Valley, California, American Society of Petroleum Geologists Bulletin, v. 51, 454-455.

Berry, F. A. F., 1966, Proposed origin of subsurface thermal brines, Imperial Valley, California (abs.), American Society of Petroleum Geologists Bulletin, v. 50, 644-645.

Berry, F. A. F., 1960, Geologic field evidence suggesting membrane properties of shales, American Society of Petroleum Geologists Bulletin, v. 44, 953-954.

Berry, F. A. F., 1959, Hydrodynamics and geochemistry of the Jurassic and Cretaceous systems in the San Juan Basin, northeastern New Mexico and southwestern Colorado, Ph.D. dissertation, Stanford University, 192 p.

Bredehoeft, J. D. Blyth, C. R., White, W. A., and Maxey, G. B., 1963, Possible mechanism for concentration of brines in subsurface formations. American Assoc. Pet. Geologists Bull. 42, 257-269.

Briggs, L. J., 1902, Filtration of suspended clay from solutions, U.S. Bur. of Soils Bulletin No. 19, p. 31-39.

Campbell, D. J., 1985, Fractionation of stable chlorine isotopes during transport through semipermeable membranes. M.S. thesis, University of Arizona, 103 p.

Coplen, T. B., and Hanshaw, B. B., 1973, Ultrafiltration by a compacted membrane--I. Oxygen and hydrogen isotope fractionation., Geochimica et Cosmochimica Acta, v 37, p. 2205-2310.

Demir, I., 1988, Studies of smectite membrane behavior: Electrokinetic, osmotic, and isotopic fractionation processes at elevated pressures. Geochimica et Cosmochimica Acta, v 52, p. 727-737.

Deobald, William B., Buchanan, John P., and Durham, Fritz E., 2003, Hydrogeology of the Northeastern Columbia Plateau, Department of Ecology, Recent Abstracts, August.

Domenico, P. A. and Schwartz, F. A., 1990, Physical and chemical hydrogeology, John Wiley and Sons, New York, 824 p.

Durbin, R. P., 1960, Osmotic flow of water across permeable cellulose membranes. J. Gen. Physiol. v. 44. p. 315-326.

Fetter, C. W., 1988, Applied Hydrogeology, Merril, Columbus Ohio, 592 p.

Freeze, R. A. and Cherry, J. A., 1979, Groundwater, Prentice-Hall, Englewood Cliffs, N. J., 604 p.

Fritz, S. J., Hinz, D. L., and Grossman, E. L., 1987, Hyperfiltration-induced fractionation of carbon isotopes, Geochemica et. Cosmochemica Acta , v 51, p. 1121-1134, .

Fritz, S. J., 1986, Ideality of clay membranes in osmotic processes: a review, Clays and Clay Minerals, v. 34, 214-223.

Fritz, S. J. and Whitworth, T. M., 1994, Hyperfiltration-induced fractionation of lithium isotopes: ramifications relating to representativeness of aquifer sampling, Water Resources Research, v. 30, p. 225-235.

Fritz, S. J. and Eady, C. D., 1985, Hyperfiltration-induced precipitation of calcite. Geochimica et Cosmochimica Acta, v 49, p. 761-768.

Fritz, S. J. and Marine, I. W., 1983, Experimental support for a predictive osmotic model of clay membranes. Geochimica et Cosmochimica Acta, v 47, p. 1515-1522.

Graf, D. L., Meents, W. F., Friedman, I., and Shimp, N. F., 1966, The origin of saline formation waters III: calcium chloride waters, Illinois Geological Survey Circular 397, 60 p.

Graf, D. L., Friedman, I., and Meents, W. F., 1965,The origin of saline pore waters, II: Isotopic fractionation by shale micropore systems, Illinois State Geological Survey Circular 393, 32 p.

Greenberg, J. A., Mitchell, J. K., and Witherspoon, P. A., 1973, Coupled salt and water flows in a groundwater basin, Journal of Geophysical Research, v. 78, 6341-6353.

Grim, R. E., 1968, Clay Mineralogy, McGraw-Hill, New York.

Hanshaw, B. B., and Hill, G. A., 1969, Geochemistry and hydrodynamics of the Paradox Basin Region, Utah, Colorado, and New Mexico, Chemical Geology, v. 4, 263-294.

Harris, F. L., Humphreys, G. B., and Spiegler, K. S., 1976, Reverse osmosis (hyperfiltration) in water desalination, in P. Meares, ed., Membrane Separation Processes, Elsevier, Amsterdam, Chapter 4.

Haydon, P. R., and Graf, D. L., 1986, Studies of smectite membrane behavior: Temperature dependence, 20-180°C, Geochemica et. Cosmochemica Acta , v. 50, 115-121.

Kedem, O. and Katchalsky, A., 1962, A physical interpretation of the phenomenological coefficients of membrane permeability, Journal of General Physiology, v. 45., p.143-179.

Kemper, W. D. and Evans, N. A., 1963, Movement of water as effected by free energy and pressure gradients III: Restriction of solutes by membranes, Soil Science Society of America Proceedings, v. 27.. 485-490.

Kemper, W. D., 1961, Movement of water as effected by free energy and pressure gradients. I. Application of classic equations for viscous and diffusive movements to the liquid phase in finely porous media. II. Experimental analysis of porous systems in which free energy and pressure gradients act in opposite directions, Proc. Soil Sci. America, v. 25, p. 255-265.

Kemper, W. D., 1960, Water and ion movement in thin films as influenced by the electrostatic charge and diffuse layer of cations associated with clay mineral surfaces, Soil Science Society Proceedings, p. 10-16.

Kemper, W. D. and Rollins, J. B., 1966, Osmotic efficiency coefficients across compacted clays, Soil Science Society of America, v. 30, 529-534.

Kharaka, Y. K. and Smalley, W. C. , 1976, Flow of water and solutes through compacted clays. American Assoc. Pet. Geol. Bull., v 60, p. 973-980.

Kharaka, Y. K. and Berry, F. A. F., 1973, Simultaneous flow of water and solutes through geologic membranes, I. Experimental investigation, Geochimica et Cosmochimica Acta, v 37, p. 2577-2603.

Kharaka, Y. K., Berry, F. A. F., and Friedman, I., 1973, Isotopic compositions of oil-field brines from Kettleman North Dome, California, and their geologic implications, Geochimica et Cosmochimica Acta, v 37, p. 1899-1908.

Marcus, Yizhak., 1997, Ion Properties, Marcel Drakker, New York.

Mariñas, B. J. and Selleck, R. E., 1992, Reverse Osmosis treatment of multicomponent electrolyte solutions, Journal of Membrane Science, v 72, p. 211-229.

Marshall, C. E., 1948, The electrochemical properties of mineral membranes III, J. Physical Chem., vol 52, 1284-1295.

McCalpin, J.P., 1999, Geomorphology, hydrology, and hydrogeology of Medano Creek, Great Sand Dunes National Monument, southern Colorado, in Schenk, C. J. (ed.), Hydrologic, geologic, and biologic research at Great Sand Dunes National Monument and vicinity, Colorado: Proceedings of National Park Service Research Symposium No. 1: U.S. Geological Survey, p. 8-30.

McKelvey, J. G. and Milne, I. H., 1963, Permeability and salt-filtering properties of compacted clay, Clays and Clay Minerals, (extended abstract) Monograph No. 13, The MacMillan Company, pp 250-251.

McKelvey, J. G. and Milne, I. H., 1960, The flow of salt solutions through compacted clay, Clays and Clay Minerals, v. 9, p. 248-259, Pergamon Press, Inc..

Milne, I. H., McKelvey, J. G., and Trump, R. P., 1964, Semi-permeability of bentonite membranes to brines, American Assoc. Petroleum Geol. Bull., v 48, pp 102-105.

Milne, I. H., McKelvey, J. G., and Trump, R. P., 1963, Permeability and salt-filtering properties of compacted clay, Clays and Clay Minerals, Monograph No. 13, The MacMillan Company, New York, p. 250-251.

Newman et al., Phytoremediation of MTBE at a California naval site, Soil & Ground water Cleanup. Feb/Mar. 1999, p. 42.

Nuezil, C. E., 2000, Osmotic generation of 'anomalous' fluid pressures in geological environments, Nature, v. 403, 182-184.

Nuezil, C. E., 1986, Groundwater flow in low-permeability environments, Water Resources Research, Vol. 22, pp. 1163-1195.

Olsen, H. W., 1972, Liquid movement through kaolinite under hydraulic, electric, and osmotic gradients, American Association of Petroleum Geologists Bulletin, v. 56, 2022-2028.

Olsen, H. W., 1969, Simultaneous fluxes of liquid and charge in saturated kaolinite, Soil Science Society of America Proceedings, v. 33, 338-344.

Phillips, F. M.; Bentley, H. M.; Davis, S. N.; Elmnore, D.; and Swanick, G. H., 1986, Chlorine 36 dating of very old groundwater 2. Milk River Aquifer, Alberta, Canada, Water Resources Research, v. 22. 2003-2016.

Spiegler, K. S. and Kedem, O., 1966, Thermodynamics of hyperfiltration (reverse osmosis): criteria for efficient membranes, Desalination, v 1, p. 311-326.

Srivastava, R. C. and Jain, A. K., 1975, Non-equilibrium thermodynamics of electro-osmosis of water through composite clay membranes, 1. The electro-kinetic energy conversion. Journal of Hydrology, Vol. 25, 307-324.

Whitworth, T. M., 1999, Clay Minerals: Ion Exchange, Encyclopedia of Geochemistry, Kluwer Academic Publishers, AH Dordrecht, The Netherlands.

Whitworth, T. M., et al., 1999, Solute-Sieving-Induced Calcite Precipitation on Pulverized Quartz Sand: Experimental Results and Implications for the Membrane Behavior of Fault Gouge, American Geophysical Union, 149-157.

Whitworth, T. M., 1998, Steady-state mathematical modeling of geologic membrane processes in aquifer systems. WERC/WRHSRC/NMHWMS Joint Conference on the Environment, Proceedings, Albuquerque, NM, March 31—April 2, 1998, pp. 37-41.

Whitworth, T. M. and DeRosa, G., 1997, Geologic Membrane Controls on Saturated Zone Heavy Metal Transport. New Mexico Water Resources Research Institute Report No. 303, Las Cruces, New Mexico, 88 p.

Whitworth, T. M., Marinas, B. J., and Fritz, S. J., 1994, Isotopic fractionation and overall permeation of lithium by a thin-film composite polyamide reverse osmosis membrane, Journal of Membrane Science, 88, 231-241.

Whitworth, T. M. and Fritz, S. J., 1994, Electrolyte-induced solute permeability effects in compacted smectite membranes, Applied Geochemistry, v 9, 533-546.

Wood, W. W., 1976, A hypothesis of ion filtration in a potable-water aquifer system, Ground Water, v. 14, 233-244.

Wyllie, M. R. J., 1949, A quantitative analysis of the electrochemical component of the S. P. curve, J. Petroleum Tech., v 1, p. 17-26.

Wyllie, M. R. J., 1948, Some electrochemical properties of shales, Science, v 108, p. 684-685.

Young, A. and Low, P. F., 1965, Osmosis in argillaceous rocks, American Association of Petroleum Geologists Bulletin, v. 49, 1004-1008.

# VITA

Megan Leanore Hart was born in Dallas, Texas on November 15, 1976. In March 2001 she received her first B.S. Geology from Western Washington University. Megan enrolled at the former University of Missouri – Rolla, currently named Missouri University of Science and Technology in order to obtain her Masters of Science in Geological Engineering in May 2004. She also graduated at that time with her second Bachelor's of Science in Geological Engineering. Throughout this time Megan was a graduate teaching assistant in the Department of Geological Engineering and taught multiple courses and lab courses including: Geology for Engineers, Environmental aspects of Geological Engineering, Subsurface Exploration, Geomorphology and Map Interpretation. Megan was a field engineer during the Summer of 2005 working at the company SAIC located in St. Louis, MO at which she helped perform soil remediation of FUSRAP sites in Saint Louis, MO, water monitoring, air monitoring, permit writing, and surveying. Megan re-enrolled at the University of Missouri – Rolla, in August 2004 as a graduate student in Geological Engineering in order to obtain her doctorate of philosophy in August, 2009. Megan left UMR in 2006 to work full time and still currently works full time as an environmental engineer at the Missouri Department of Natural Resources performing wastewater and water plan review and implementation, stakeholders committees, remedial alternatives analysis and construction requirements.